

# LOW SURFACE BRIGHTNESS GALAXY CATALOGUE SELECTED FROM THE $\alpha$ .40-SDSS DR7 SURVEY AND TULLY-FISHER RELATION

DU WEI<sup>1,2</sup> AND CHENG CHENG<sup>1,3</sup>

WU HONG<sup>1,2</sup>

ZHU MING<sup>1,4</sup>

WANG YOUGANG<sup>1,5</sup>

<sup>1</sup>*National Astronomical Observatories, Chinese Academy of Sciences, 20A Datun Road, Chaoyang District, Beijing 100012, China*

<sup>2</sup>*Key Laboratory of Optical Astronomy, National Astronomical Observatories, Chinese Academy of Sciences, 20A Datun Road, Chaoyang District, Beijing 100012, China*

<sup>3</sup>*Chinese Academy of Sciences South America Center for Astronomy, National Astronomical Observatories, Chinese Academy of Sciences, 20A Datun Road, Chaoyang District, Beijing 100012, China*

<sup>4</sup>*Chinese Academy of Sciences Key Laboratory of FAST, National Astronomical Observatories, Chinese Academy of Sciences, 20A Datun Road, Chaoyang District, Beijing 100012, China*

<sup>5</sup>*Key Laboratory of Computational Astrophysics, National Astronomical Observatories, Chinese Academy of Sciences, 20A Datun Road, Chaoyang District, Beijing 100012, China*

(Received; Revised; Accepted November 13, 2018)

Submitted to

## ABSTRACT

We present a catalogue of an HI-selected sample of 1129 low surface brightness galaxies (LSBGs) searched from the  $\alpha$ .40-SDSS DR7 survey. This sample, consisting of various types of galaxies in terms of luminosity and morphology, has extended the parameter space covered by the existing LSBG samples. Based on a subsample of 173 LSBGs which are selected from our entire LSBG sample to have the 2-horn shapes of the HI line profiles, minor-to-major axial ratios ( $b/a$ ) less than 0.6 and signal-to-noise ratio (S/N) of HI detection greater than 6.5, we investigated the Tully-Fisher relation (TFr) of LSBGs in the optical  $B$ ,  $g$  and  $r$  bands and near-infrared  $J$ ,  $H$  and  $K$  bands as well. In optical bands, the LSBG subsample follows the fundamental TFr which was previously defined for normal spiral galaxies. In NIR bands, the TFrs for our LSBG subsample are slightly different from the TFrs for the normal bright galaxies. This might be due to the internal extinction issue. Furthermore, the mass-to-light ratio ( $M/L$ ), disk scale length ( $h$ ) and mass surface density ( $\bar{\sigma}$ ) for our LSBG subsample were deduced from the optical TFr results. Compared with High Surface Brightness Galaxies (HSBGs), our LSBGs have higher  $M/L$ , larger  $h$  and lower  $\bar{\sigma}$  than HSBGs.

*Keywords:* Catalogues-Galaxies:dwarf-Galaxies:irregular-Galaxies:fundamental parameters

## 1. INTRODUCTION

Low Surface Brightness Galaxies (LSBGs) are galaxies that have central surface brightness fainter than the night sky ( $\sim 22.5 B$  mag arcsec $^{-2}$ ) (e.g. Impey & Bothun 1997; Impey et al. 2001; Ceccarelli et al. 2012). Comparing with their High Surface Brightness Galaxy (HSBG) counterparts, they are gas-rich, metal-poor ( $\leq 1/3$  solar abundance; McGaugh & Bothun (1994)), dust-poor (e.g., Matthews et al. 2001), and with diffuse, low-density stellar disks, (e.g. de Blok et al. 1996; Burkholder et al. 2001; O’Neil et al. 2004; Trachternach et al. 2006), which indicates that they are low in star formation and insufficiently evolved (e.g., Das et al. 2009; Galaz et al. 2011; Lei et al. 2018). Usually, dwarf galaxies can mostly satisfy the definition of LSBGs, so dwarf galaxies make a great contribution to the LSBG family. Meanwhile, some of the giant galaxies have very extended and thus faint disk. LSBGs between dwarf and giant types are more similar to late-type spiral galaxies in general properties (Chung et al. 2002). These main types of LSBGs are proposed to have fundamentally different formation and evolutionary histories from each other.

LSBGs contribute 30%–60% to the number density of local galaxies (McGaugh et al. 1995; McGaugh 1996; Bothun et al. 1997; O’Neil et al. 2000; Trachternach et al. 2006; Haberzettl et al. 2007) and  $\sim 20\%$  to the dynamical mass of galaxies (Minchin et al. 2004), making them cosmologically significant. However, due to the observational capability and selection effects, LSBGs are seriously underrepresented in the present-day galaxy catalogues, which inevitably leads a bias (towards HSB galaxies) to our understanding of the galaxy formation and evolution. More LSBG samples are necessary. The first LSBG samples were mainly composed of LSBGs in the bright end of surface brightness (McGaugh & Bothun 1994; de Blok et al. 1995; Schombert et al. 1992; Impey et al. 1996). Afterwards, Zhong et al. (2008) derived a large sample of 12282 LSBGs from the main galaxy sample of SDSS DR4 (Adelman-McCarthy et al. 2006), with dwarf galaxies removed. Williams et al. (2016) discovered LSBGs which have fainter surface brightness ( $\mu_0(B) \sim 24 - 28$  mag arcsec $^{-2}$ ) by using SDSS *gri* combined images within the GAMA equatorial fields (Driver et al. 2011; Liske et al. 2015). As LSBGs are mostly rich in HI gas, the extragalactic HI surveys, such as the Arecibo Legacy Fast Arecibo L-band Feed Array (ALFALFA; Giovanelli et al. (2005)), are good databases for searching LSBGs. So we have established a sample of 1129 LSBGs from the combination of 40% data release of ALFALFA ( $\alpha.40$ ; Haynes et al. (2011)) and SDSS DR7 (Abazajian et al. 2009) imaging survey. The sample establishment, including the key steps of sky subtraction and surface photometry, have been detailedly reported in Du et al. (2015), which is the first paper of a series of our papers on LSBG studies. In the current paper, we expect to release the catalogue of the  $\alpha.40$ -SDSS DR7 LSBG sample.

Additionally, Tully-Fisher relation (TFr), an empirically linear correlation between the rotational velocity and the total absolute magnitude, was first discovered for HSB spiral galaxies in Tully & Fisher (1977). The TFr has been widely studied for various samples of HSB spiral galaxies in optical bands (Tully & Fisher 1977; Bottinelli et al. 1986; Fouque et al. 1990; Sprayberry, Bernstein & Impey 1995; Courteau et al. 1997; Pizagno et al. 2007). Later, because near-infrared (NIR) luminosity suffers less from Galactic and internal extinction than optical luminosity, and is more sensitive to stellar mass and thus correlates more tightly with the rotational velocity, many TFr studies have been performed in NIR passbands (Burstein 1982; Freedman 1990; Liu et al. 2008; Theureau et al. 2007; Masters et al. 2008; Tiley et al. 2016), in mid-infrared passbands (Sorce et al. 2012, 2013), and even in multi-wavelength passbands from optical to NIR (Sakai et al. 2000; Bell & de Jong 2001; Ponomareva et al. 2017). Recently, the baryonic TFr, a relation between the rotational velocity and the total baryonic mass (including both stellar and gas mass), has received a lot of attention (McGaugh et al. 2000; McGaugh 2005; Begum et al. 2008; Trachternach et al. 2009; Gurovich et al. 2010; McGaugh 2012; Zaritsky et al. 2014; Papastergis et al. 2016). So far, TFr studies for LSBGs are deficient due to the lack of LSBG samples (Zwaan et al. 1995; Sprayberry, Bernstein & Impey 1995; O’Neil et al. 2000; Chung et al. 2002). The TFr studies are all performed in optical passbands. Zwaan et al. (1995) gathered 42 LSBGs from literature, and showed that their LSBGs followed the fundamental TFr defined for HSB spiral galaxies. This draws a picture that LSBGs may not be fundamentally different from normal HSBGs. However, basing on a homogeneous sample of 43 LSBGs, O’Neil et al. (2000) claimed that their LSBGs did not show any significant correlation between the velocity width and the optical absolute magnitude. This conclusion was later proved by Chung et al. (2002). In this paper, we expect to investigate the TFr of LSBGs based on our own LSBG sample.

In this paper, we briefly introduce the establishment of our LSBG sample in §2.1 and release the complete catalogue in §2.2. We perform a luminosity classification in §3.1 and a morphological classification for our LSBG sample by machine learning in §3.2. The optical and radio properties are studied in §4. In §5, we study the optical and near-infrared (NIR) TFr for a subsample from our entire LSBG sample. The strength and weakness of this LSBG sample are discussed in §6.1. The mass-to-light ratios, disk scale length and mass surface density deduced from the TFr results

on the basis of our LSBG subsample are discussed in §6.2~6.4. Finally, we summarize the paper in §7. Through this paper, the distances that we used to convert angular sizes to physical (kpc) sizes are directly the ones listed in the  $\alpha.40$  catalogue (Haynes et al. 2011), which adopted the Hubble constant to be  $H_0=70 \text{ km s}^{-1} \text{ Mpc}^{-1}$ . Magnitudes in this paper are all in the AB magnitude system.

## 2. OUR $\alpha.40$ -SDSS DR7 LSBG SAMPLE

### 2.1. A brief review of sample establishment

In Du et al. (2015), we have constructed a sample of LSBGs which is searched from the  $\alpha.40$ -SDSS DR7 survey combination. We just make a brief introduction of the sample selection in this section because details have already been reported in Du et al. (2015).

First of all, we reconstructed the sky background maps for SDSS DR7  $g$ - and  $r$ -band images for each galaxy of the entire  $\alpha.40$ -SDSS DR7 sample (12,423 galaxies). The method we used for reconstructing sky background map is to fit the sky pixels on the object-subtracted image row-by-row and column-by-column (Wu et al. 2002; Zheng et al. 1999), which is a better method of constructing sky background for bright galaxies with faint extended outskirts and in particular for LSBGs (Du et al. 2015). After subtracting the sky background of galaxies, we made surface photometry by using SExtractor (Bertin & Arnouts 1996) and made radial profile fitting by using Galfit (Peng et al. 2002). Afterwards, on the basis of the photometric and fitting results, the  $g$ - and  $r$ -band central surface brightnesses ( $\mu_0$ ) were calculated and then converted to the  $B$ -band values ( $\mu_0(B)$ ). Finally, 1129 galaxies which have  $\mu_0(B)$  fainter than  $22.5 \text{ mag arcsec}^{-2}$  and minor-to-major axial ratios ( $b/a$ ) in both  $g$  and  $r$  bands larger than 0.3 were selected to be our LSBG sample. It is an HI-selected LSBG sample, of which the data reduction, sky subtraction, surface photometry, profile fitting, selection criteria and environment properties have been detailedly reported and studied in Du et al. (2015). In this paper, we aim to make the catalogue of this LSBG sample released to the public who might be interested in this sample and also investigate the Tully-Fisher relations of LSBGs in the optical and NIR bands based on this LSBG sample.

### 2.2. Catalogue

We present the entire catalogue of our LSBG sample in this paper. A short list of the catalogue is shown in Table 2 and the long rest list is shown in Table 4 in Appendix. The column descriptions of both tables are shown below:

Column 1: galaxy name as it appears in the  $\alpha.40$  catalogue.

Column 2: velocity width of the HI line profile measured at the 50% level of the peak (stemmed from the  $\alpha.40$  catalogue).

Columns 3 & 4:  $g$ - and  $r$ -band magnitudes and errors measured on the sky-subtracted images of galaxies within the automatic aperture (AUTO) by SExtractor. As mentioned before, the sky subtraction was performed by using a column-by-column and row-by-row fitting method which was more precise (details in Section 3.1 in Du et al. (2015)). These magnitudes have already been corrected for the Galactic extinction by using the dust maps of Schlegel et al. (1998)(SFD98). It is worth noting that SExtractor has computed several types of magnitudes: isophotal, corrected isophotal, fixed-aperture, automatic aperture and petrosian magnitudes. Thereinto, the automatic aperture, inspired by Kron’s “first moment” algorithm (see details in Kron (1980)), is an flexible and accurate elliptical aperture whose elongation  $\epsilon$  and position angle  $\theta$  are defined by the second order moments of the object’s light distribution. Then, within this aperture, the characteristic radius  $r_1$  is defined as that weighted by the light distribution function ( $r_1 = \frac{\sum r^2 I(r)}{\sum I(r)}$ ). Kron (1980) and Infante (1987) have verified that for stars and galaxy profiles convolved with Gaussian seeing, more than 90% of the flux is expected to lie within a circular aperture of radius  $kr_1$  if  $k=2$ , almost independently of their magnitudes. This picture remains unchanged if they consider an ellipse with  $\epsilon kr_1$  and  $\frac{kr_1}{\epsilon}$  as the principal axes. By choosing a larger  $k=2.5$ , more than 96% of the flux is captured within the elliptical aperture. So, the AUTO magnitudes are intended to give the most precise estimate of “total magnitudes”, at least for galaxies. More details about the Kron radius and the automatic aperture photometry used in SExtractor have been reported in SExtractor manual and Kron (1980); Infante (1987); Bertin & Arnouts (1996). For our automatic photometry using SExtractor, we keep  $k=2.5$  that is also the default setting of SExtractor (Bertin & Arnouts 1996) and our following studies and analysis would all base on the AUTO magnitudes in this table.

Column 5:  $B$ -band AUTO magnitude converted from the combination of AUTO magnitudes in both  $g$ - and  $r$  bands by using the transformation formula in Smith et al. (2002) (also listed as Equation (1) below). The errors on  $B$ -band magnitudes in this table were propagated from the errors on magnitudes in  $g$  and  $r$  bands by the error propagation

method.

$$B = g + 0.47(g - r) + 0.17 \quad (1)$$

Columns 6 & 7:  $g$ -band major-to-minor axis ratio ( $b/a$ ) and disk scale length ( $h(g)$ ) which were derived from fitting the sky-subtracted image of the galaxy with a single exponential profile by using Galfit (Peng et al. 2002). The details about our fitting processes have been reported in Section 3.3 in Du et al. (2015)). No uncertainties on  $b/a$  or  $h(g)$  are listed in this table because Galfit did not provide any errors for these outputs. Galfit gave the disk scale length in angular size and we converted the angular size to the physical size (kpc) by using the distance information from the  $\alpha.40$  catalogue (Haynes et al. 2011).

Column 8:  $g$ -band effective radius ( $R_{eff}(g)$ ) given by SExtractor. SExtractor gave the effective radius in angular size and we then converted the angular size to the physical size by using the distance information from the  $\alpha.40$  catalogue. No uncertainties on  $R_{eff}(g)$  are listed in this table because SExtractor did not provide the uncertainties for this parameter.

Column 9:  $g$ -band central surface brightness in mag arcsec $^{-2}$ ,  $\mu_{0,g}$ , which is calculated from the combination of  $g$ -band automatic aperture magnitude,  $g$ , (Column 3), major-to-minor axis ratio,  $b/a$  (Column 6) and disk scale length,  $h(g)$  (Column 7), according to the calculation formula (1b) in Du et al. (2015). As we have no available uncertainties on  $b/a$  and  $h(g)$ , unfortunately we could not provide the uncertainties on  $\mu_{0,g}$ . Additionally, the  $g$ -band effective radius and central surface brightness in columns 8 & 9 are listed in this table only because they might be useful for readers who would like to pick out candidates of Ultra Diffuse Galaxies (UDGs) from this LSBG sample.

Column 10:  $B$ -band central surface brightness in mag arcsec $^{-2}$ ,  $\mu_{0,B}$ . This value was converted from  $\mu_{0,g}$  (Column 9) and  $\mu_{0,r}$  according to the transformation formula in Smith et al. (2002) which was also listed as formula (1c) in Du et al. (2015) for convenience.  $\mu_{0,r}$  was calculated using the same method as  $\mu_{0,g}$  in Column 9. As we have no available uncertainties on both  $\mu_{0,g}$  and  $\mu_{0,r}$ , we can not provide any uncertainties on  $\mu_{0,B}$ .

Columns 11~14: Besides the central surface brightness based on the AUTO magnitudes (Column 10), we also list the  $B$ -band central surface brightnesses based on the isophotal (ISO), corrected isophotal (ISOCOR), petrosian (PETRO) magnitudes and the average of the four (AVE) for each galaxy. As we have difficulty in providing the errors on these central surface brightnesses of each type, we wish that readers could make their own impression and constraints on the uncertainties of the central surface brightness by comparing  $\mu_0$  based on different magnitude types.

Column 15: morphological type by decision trees with Random Forest of Machine Learning (see details in § 3.2)

Column 16: luminosity type in terms of  $B$ -band absolute magnitude. D, G and M denote dwarf LSBGs, giant LSBGs and moderate-luminosity LSBGs (see details in § 3.1).

More useful parameters, such as ra, dec, distance, radial velocity and the HI mass, can be easily accessed from the  $\alpha.40$  catalogue (Haynes et al. 2011) or the entire ALFALFA catalogue (Haynes et al. 2018).

**Table 1.** A subset of the catalogue of our LSBG sample from the  $\alpha$ .40–SDSS DR7.

AGC	W50	g	r	B	b/a	h(g)	$R_{eff}(g)$	$\mu_{0,g}$	$\mu_{0,B}$	$\mu_{0,B}$	$\mu_{0,B}$	$\mu_{0,B}$	T1	T2
	(km s $^{-1}$ )	(mag)	(mag)	(mag)		(kpc)	(kpc)	(AUTO)	( AUTO)	ISO	ISOCOR	PETRO	AVE	
17	102 $\pm$ 2	14.66 $\pm$ 0.005	14.20 $\pm$ 0.005	15.05 $\pm$ 0.008	0.62	1.52	1.87	23.08	23.44	24.96	23.59	23.40	23.85	S D
273	157 $\pm$ 11	16.38 $\pm$ 0.010	16.01 $\pm$ 0.010	16.73 $\pm$ 0.015	0.53	3.23	4.31	22.26	22.65	23.58	23.04	22.67	22.98	L M
337	144 $\pm$ 13	15.66 $\pm$ 0.006	15.36 $\pm$ 0.007	15.98 $\pm$ 0.010	0.78	3.32	5.67	22.13	22.55	23.63	23.16	22.56	22.98	L M
1084	59 $\pm$ 3	16.41 $\pm$ 0.011	16.03 $\pm$ 0.011	16.75 $\pm$ 0.017	0.74	2.49	3.20	23.26	23.63	25.31	24.23	23.56	24.18	L D
1211	156 $\pm$ 5	14.92 $\pm$ 0.005	14.55 $\pm$ 0.006	15.27 $\pm$ 0.008	0.70	2.68	3.67	22.67	23.14	24.51	23.54	23.10	23.57	S M
1362	151 $\pm$ 8	16.46 $\pm$ 0.012	16.00 $\pm$ 0.012	16.85 $\pm$ 0.019	0.76	3.99	5.72	22.45	22.90	23.99	22.88	22.88	23.16	S M
1693	95 $\pm$ 2	15.33 $\pm$ 0.007	15.01 $\pm$ 0.008	15.65 $\pm$ 0.012	0.84	3.60	5.01	22.86	23.23	24.99	23.18	23.22	23.66	S M
2144	130 $\pm$ 7	15.27 $\pm$ 0.007	14.79 $\pm$ 0.006	15.67 $\pm$ 0.010	0.86	3.64	4.99	22.34	22.77	23.40	22.28	22.73	22.79	S M
4528	88 $\pm$ 6	15.65 $\pm$ 0.006	15.35 $\pm$ 0.008	15.96 $\pm$ 0.010	0.92	2.92	5.10	22.39	22.90	24.18	23.59	22.86	23.38	L M
4542	143 $\pm$ 2	14.97 $\pm$ 0.005	14.52 $\pm$ 0.005	15.35 $\pm$ 0.008	0.84	4.78	6.73	22.29	22.75	23.43	22.63	22.70	22.88	S G
4626	103 $\pm$ 2	15.78 $\pm$ 0.009	15.36 $\pm$ 0.008	16.15 $\pm$ 0.014	0.79	3.25	3.75	23.55	23.67	25.29	24.04	23.60	24.15	L D
4797	73 $\pm$ 2	14.13 $\pm$ 0.003	13.69 $\pm$ 0.004	14.51 $\pm$ 0.006	0.77	2.93	3.32	23.13	23.48	24.64	23.51	23.44	23.77	S M
5284	185 $\pm$ 2	15.67 $\pm$ 0.007	15.24 $\pm$ 0.007	16.04 $\pm$ 0.011	0.66	3.65	5.17	22.16	22.65	23.63	22.98	22.64	22.97	S M
5633	167 $\pm$ 2	13.85 $\pm$ 0.004	13.43 $\pm$ 0.004	14.22 $\pm$ 0.006	0.54	2.91	3.52	22.29	22.67	23.73	22.89	22.71	23.00	S M
5716	122 $\pm$ 2	15.24 $\pm$ 0.005	15.06 $\pm$ 0.007	15.50 $\pm$ 0.008	0.79	1.35	1.90	22.57	22.93	24.10	23.47	22.81	23.33	L D
5758	121 $\pm$ 4	16.41 $\pm$ 0.010	16.12 $\pm$ 0.013	16.71 $\pm$ 0.016	0.54	2.16	2.48	22.67	22.99	24.09	23.36	22.99	23.36	L D
5781	166 $\pm$ 3	20.92 $\pm$ 0.061	20.61 $\pm$ 0.071	21.24 $\pm$ 0.095	0.44	2.52	0.43	27.27	27.64	30.99	26.79	27.66	28.27	L D
5889	46 $\pm$ 2	13.71 $\pm$ 0.002	13.26 $\pm$ 0.003	14.08 $\pm$ 0.004	0.89	1.06	1.49	22.44	22.83	23.51	22.96	22.82	23.03	S D
5999	68 $\pm$ 2	16.24 $\pm$ 0.009	15.97 $\pm$ 0.010	16.54 $\pm$ 0.015	0.67	4.56	4.10	24.09	24.47	26.60	25.72	24.35	25.28	L M
6122	75 $\pm$ 5	15.53 $\pm$ 0.007	15.15 $\pm$ 0.008	15.88 $\pm$ 0.011	0.94	4.80	7.73	22.44	22.94	24.08	23.18	22.92	23.28	S G
6130	219 $\pm$ 6	16.68 $\pm$ 0.011	16.16 $\pm$ 0.008	17.10 $\pm$ 0.018	0.92	7.68	4.28	24.01	24.51	25.05	24.89	24.23	24.67	S M
6248	26 $\pm$ 3	15.72 $\pm$ 0.009	15.27 $\pm$ 0.008	16.10 $\pm$ 0.014	0.84	1.25	1.73	23.37	23.67	25.56	22.96	23.58	23.94	L D
6287	62 $\pm$ 5	16.59 $\pm$ 0.010	16.29 $\pm$ 0.013	16.91 $\pm$ 0.016	0.59	4.91	5.76	23.10	23.39	24.98	24.38	23.26	24.00	L M
6486	113 $\pm$ 3	15.68 $\pm$ 0.007	15.30 $\pm$ 0.008	16.03 $\pm$ 0.011	0.93	2.71	4.15	22.86	23.15	24.63	23.88	23.13	23.70	S M
6599	118 $\pm$ 2	15.18 $\pm$ 0.005	14.83 $\pm$ 0.006	15.52 $\pm$ 0.008	0.41	2.28	2.69	22.48	22.89	23.95	23.41	22.76	23.25	S D
6647	207 $\pm$ 2	15.01 $\pm$ 0.005	14.53 $\pm$ 0.006	15.41 $\pm$ 0.008	0.82	5.47	7.20	22.10	22.68	23.40	22.83	22.63	22.89	S G
6669	65 $\pm$ 4	15.84 $\pm$ 0.007	15.68 $\pm$ 0.009	16.08 $\pm$ 0.011	0.31	2.26	1.72	23.86	24.05	26.91	26.18	24.05	25.30	L D
6717	61 $\pm$ 1	15.16 $\pm$ 0.006	14.82 $\pm$ 0.006	15.49 $\pm$ 0.010	0.79	4.22	4.96	23.37	23.70	25.34	24.35	23.67	24.26	S M
6807	140 $\pm$ 2	15.86 $\pm$ 0.006	15.61 $\pm$ 0.008	16.15 $\pm$ 0.010	0.87	2.42	4.04	22.43	22.88	24.21	23.84	22.87	23.45	L M
6980	36 $\pm$ 3	15.96 $\pm$ 0.007	15.85 $\pm$ 0.010	16.18 $\pm$ 0.011	0.48	2.98	3.39	22.56	22.86	24.26	23.95	22.80	23.47	L M
7003	127 $\pm$ 1	16.22 $\pm$ 0.010	15.82 $\pm$ 0.011	16.58 $\pm$ 0.016	0.46	1.65	1.77	23.19	23.52	25.14	24.13	23.49	24.07	L D
7038	90 $\pm$ 1	15.90 $\pm$ 0.007	15.56 $\pm$ 0.008	16.24 $\pm$ 0.011	0.61	0.82	0.86	23.53	23.80	26.11	24.92	23.78	24.65	L D
7138	145 $\pm$ 2	14.51 $\pm$ 0.004	14.12 $\pm$ 0.003	14.87 $\pm$ 0.006	0.64	2.75	3.57	22.11	22.56	23.13	22.82	22.54	22.76	S M
7149	131 $\pm$ 3	15.10 $\pm$ 0.005	14.63 $\pm$ 0.005	15.49 $\pm$ 0.008	0.71	1.83	2.40	22.19	22.61	23.22	22.46	22.54	22.71	S D
7150	44 $\pm$ 1	15.53 $\pm$ 0.007	15.35 $\pm$ 0.009	15.79 $\pm$ 0.011	0.58	1.15	1.28	22.71	23.05	24.12	23.49	22.96	23.41	L D

### 3. CLASSIFICATION OF THE LSBG SAMPLE

#### 3.1. Luminosity classification

The surface brightnesses of galaxies show a continuous distribution, so the traditional definition of an LSBG (Impey & Bothun 1997) based on a simple threshold in central surface brightness is in fact unphysical. This broad definition means that the existing LSBG catalogues must include LSBGs of different types. To date, three main types have been discovered in the LSBG regime. They are dwarf LSBGs (Sandage & Binggeli 1984; Impey, Bothun & Malin 1988), giant LSBGs (Bothun et al. 1987, 1990; Sprayberry et al. 1993), and we call the LSBGs with luminosities between dwarfs and giants the 'moderate-luminosity' LSBGs. Majority of existing LSBG catalogues include a large fraction of moderate-luminosity LSBGs, such as Impey et al. (1996); Zhong et al. (2008)

(1) dwarf LSBGs: Generally, galaxies with  $M_B > -17$  mag are considered as dwarf galaxies (Dunn (2010) and references therein), which can easily satisfy the definition for LSBGs. Among the dwarf LSBGs, a population of Ultra Diffuse Galaxy (UDG) (van Dokkum et al. 2015) is special because they have faint ( $\mu_g(0) > 24$  mag arcsec $^{-2}$ ) and very extended disks (effective radius,  $R_{eff} > 1.5$  kpc).

(2) giant LSBGs: They are bright ( $M_B > -19$  mag)(Sabatini et al. 2003), but their disk surface brightness are quite faint because their disks are very extended. For example, the disk of Malin-1, an extreme giant LSB galaxy, has extended to  $\sim 160$  kpc in diameter (Galaz et al. 2015; Boissier et al. 2016). Compared with the dwarf LSBGs, giant LSBGs are often redder in color.

(3) morderate-luminosity LSBGs: LSBGs with moderate luminosity ( $-19 < M_B < -17$  mag) are more similar to late-type spiral galaxies in appearance and general properties, except for the overall low surface brightness and surface density. Up to now, it is proposed that different types of LSBGs may have distinct formation and evolutionary histories from each other (Matthews et al. 2001).

In Figure 1(a), We classified the galaxies in our LSBG sample in terms of  $B$ -band absolute magnitude. Out of the total 1129 galaxies , 39 galaxies are giants ( $M_B \leq -19.0$  mag), 607 galaxies are dwarfs ( $M_B \geq -17.0$  mag), among which 28 galaxies are UDG candidates with  $\mu_g(0) > 24$  mag arcsec $^{-2}$  and  $R_{g,e} > 1.5$  kpc. and the rest 483 galaxies are moderate-luminosity LSBGs ( $-19.0 < M_B < -17.0$  mag) . Additionally, in  $B-V$  color, our sample is dominated by blue galaxies since it has 909 blue ( $B-V \leq 0.6$  mag) and 220 red galaxies ( $B - V > 0.6$  mag)(Figure 1(b)).

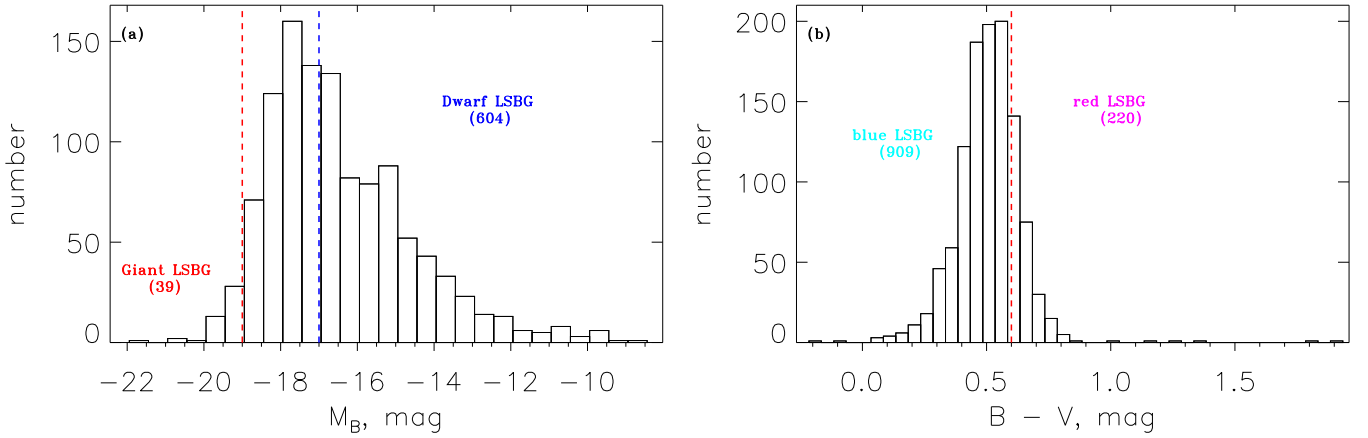


**Figure 1.** Histogram distributions. The  $B$ -band absolute magnitude (panel (a)) and and  $B-V$  color (panel (b)) distributions for the entire LSBG sample are shown. In panel (a), the red dashed line represents  $M_B = -19.0$  mag that distinguishes giants apart from other galaxies, and the blue dashed line represents  $M_B = -17.0$  mag that distinguishes dwarfs from other galaxies. Galaxies between the two lines ( $-19.0 < M_B < -17.0$ ) are considered as galaxies with moderate luminosities. In panel (b), the red dashed line of  $B-V = 0.6$  mag is used to divide LSBGs into blue and red.

### 3.2. Morphological Classification by Machine Learning

For a statistical information of the morphologies of our LSBG sample, we made morphological classification for our sample using Machine Learning Technique. Among various machine learning classifiers, we chose the classifier of decision trees with Random Forests which has been proved to have the highest accuracy for classification (Dobrycheva et al. 2017).

Above all, we should derive a training sample to train the classifier. There is a catalogue of 14,034 SDSS galaxies with detailed visual classifications (Nair & Abraham 2010), covering morphological types from T=-5 to 10 (E to Im) in de Vaucouleurs system. We randomly selected 80% of galaxies from this catalogue as the training sample and the rest 20% as the test sample.

First of all, the attributes of redshift ( $z$ ),  $g$ -band magnitude ( $g$ ) and absolute magnitude( $M_g$ ),  $r$ -band magnitude( $r$ ),  $g-r$  color, and the concentration index ( $R_{90}/R_{50}$ ) of galaxies in the training sample were adopted to train the Random Forests Classifier model. The trained Classifier was then fed into the test sample to predict the morphological types and test the accuracy. The accuracy of the trained classifier was 82.5% for the total test sample and 88.8% for E type (E, S0), 82.8% for S type (Sa, Sab, Sb, Sbc, Sc, Scd), 31.4% for L type (Sd, Sm, Im) and 12.8% for U type (unknown) of the test sample. Secondly, we adopted this trained Random Forests classifier to predict the morphological types (E, S, L, or U) of our LSBG sample. The results from the classifier show that out of the total 1129 galaxies in our sample, 950 galaxies (84.1%) are classified into L type, 151 galaxies (13.4%) are classified into S type, 2 galaxies (0.2%) are classified into E type and 26 galaxies (2.3%) are classified into U type, which indicates that our LSBG sample are dominating by the late-type galaxies in morphology. For a general review, the morphological classification results are listed in the column of  $T_M$  in Table 2.

Additionally, in Figure 2, we checked the fraction of galaxies of E, S and L types for our LSBGs of different luminosity types of giant, moderate-luminosity and dwarf LSBGs classified in § 3.1. For giant LSBGs (red), the morphological types of galaxies are dominated by earlier morphological types (S). For moderate-luminosity LSBGs (green), the morphological types of galaxies are composed of less S and more L types. For dwarf LSBGs (blue), the morphological types of galaxies are absolutely dominated by very late morphological type (L). Therefore, for our LSBG sample of different luminosity types from giant to dwarf, the dominance of morphological types have changed from earlier types (S) to later types (L). So the morphological classifications by Machine Learning technique agrees statistically with the luminosity classification for the three luminosity types of LSBGs in our sample.

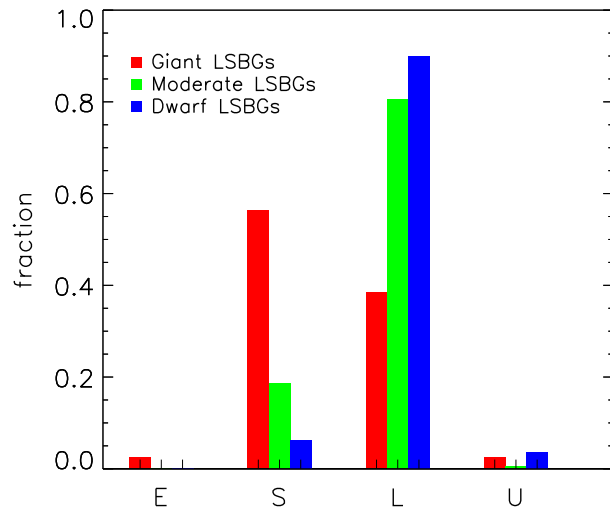


**Figure 2.** Distributions of different morphological types (E, S and L) for giant (red), moderate-luminosity (green) and dwarf (blue) LSBGs of our sample. E represents E and S0 types. S represents Sa, Sab, Sb, Sbc, Sc and Scd types. L represents Sd, Sm and Im types. U represents the unknown morphological type since the morphological type for those galaxies could not be successfully recognized from the Machine Learning technique.

#### 4. OPTICAL AND RADIO PROPERTIES

We show the optical and radio properties of the LSBG sample in Figure 3. In each panel, dwarf, moderate-luminosity and giant LSBGs in our sample are represented by the cyan, green and red circles. Additionally, we compare our LSBG sample with the 21 HSBGs (purple stars) which have optical band photometry from Ponomareva et al. (2017) and Ponomareva et al. (2017) and also with the available LSBGs from McGaugh & Bothun (1994)(open triangles), O’Neil et al. (2000) (open squares) and de Blok et al. (1995)(asterisks) in the figure.

We show the  $g$ - and  $r$ -band AUTO magnitude distributions for both our LSBG sample (black) and the HSBGs (purple) in panels (a) and (b). In order to show the distribution of the HSBGs clearly, the zoom-in windows are also plotted within each panel. The  $g$ -band magnitude of our LSBGs peaks at 17.57 mag and has an Gaussian FWHM of 2.05 mag in  $g$  band. The  $r$ -band magnitude of our LSBGs peaks at 17.26 mag and has an Gaussian FWHM of 2.17 mag in  $r$  band. Comparing with the HSBGs, our LSBGs are entirely much fainter.

In panels (c) and (d), both our LSBG sample and the HSBGs are shown in the size - central surface brightness plane. Comparing with our LSBGs, the HSBGs are systematically brighter in central surface brightness and larger in apparent size. As the Point Spread Function (PSF) widths of the SDSS  $g$ - and  $r$ -band images are statistically 1.0~2.0 ‐, galaxies with very small measured disk scale length (below  $h = 1.0''$  line) are better to be considered to be spurious. In order to show the distribution of LSBGs and the  $h = 1.0''$  line clearly, we over-plot the zoom-in windows within panels (c) and (d). Fortunately, no galaxies in our sample have measured disk scale lengths less than 1.0''. For the SDSS survey, Kniazev et al. (2004) found that the  $3\sigma$  limiting surface brightness goes down to  $\sim 26.4$  mag/arcsec $^2$  in  $g$  band and goes down to  $\sim 26.2$  mag/arcsec $^2$  in  $r$  band in a circular aperture of a radius of 12''. Therefore, we should have lower confidence in our measured  $\mu_0$  values for those galaxies which have measured  $\mu_{0,g}$  fainter than 26.4 mag/arcsec $^2$  or  $\mu_{0,r}$  fainter than 26.2 mag/arcsec $^2$  but the disk scale lengths are measured to be smaller than 12''. Furthermore, for those galaxies which are extended to have measured disk scale lengths larger than 12'', it is logically reasonable for them to have  $\mu_{0,g}$  fainter than 26.4 mag/arcsec $^2$  or  $\mu_{0,r}$  fainter than 26.2 mag/arcsec $^2$ . It mainly depends on the sizes of those galaxies that how faint their central surface brightness could reach? From the literature, Pohlen & Trujillo (2006) found that the  $3\sigma$  limiting surface brightness of the SDSS images could go down to  $\sim 27.0$  mag/arcsec $^2$  at a very large circular radius of 150'' in both  $g$  and  $r$  bands. Therefore, the central surface brightness are not expected to be measured fainter than  $\sim 27.0$  mag/arcsec $^2$  for our LSBGs which have disk scale length measured to be far less than 150''. So, for our LSBGs which have disk scale length measured to be larger than 12'' but smaller than 150'', the  $\mu_0$  measurements for these galaxies that are measured to be fainter than or around  $\sim 27.0$  mag/arcsec $^2$  might be unreliable. For a reminder, all of the 7 galaxies with such unreliable measurements of  $\mu_0$  were marked (as black filled circles) to the right of the  $3\sigma$  limiting line (red dashed lines) that was extracted by (Kniazev et al. 2004) for the SDSS imaging survey in Figure 3(c) and (d). For emphasis, they were still marked in the following panels. For further reminders, in Table 2, the AGC names of these 7 galaxies are labeled by adding a star symbol. It is necessary to note ahead of time that these 7 galaxies that have unreliable measurements of central surface brightness would be excluded in the Tully-Fisher relation studies later in § 5.

In panel (e), it shows that LSBGs and HSBGs almost cover the similar range in physical size. For the LSBG sample itself, it shows that LSBGs which have higher luminosities tends to be larger in physical size. Additionally, there are 24 dwarf LSBGs (over-plotted with black plus) which can be candidates of Ultra Diffuse Galaxies (UDGs) because they have  $\mu_0(g) > 24.0$  mag arcsec $^{-2}$  and effective radius  $R_{eff}(g) > 1.5$  kpc (van Dokkum et al. 2015).

In panels (f) and (g), HSBGs (purple stars) are at the bottom edge or below the LSBGs (circles), implying that LSBGs usually have larger physical size and have higher HI mass than the HSBGs with the same level of luminosity. For the LSBG sample itself, it shows that our LSBGs which have fainter luminosities tends to be lower in HI mass and smaller in size. This phenomenon for our LSBGs agrees with that for other LSBG samples from O’Neil et al. (2000) (black open squares) and McGaugh & Bothun (1994) (black open triangles). Comparatively, for our sample, giant LSBGs (red circles) have the highest HI masses and largest sizes, then the moderate-luminosity LSBGs (green open circles), and the dwarf LSBGs have the lowest HI masses and smallest sizes. It is worth noting that in panel (g), an outlier with disk scale length smaller than  $\sim 0.1$  kpc (the black dashed line which is a widely accepted lower size cutoff for a galaxy) deviates from most of the LSBGs in size. We checked this outlier (AGC 748778) and found that it is very nearby (radial velocity=258 km/s), has a very low HI mass ( $M(HI)=10^{6.36} M_\odot$ ) and a very narrow width of the HI line profile, and appears to be extremely faint, irregular and small in SDSS  $gri$  combined images. Such a galaxy image was not expected to be well fitted by an exponential profile model by using Galfit. So, the disk scale length measured for this outlier (AGC 748778) might be unreliable. However, it will not seriously affect the statistical trend of the sample

distribution in the disk scale length – luminosity plane. For a reminder, in Table 2, the AGC name, 748778 which might have unreliable measurements for disk scale length value is labeled by adding an asterisk symbol. Additionally, this galaxy would also be excluded in the Tully-Fisher relation fitting later in this paper.

In panel (h), The HSBGs are systematically brighter in both central surface brightness and luminosity than the LSBGs. By comparison, there are obviously no LSBGs with  $\mu_0(B) < 22.5$  mag arcsec $^{-2}$ . This is due to our selection threshold. It is interesting that in the  $\mu_0(B)$  –  $M(B)$  plane, there is a void at the lower left corner for our sample and another sample of [McGaugh & Bothun \(1994\)](#) (open triangles). This void space should have been populated by very low surface brightness, but intrinsically very luminous and large galaxies, which are in fact the giant LSBGs. This void might be either due to the low number density of giant LSBGs or that our sample actually lacks for LSBGs with bulges due to our selection method (see more in Section 6.1 or in [Du et al. \(2015\)](#)).

In panels (i)~(l), comparing with LSBGs, the HSBGs are systematically redder in color. For the LSBGs, while our sample has extended the parameter space covered by the previous samples towards lower luminosity and lower HI mass, the previous samples also cover parameter space that is not covered by our sample, specifically towards redder B-V color and higher HI mass-to-luminosity ratio. The main reason might be that our sample lacks for LSBGs with bulges which are generally redder than disk and dwarf galaxies due to the selection method (see more discussions in Section 6.1 or in [Du et al. \(2015\)](#)), although five LSBGs (over-plotted with open diamonds) in our sample appear to be very red ( $B-V > 1.0$  mag), low-luminosity ( $M(B) > -17.0$  mag) (panel (i)) and gas-rich ( $M_{HI}/L_B > 1.0$ ; panels (k) and (l)). In panel (l), a clear trend between absolute magnitude and gas-to-star ratio appears to exist for the entire LSBG sample, showing that fainter LSBGs would be larger in gas-to-star ratio, however, it shows no color–absolute magnitude relation (panel (i)), color–gas content correlation (panel (j)) nor color–gas-to-star relation (panel (k)).

## 5. TULLY-FISHER RELATION

The Tully-Fisher relation (TFr) has been well defined between the luminosity and the maximal rotational velocity for late-type spiral galaxies (with high surface brightness) ([Tully & Fisher 1977](#)).

There are two main methods to measure the maximal rotational velocities,  $V_{max}$ , of spiral galaxies. Firstly,  $V_{max}$  could be measured from the width of the global HI line profile, as the observed width of the HI line profile, in km/s, gives the observed Doppler broadening due principally to the galaxy's rotation. In the literature, the width of the HI line profile at 50% of peak flux,  $W_{50}$ , has been greatly used as a good measure of the  $V_{max}$  of a galaxy to, study the TFr of spiral galaxies in the absolute magnitude -  $W_{50}$  plane ([Zwaan et al. 1995](#); [O'Neil et al. 2000](#); [Chung et al. 2002](#)). Secondly,  $V_{max}$  could be measured from the high-quality rotation curves which can be derived from spatially-resolved HI velocity maps of galaxies. It is clearly demonstrated in [Ponomareva et al. \(2017\)](#) that the shape of the global HI line profile may hint at the shape of the rotation curve of a galaxy in several cases. Generally, the global HI line profile can be observationally obtained much faster than the high-quality HI velocity map for a galaxy, so the first method which use the line width to measure the maximal rotation velocity of a spiral galaxy is feasible for large samples of galaxies. A detailed comparisons in Figure 6 in [Ponomareva et al. \(2017\)](#) demonstrated that the rotational velocity measured from  $W_{50}$  will be underestimated in comparison with  $V_{max}$  derived from the high-quality rotation curve for those dwarf galaxies which mostly have slowly rising rotation curves or for those massive spiral galaxies which mostly have declining rotation curves. However, for those galaxies which have the classical double peak (2-horn) profiles, the rotational velocity measured from  $W_{50}$  are generally consistent with  $V_{max}$  derived from the rotation curves. Because the 2-horn line profile gives an indication that the rotation curve of a galaxy will reach its flat part. In view of this, our entire sample which is composed of a variety of galaxy types from dwarf to giant in luminosity and from disk-like to irregular in morphology, corresponding to various rotation curves, should be carefully refined in terms of HI line profile for better studying TFr.

In order to make sure that the  $W_{50}$  is a good measure of  $V_{max}$  of the galaxy, first of all, with the examples of good 2-horn HI profiles given in [Courtois et al. \(2009\)](#) as standards, we manually inspected the HI line profile for every LSBG of our entire sample and selected those galaxies which have 2-horn HI line profiles. For example, we show the 2-horn HI line profiles of several of our LSBGs to give an idea of our identification for the 2-horn profiles in Figure ???. These example LSBGs were chosen to have their signal-to-noise (SNR) of HI detection ranging from high to low. Secondly, we are recommended by the  $\alpha.40$  release paper ([Haynes et al. 2011](#)) to have those galaxies with the signal-to-noise ratio (SNR) of the HI line less than 6.5 excluded. Because it is claimed in [Haynes et al. \(2011\)](#) that the detection of HI with SNR>6.5 by ALFALFA is a real detection. Thirdly, large uncertainties might be inherent in inclination correction for  $W_{50}$  for less inclined galaxies (nearly face-on, with large minor-to-major axis ratio,  $b/a$ ).

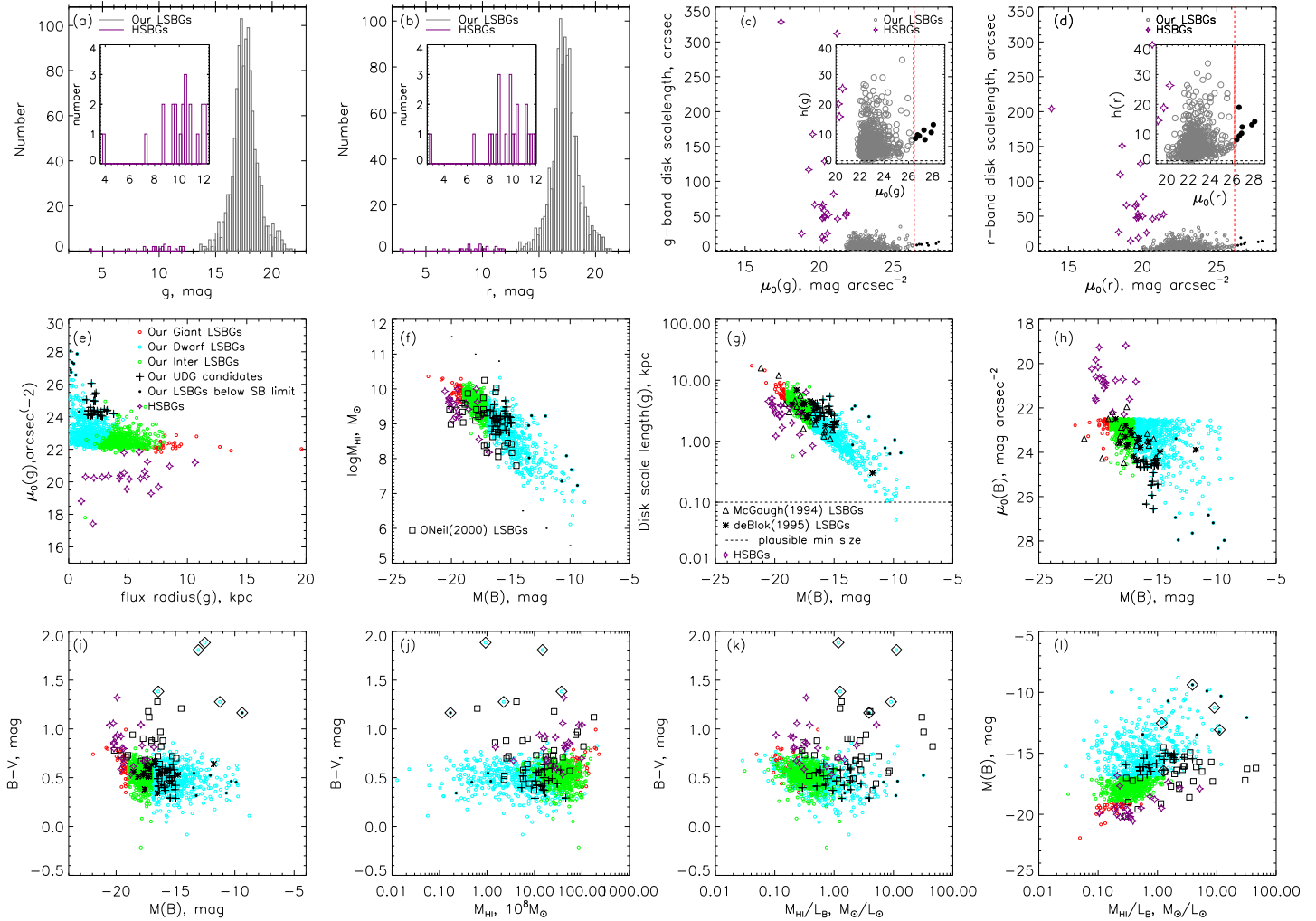


**Figure 3.** Optical and radio properties of our LSBG sample (open circles), compared with HSBGs (purple stars) from Ponomareva et al. (2017) and Ponomareva et al. (2017) and other available LSBGs from O’Neil et al. (2000) (open squares), McGaugh & Bothun (1994) (open triangles) and de Blok et al. (1995) (asterisks). In all panels, the cyan, red and green open circles represent dwarf, giant and moderate-luminosity LSBGs in our sample. The overlaid black filled circles mark the 7 galaxies in our sample for which we have low confidence in their measurements of central surface brightness. The over-plotted black plus symbols represent candidates of Ultra Diffuse Galaxies in our LSBG sample. In panels (a) and (b), the magnitudes which were measured by using SExtractor AUTO aperture in  $g$  and  $r$  bands for our entire LSBG sample are shown. In panels (c) and (d), the red dashed lines represent the  $3\sigma$  surface brightness limitings of  $g \sim 26.4$  mag/arcsec $^2$  and  $r \sim 26.2$  mag/arcsec $^2$  (within circular apertures of radii of  $12''$ ) for the SDSS imaging survey. The black dashed lines represent the half of the maximum PSF width for the SDSS images. Within these 4 panels, the zoom-in plots are shown to show the details of data distribution in small subregions. In panel (e), the flux radius versus the  $g$ -band central surface brightness of our entire LSBG sample are shown. In panel (f), the  $B$ -band absolute magnitude versus HI mass are shown. In panel (g),  $B$ -band absolute magnitude versus the optical disk scale length are shown and the black dashed line is a widely accepted lower size cutoff for a galaxy. In panel (h), the  $B$ -band absolute magnitude versus central surface brightness are shown. In panels (i)~(l), our LSBGs which have very red color ( $B-V > 1.0$  mag) but are low in luminosity ( $M(B) > -17.0$  mag) and gas-rich ( $M_{HI}/L_B > 1.0$ ) are over-marked by open diamonds.

This problem could be largely mitigated for largely inclined galaxies (nearly edge-on, with small  $b/a$ ), in particular for edge-on galaxies, so we decided to further have those less inclined galaxies ( $g$ -band  $b/a \leq 0.6$ ) excluded. This step is only to mitigate the large uncertainties inherent in inclination correction for  $W_{50}$  of less inclined galaxies.

After the above criteria of HI-line profile shape, the SNR of HI line and the b/a, a subsample of 175 LSBGs were selected from our entire sample. This subsample is appropriate for the TFr studies because the key point is that, for this subsample galaxies, the  $W_{50}$  of the HI line can accurately measure the maximal rotational velocities. To make the results more reliable, we removed the galaxies which are members of the 7 galaxies that were mentioned in Section 4 to have unreliable measurements of central surface brightness and also removed the galaxy AGC 748778 that was also mentioned in Section 4 to have very small disk scale length measurements from this subsample. After such removal, our final subsample for TFr studies contains 173 LSBGs. We list these 173 LSBGs in Table ?? which includes the AGC name, inclination angle,  $i$ , calculated following Equation (3), corrected  $W_{50}$  calculated by Equation (2), distance from the released entire ALFALFA catalogue, and the  $B$ -band absolute magnitude which has been corrected for Galactic and internal extinction following Equation (4), the NIR-band absolute magnitudes which have been corrected only for Galactic extinction. For those galaxies with no UKIDSS observations, we just leave their corrected  $J$ -,  $H$ - and  $K$ -band absolute magnitudes blank in Table ??.

Although this subsample is only 15% of the entire sample in size, it includes all of the galaxies in the entire sample that are better suitable for TFr studies because the maximum rotation velocity of these galaxies could be properly measured by the width of the HI line and these galaxies also suffered less from the uncertainties induced by the inclination correction for the HI line width.

**Table 2.** A subset of the catalogue of our LSBG sample from the  $\alpha.40$ –SDSS DR7.

AGC	i	$W_{50,cor}$	Dist	$B_{cor}$	$J_{cor}$	$H_{cor}$	$K_{cor}$
	(deg)	(km/s)	(Mpc)	(mag)	mag	(mag)	(mag)
273	59.4	$182.4 \pm 12.78$	$78.9 \pm 2.30$	$-18.84 \pm 0.07$	—	—	—
5633	58.8	$195.3 \pm 2.34$	$22.5 \pm 4.20$	$-18.68 \pm 0.41$	—	—	—
5758	59.2	$140.9 \pm 4.66$	$45.4 \pm 4.20$	$-17.53 \pm 0.202$	$-17.02 \pm 0.227$	$-17.41 \pm 0.207$	$-17.19 \pm 0.215$
6287	55.4	$75.3 \pm 6.07$	$93.9 \pm 2.40$	$-18.88 \pm 0.06$	—	—	—
6599	68.1	$127.2 \pm 2.16$	$26.2 \pm 2.30$	$-17.78 \pm 0.19$	—	—	—
6669	76.0	$67.0 \pm 4.12$	$16.1 \pm 2.10$	$-16.05 \pm 0.285$	$-15.59 \pm 0.299$	$-15.57 \pm 0.295$	$-15.41 \pm 0.301$
7003	64.4	$140.8 \pm 1.11$	$25.5 \pm 4.20$	$-16.66 \pm 0.358$	$-16.32 \pm 0.373$	$-16.46 \pm 0.365$	$-16.43 \pm 0.366$
7737	70.9	$109.0 \pm 1.06$	$16.7 \pm 1.20$	$-16.94 \pm 0.158$	$-16.15 \pm 0.163$	$-16.27 \pm 0.160$	$-15.72 \pm 0.165$
8030	67.7	$57.3 \pm 2.16$	$7.8 \pm 2.30$	$-14.67 \pm 0.64$	—	—	—
8055	62.8	$100.0 \pm 2.25$	$16.6 \pm 4.30$	$-15.97 \pm 0.563$	$-15.74 \pm 0.568$	$-15.46 \pm 0.566$	$-15.79 \pm 0.567$
8276	62.2	$76.8 \pm 2.26$	$16.9 \pm 2.20$	$-15.61 \pm 0.283$	$-15.28 \pm 0.302$	$-15.26 \pm 0.292$	$-15.17 \pm 0.296$
8762	59.4	$176.7 \pm 3.49$	$51.7 \pm 2.20$	$-19.27 \pm 0.094$	$-18.00 \pm 0.148$	$-18.76 \pm 0.100$	$-18.43 \pm 0.113$
8915	63.8	$176.1 \pm 2.23$	$37.3 \pm 2.30$	$-17.75 \pm 0.135$	$-17.36 \pm 0.151$	$-17.46 \pm 0.137$	$-17.22 \pm 0.148$
9002	67.9	$103.6 \pm 4.32$	$60.8 \pm 2.30$	$-19.80 \pm 0.084$	$-18.90 \pm 0.099$	$-19.24 \pm 0.086$	$-18.87 \pm 0.089$
9063	76.1	$181.3 \pm 3.09$	$87.9 \pm 4.20$	$-19.98 \pm 0.107$	$-18.91 \pm 0.127$	$-19.16 \pm 0.111$	$-18.71 \pm 0.121$
9380	66.0	$104.0 \pm 2.19$	$27.8 \pm 4.40$	$-17.95 \pm 0.344$	$-17.23 \pm 0.351$	$-17.33 \pm 0.347$	$-16.99 \pm 0.351$
10009	71.7	$130.6 \pm 4.21$	$32.8 \pm 2.40$	$-17.55 \pm 0.161$	$-16.58 \pm 0.201$	$-17.04 \pm 0.163$	$-17.12 \pm 0.166$
100350	61.1	$122.2 \pm 14.84$	$64.2 \pm 4.30$	$-17.05 \pm 0.15$	—	—	—
101812	69.7	$99.1 \pm 3.20$	$27.0 \pm 2.30$	$-15.06 \pm 0.19$	—	—	—
101877	66.4	$201.9 \pm 4.36$	$72.9 \pm 2.50$	$-18.28 \pm 0.078$	$-18.01 \pm 0.169$	$-18.18 \pm 0.116$	$-18.31 \pm 0.117$
101942	55.2	$92.6 \pm 9.75$	$79.7 \pm 2.30$	$-17.27 \pm 0.070$	$-17.89 \pm 0.129$	$-17.45 \pm 0.147$	$-16.14 \pm 0.491$
102229	60.6	$94.1 \pm 9.18$	$45.9 \pm 2.20$	$-16.34 \pm 0.11$	—	—	—
102729	67.1	$57.5 \pm 6.51$	$65.4 \pm 2.10$	$-16.24 \pm 0.08$	—	—	—
102900	61.2	$151.8 \pm 4.57$	$168.6 \pm 2.20$	$-17.42 \pm 0.05$	—	—	—
110398	62.2	$198.9 \pm 7.91$	$92.3 \pm 2.30$	$-19.55 \pm 0.057$	$-19.35 \pm 0.090$	$-19.33 \pm 0.069$	$-18.94 \pm 0.090$
113200	56.9	$120.5 \pm 47.74$	$102.3 \pm 2.20$	$-17.78 \pm 0.057$	$-17.51 \pm 0.320$	$-17.62 \pm 0.200$	$-17.01 \pm 0.352$
113752	57.0	$108.6 \pm 8.35$	$173.3 \pm 2.30$	$-17.89 \pm 0.05$	—	—	—
113825	73.6	$111.5 \pm 9.38$	$52.4 \pm 2.40$	$-16.34 \pm 0.11$	—	—	—
121174	63.3	$88.4 \pm 3.36$	$9.7 \pm 2.30$	$-12.76 \pm 0.52$	—	—	—
122218	72.1	$103.0 \pm 2.10$	$35.9 \pm 2.30$	$-15.94 \pm 0.14$	—	—	—
122341	60.8	$195.9 \pm 4.58$	$156.8 \pm 2.30$	$-19.47 \pm 0.041$	$-18.74 \pm 0.130$	$-19.43 \pm 0.053$	$-19.14 \pm 0.068$
122874	62.0	$152.8 \pm 11.32$	$87.8 \pm 2.30$	$-17.76 \pm 0.06$	—	—	—
122877	56.2	$97.5 \pm 6.02$	$85.0 \pm 2.30$	$-18.08 \pm 0.06$	—	—	—
123047	60.1	$70.4 \pm 9.23$	$142.7 \pm 2.40$	$-17.97 \pm 0.06$	—	—	—

Table 2 continued on next page

**Table 2** (*continued*)

AGC	i	$W50_{cor}$	Dist	$B_{cor}$	$J_{cor}$	$H_{cor}$	$K_{cor}$
	(deg)	(km/s)	(Mpc)	(mag)	mag	(mag)	(mag)
123172	69.0	171.4± 3.21	74.5±2.30	-18.43±0.07	—	—	—
171585	61.0	144.0± 9.15	69.1±2.50	-17.86±0.081	-17.60±0.105	-17.76±0.097	-17.71±0.103
174601	65.7	189.9± 3.29	72.7±2.10	-19.09±0.07	—	—	—
181471	73.5	94.9± 5.21	30.3±2.40	-16.44±0.17	—	—	—
181571	70.0	73.4± 3.19	62.3±2.30	-18.08±0.084	-17.27±0.155	-17.56±0.106	-17.11±0.148
181762	61.8	240.6±24.97	192.3±2.40	-20.60±0.033	-20.44±0.074	-20.77±0.043	-20.34±0.054
182466	58.6	93.8± 2.34	29.6±2.30	-14.73±0.17	—	—	—
182467	59.8	39.3± 9.25	59.6±2.10	-15.19±0.09	—	—	—
182477	55.3	102.2± 3.65	62.2±2.20	-16.05±0.09	—	—	—
182608	69.6	116.3± 4.27	67.9±2.30	-17.44±0.080	-16.86±0.164	-17.32±0.128	-16.69±0.232
182924	64.5	247.0± 7.75	167.7±2.60	-19.05±0.044	-19.14±0.165	-19.13±0.187	-19.57±0.123
183068	66.6	179.8± 7.63	183.4±2.40	-20.11±0.036	-19.86±0.091	-20.39±0.071	-19.96±0.108
183138	57.4	151.9±13.05	171.2±2.20	-20.03±0.033	-19.89±0.070	-20.18±0.069	-20.09±0.082
183691	61.5	172.9±13.65	124.8±2.30	-18.89±0.046	-18.62±0.122	-19.02±0.100	-18.91±0.102
184304	70.1	175.4± 7.44	78.1±2.30	-17.56±0.072	-16.97±0.166	-17.50±0.123	-16.86±0.182
191817	65.6	136.2± 2.20	40.6±2.30	-17.07±0.125	-16.77±0.145	-16.59±0.141	-16.36±0.154
191906	71.0	125.8± 3.17	48.6±2.10	-16.60±0.099	-15.94±0.262	-16.19±0.176	-15.90±0.181
191989	56.6	130.6± 5.99	48.9±2.20	-17.64±0.10	—	—	—
192118	61.5	182.0± 3.41	83.1±2.30	-18.16±0.064	-17.75±0.131	-17.74±0.093	-17.41±0.113
192165	57.9	131.0± 7.08	123.2±2.30	-19.23±0.045	-19.35±0.067	-19.50±0.070	-19.31±0.067
193781	58.9	177.4± 4.67	121.5±2.30	-18.14±0.05	—	—	—
193802	70.4	45.6± 3.18	23.5±2.30	-13.55±0.216	-14.28±0.303	-13.98±0.291	-13.78±0.322
193862	68.4	180.7± 8.60	56.6±2.20	-17.19±0.09	—	—	—
193905	62.5	92.4± 7.89	115.6±2.40	-17.82±0.06	—	—	—
194002	63.7	85.9± 3.35	38.1±2.20	-16.34±0.13	—	—	—
198454	68.5	48.4± 6.45	22.0±2.20	-13.40±0.22	—	—	—
198456	69.9	60.7± 6.39	29.5±2.20	-14.58±0.167	-13.79±0.295	-14.16±0.195	-14.01±0.228
202040	64.0	106.8± 4.45	17.5±3.30	-14.63±0.410	-14.58±0.437	-14.77±0.420	-14.12±0.449
202257	68.7	54.7± 2.15	10.4±4.30	-14.77±0.898	-14.43±0.904	-14.62±0.902	-14.60±0.902
202704	61.0	101.7± 8.00	99.2±2.40	-18.49±0.057	-17.96±0.176	-18.30±0.086	-18.02±0.109
203515	54.9	227.4± 7.33	100.7±2.20	-18.44±0.05	—	—	—
203667	56.7	86.1± 8.37	56.6±2.30	-16.98±0.091	-16.89±0.288	-16.76±0.155	-16.01±0.312
204112	71.5	95.9±23.19	185.7±2.20	-20.10±0.037	-19.62±0.082	-19.79±0.056	-19.84±0.064
205062	67.1	58.6± 6.51	99.2±2.40	-16.16±0.08	—	—	—
205205	69.3	110.1± 6.41	43.7±2.30	-15.91±0.121	-15.37±0.245	-15.52±0.154	-14.98±0.271
205216	55.9	48.3± 3.62	47.5±2.30	-15.31±0.111	-15.51±0.243	-14.85±0.293	-13.80±0.816

Table 2 continued on next page

**Table 2** (*continued*)

AGC	i	$W50_{cor}$	Dist	$B_{cor}$	$J_{cor}$	$H_{cor}$	$K_{cor}$
		(deg)	(km/s)	(Mpc)	(mag)	mag	(mag)
205336	56.5	92.3±14.39	158.7±2.40	-15.28±0.123	-16.86±0.379	-16.40±0.447	-16.60±0.362
206787	60.6	308.9± 5.74	163.9±2.20	-20.58±0.03	—	—	—
208385	59.6	131.1± 2.32	55.1±2.40	-17.19±0.10	—	—	—
214098	59.9	164.2± 3.47	96.8±2.30	-18.60±0.056	-18.21±0.141	-18.33±0.140	-18.79±0.101
215197	62.1	113.2± 7.92	50.5±2.10	-16.68±0.094	-16.47±0.174	-16.46±0.134	-16.10±0.169
215213	76.1	70.0± 1.03	9.0±2.30	-13.61±0.556	-13.25±0.567	-13.02±0.564	-13.03±0.564
215222	59.1	179.4± 9.32	97.3±2.30	-18.53±0.056	-18.18±0.119	-18.61±0.075	-17.97±0.111
215256	71.7	110.6±11.58	21.0±2.30	-16.49±0.24	—	—	—
215262	66.0	68.9± 6.57	17.5±3.60	-14.29±0.45	—	—	—
215265	64.0	139.0± 7.79	140.3±2.20	-18.58±0.045	-18.76±0.119	-18.60±0.102	-18.44±0.144
215280	73.4	97.1± 4.17	17.5±3.70	-14.05±0.46	—	—	—
215283	59.9	126.0± 3.47	90.9±2.30	-16.48±0.07	—	—	—
215630	55.1	137.8± 6.10	90.5±2.30	-17.79±0.060	-17.74±0.123	-17.17±0.157	-17.15±0.168
215716	74.8	103.6±13.47	38.3±2.40	-16.62±0.139	-15.90±0.189	-15.91±0.166	-15.89±0.182
219206	68.5	148.4± 4.30	97.6±2.30	-17.34±0.067	-16.07±0.389	-16.27±0.336	-16.83±0.228
219232	54.9	58.6±12.22	146.8±2.10	-16.53±0.077	-16.57±0.423	-16.59±0.201	-15.86±0.522
220005	54.8	91.7± 0.00	104.0±2.30	-17.73±0.06	—	—	—
220299	70.8	98.5± 4.24	63.4±2.10	-17.27±0.078	-16.49±0.362	-17.41±0.170	-17.05±0.171
220351	67.3	78.1± 3.25	16.7±1.20	-15.84±0.157	-15.24±0.169	-15.11±0.162	-14.97±0.167
220580	76.1	118.5±18.54	61.8±2.30	-18.23±0.086	-17.48±0.133	-17.75±0.098	-17.60±0.115
220762	66.4	96.1± 3.27	16.6±4.30	-15.81±0.563	-15.31±0.570	-15.34±0.565	-15.07±0.570
220939	63.4	76.0± 3.35	16.5±1.20	-15.35±0.159	-14.97±0.186	-15.10±0.164	-14.63±0.194
221085	63.3	99.6± 1.12	16.6±2.40	-15.16±0.315	-15.01±0.341	-14.74±0.332	-14.89±0.331
223279	75.6	124.9± 5.16	89.1±2.30	-17.86±0.066	-17.64±0.168	-17.44±0.115	-17.64±0.127
223295	71.6	159.2±16.87	106.8±2.30	-17.65±0.06	—	—	—
223392	63.6	92.7± 6.70	24.2±4.20	-15.39±0.378	-15.70±0.402	-15.33±0.385	-15.17±0.389
224075	67.0	151.0±23.89	97.5±2.30	-18.11±0.059	-17.94±0.188	-17.85±0.142	-17.91±0.144
224094	55.8	128.2± 6.05	30.1±2.30	-15.97±0.167	-16.16±0.200	-15.61±0.210	-15.75±0.205
225297	67.9	136.0± 6.48	78.9±2.10	-17.66±0.065	-18.21±0.140	-17.68±0.134	-17.30±0.189
225849	61.0	98.3± 5.72	16.3±2.30	-14.81±0.307	-14.43±0.324	-14.03±0.349	-13.76±0.425
225876	59.3	45.4±10.47	16.6±4.30	-12.41±0.565	-11.49±1.060	-11.44±0.783	-12.03±0.680
225992	64.6	160.5±12.18	90.9±2.20	-17.08±0.063	-16.86±0.243	-16.89±0.125	-16.56±0.219
228097	59.6	78.9± 8.12	88.6±2.20	-17.70±0.060	-17.86±0.155	-18.06±0.099	-17.55±0.154
232871	56.8	215.2± 8.37	112.7±2.30	-17.97±0.052	-18.04±0.173	-17.61±0.137	-17.68±0.163
232879	56.2	178.2±14.45	88.6±2.30	-18.60±0.060	-18.38±0.136	-18.59±0.081	-18.42±0.103
233571	56.6	131.8± 2.40	22.9±2.20	-16.15±0.21	—	—	—

Table 2 continued on next page

**Table 2** (*continued*)

AGC	i	$W50_{cor}$	Dist	$B_{cor}$	$J_{cor}$	$H_{cor}$	$K_{cor}$
		(deg)	(km/s)	(Mpc)	(mag)	mag	(mag)
233601	56.1	120.4± 3.61	22.3±2.30	-15.18±0.225	-15.13±0.257	-15.30±0.243	-14.56±0.281
233615	66.9	101.1± 7.61	52.1±2.20	-15.79±0.100	-15.44±0.174	-15.65±0.179	-15.65±0.186
233635	75.6	165.2± 4.13	104.9±2.30	-18.49±0.06	—	—	—
233638	56.5	74.4± 7.20	112.3±2.30	-18.03±0.05	—	—	—
233683	57.1	79.8± 3.58	96.8±2.10	-18.04±0.053	-17.72±0.108	-17.86±0.078	-17.84±0.087
233711	66.3	126.7± 4.37	83.5±2.30	-17.60±0.066	-17.04±0.186	-17.32±0.126	-17.09±0.143
238689	63.4	116.4± 8.95	57.6±2.30	-16.86±0.091	-16.68±0.195	-16.33±0.214	-15.84±0.358
238751	58.9	126.1±10.51	96.6±2.20	-18.13±0.056	-17.99±0.166	-18.16±0.103	-17.48±0.202
241275	60.8	110.0±11.46	34.2±2.10	-16.65±0.135	-16.55±0.168	-16.56±0.156	-16.16±0.167
242042	69.9	132.1± 2.13	33.0±2.30	-16.78±0.15	—	—	—
242246	63.3	113.1±10.08	61.5±2.30	-17.11±0.086	-16.50±0.177	-16.17±0.155	-16.65±0.125
242248	61.8	74.9± 3.41	102.9±4.30	-19.23±0.09	—	—	—
242284	68.1	142.3± 2.16	96.9±2.30	-18.56±0.057	-17.95±0.155	-18.10±0.068	-18.10±0.091
242296	63.4	120.8± 3.35	64.3±2.30	-18.52±0.080	-18.31±0.135	-18.36±0.103	-18.07±0.128
248896	58.0	86.1± 9.43	83.2±2.30	-16.84±0.069	-16.87±0.189	-16.78±0.144	-16.77±0.152
248914	56.1	110.8± 8.43	62.2±2.30	-18.33±0.082	-17.86±0.121	-18.04±0.087	-17.87±0.102
248970	58.3	161.1± 8.23	133.6±2.20	-18.81±0.04	—	—	—
249100	61.5	190.1± 3.41	165.1±2.30	-19.98±0.036	-19.90±0.077	-19.68±0.071	-19.61±0.072
249304	61.3	115.2± 6.84	103.0±2.30	-17.91±0.056	-16.99±0.285	-18.24±0.079	-16.55±0.340
252891	60.0	93.5±12.70	31.0±2.30	-16.79±0.16	—	—	—
257954	70.7	117.6± 7.42	76.7±2.30	-16.28±0.08	—	—	—
258263	65.9	107.3± 5.48	157.5±2.30	-17.40±0.056	-17.62±0.393	-17.89±0.199	-17.49±0.319
258268	63.5	78.2± 8.94	156.4±2.20	-18.48±0.045	-18.28±0.245	-18.28±0.181	-18.13±0.269
258407	69.1	271.9± 5.35	150.5±2.30	-19.21±0.044	-18.95±0.117	-18.81±0.086	-18.76±0.100
263839	63.0	190.8± 7.86	139.4±2.30	-19.86±0.041	-19.50±0.106	-19.07±0.168	-19.11±0.142
267948	60.7	104.4± 9.17	74.8±2.30	-19.00±0.07	—	—	—
267968	61.3	115.1± 6.84	150.7±2.20	-18.76±0.04	—	—	—
268028	71.1	199.8± 5.29	104.3±2.30	-18.89±0.05	—	—	—
268107	66.4	201.9±62.22	191.0±2.30	-20.39±0.03	—	—	—
268151	56.2	121.6± 3.61	76.5±2.20	-18.00±0.07	—	—	—
268199	71.7	196.9± 6.32	70.4±2.20	-18.54±0.07	—	—	—
320466	66.0	116.0± 2.19	43.3±2.30	-16.94±0.12	—	—	—
321385	62.0	84.9± 9.06	102.2±4.40	-17.98±0.10	—	—	—
321490	71.3	167.8±22.17	95.0±2.20	-18.10±0.06	—	—	—
332328	58.1	87.2± 7.07	68.1±2.10	-16.47±0.07	—	—	—
332861	65.7	149.2±21.95	107.5±2.20	-18.78±0.051	-18.40±0.128	-18.81±0.078	-18.52±0.096

Table 2 continued on next page

**Table 2** (*continued*)

AGC	i	$W50_{cor}$	Dist	$B_{cor}$	$J_{cor}$	$H_{cor}$	$K_{cor}$
		(deg)	(km/s)	(Mpc)	(mag)	mag	(mag)
333224	73.9	167.6± 5.21	105.4±2.30	-18.38±0.06	—	—	—
714453	68.5	248.2± 5.37	151.6±2.30	-20.85±0.04	—	—	—
716496	73.7	121.9± 4.17	28.6±2.30	-15.89±0.18	—	—	—
727027	59.0	192.4±18.66	195.3±2.20	-20.16±0.03	—	—	—
731695	55.6	121.2± 6.06	102.9±2.30	-18.50±0.05	—	—	—
731805	72.2	121.8± 6.30	54.4±2.50	-17.06±0.10	—	—	—
732178	56.9	185.0± 4.77	96.1±2.30	-17.94±0.06	—	—	—
732274	54.8	138.3± 8.57	75.1±2.30	-18.73±0.068	-18.08±0.130	-17.78±0.115	-17.82±0.117
732488	54.9	180.9±29.33	97.9±2.30	-18.40±0.055	-18.48±0.117	-18.75±0.076	-17.83±0.160
732593	67.1	146.6± 2.17	42.9±2.40	-16.88±0.124	-16.31±0.207	-16.77±0.140	-16.52±0.154
732937	60.0	170.9± 8.08	71.4±2.20	-17.79±0.07	—	—	—
733774	56.8	163.8±10.76	151.4±2.20	-19.42±0.04	—	—	—
748757	76.7	136.7± 2.06	56.1±2.40	-17.60±0.10	—	—	—
748786	67.5	161.3± 5.41	77.7±2.20	-17.49±0.070	-17.00±0.281	-17.29±0.163	-16.17±0.459
748819	74.5	55.0± 2.08	35.0±2.20	-15.28±0.141	-16.55±0.185	-15.88±0.186	-14.09±0.844
749209	69.0	155.3±25.71	103.4±2.20	-17.90±0.06	—	—	—
749230	76.5	130.6±10.28	60.4±2.30	-16.87±0.09	—	—	—
749264	58.3	170.3± 7.05	103.4±2.30	-18.29±0.053	-18.31±0.086	-18.46±0.104	-18.27±0.107
749287	71.5	157.1± 7.38	98.0±2.10	-17.77±0.06	—	—	—
749324	62.6	63.1± 5.63	24.7±2.20	-15.37±0.19	—	—	—
749362	60.3	201.4± 9.21	130.0±2.40	-18.63±0.047	-18.21±0.157	-18.80±0.107	-17.97±0.189
749363	61.5	117.2± 5.69	85.0±2.30	-17.99±0.063	-17.91±0.116	-18.13±0.101	-18.02±0.124
749368	63.6	56.9± 3.35	64.6±2.30	-15.98±0.09	—	—	—
749380	76.2	144.2± 4.12	86.0±2.40	-17.74±0.069	-17.29±0.114	-17.54±0.135	-17.08±0.174
749383	56.7	116.0± 7.18	135.4±2.30	-18.05±0.048	-17.95±0.171	-17.88±0.279	-17.97±0.264
749405	72.5	154.1±10.48	56.7±2.20	-16.75±0.09	—	—	—
749423	60.5	121.8±13.79	95.3±2.10	-18.34±0.05	—	—	—
749438	55.8	128.2± 8.46	53.4±2.30	-16.07±0.10	—	—	—
749452	59.5	92.9± 8.12	40.8±2.40	-15.32±0.13	—	—	—
749464	74.9	133.6±10.36	95.8±2.30	-17.44±0.068	-15.37±1.447	-16.51±0.407	-16.67±0.321
749475	62.0	132.5± 9.06	179.5±2.20	-18.35±0.05	—	—	—

To investigate the TFr, the W50 of the HI line should be first of all corrected for inclination effect. For the subsample galaxies, we have the minor-to-major axis ratios, b/a (q in Table 2), which were estimated by us fitting the *g*-band galaxy images with a single exponential profile model. As galaxies in this subsample are visually round, the b/a ratios derived from a single exponential model fitting for this subsample galaxies are more appropriate.

Using the b/a ratios (q), we corrected the width of the HI line width, W50, for inclination effect via Equation (2) below. The inclination angle,  $i$ , could be calculated using the formula proposed by [Hubble \(1926\)](#) which is also listed as Equation (3) below in this paper. The intrinsic axis ratio,  $q_0$ , in Equation (3) was set to be 0.2 ([Masters et al. 2008](#)) to mitigate the effect of the bulge on the most edge-on galaxies.

$$W50_{cor} = W50 / \sin(i) \quad (2)$$

$$\cos(i)^2 = \frac{q^2 - q_0^2}{1 - q_0^2} \quad (3)$$

Additionally, the W50 has already been corrected for instrumental broadening by the ALFALFA team ([Haynes et al. 2011](#)). Although the TFr was originally discovered in the optical bands, it was later proved to be even tighter in the near-infrared (NIR) bands (see more in Section 1). Therefore, we would study the TFrs in the optical *B*, *g* and *r* bands and the NIR *J*, *H* and *K* bands for the LSBG subsample.

### 5.1. Optical TFr

In this subsection, we study the optical *B*-, *g*- and *r*-band TFrs for the LSBG subsample. First of all, we converted the *B*-band magnitudes (measured by ourselves in [Du et al. \(2015\)](#) and listed in Table 2) to absolute magnitudes,  $M_B$ , for the subsample galaxies. The distances used for conversion are directly from the newly released ALFALFA Extragalactic HI source catalogue ([Haynes et al. 2018](#)). Compared with the  $\alpha.40$  catalog ([Haynes et al. 2011](#)), the newly released ALFALFA catalog has provided uncertainties on distance. So, the errors on *B*-band absolute magnitude were propagated from the errors on *B*-band magnitude and the distance (provided by the ALFALFA catalogue), based on the error transfer formula of mathematical statistics. In order to compare the TFr of our LSBGs with the TFrs of other available LSBG samples, such as the LSBG sample of [Zwaan et al. \(1995\)](#), in *B* band, we adopted the same prescription as was used in [Zwaan et al. \(1995\)](#) to correct the  $M_B$  for Galactic and internal extinction to face-on orientation. This prescription (Equation (4) below) for extinction correction was proposed by [Tully & Fouque \(1985\)](#).

$$M(B)_{corr} = M_B + 2.5 \log[f(1 + e^{-\tau sec(i)}) + (1 - 2f)(\frac{1 - e^{-\tau sec(i)}}{\tau sec(i)})] \quad (4)$$

where  $\tau$  is the optical depth, and  $f$  is the fraction of the light that is unobscured by the dust layer.  $\tau \sim 0.55$  and  $f \sim 0.25$  were adopted in most publications ([Tully & Fouque 1985; Zwaan et al. 1995](#)).

In Figure 4 (a), we plot our LSBG subsample (black dots) in the plane of corrected HI line width v.s. corrected absolute magnitude (TF plane) in *B* band. The linear regression line (black solid line) of the TFr and the corresponding 95% confidence bands (black dashed hyperbolae) of the regression line are over-plotted. The function we used for regressing the TFr line is the MPFITEXY function in IDL. This function takes into account errors in both axes and performs an inverse least squares regression which can resolve the Malmquist bias ([Willick 1994](#)) that affects the slope of the TFr. Furthermore, in order to estimate the confidence intervals for the coefficients of the regression lines, we performed pair bootstrap resampling for 1000 times. Quantitatively, the vertical scatter and the tightness of the TFr fit are also measured following the method of [Ponomareva et al. \(2017\)](#). The coefficients, confidence intervals, scatter and tightness of the TFr fit are also quantitatively listed in Table 3.

For comparison with the TFr of the LSBG sample of [Zwaan et al. \(1995\)](#), we over-plotted the *B*-band TFr line which is followed by the LSBG sample of [Zwaan et al. \(1995\)](#) as the red line in Figure 4(a). Apparently in Figure 4(a), the slope of the TFr line (black solid line) for our LSBG subsample seem to be well consistent with the slope of the TFr line (red solid line) for the LSBG sample of [Zwaan et al. \(1995\)](#). Importantly, this blue TFr line was in [Zwaan et al. \(1995\)](#) to be well consistent with the TFr of the High Surface Brightness Galaxies (HSBGs) compiled by [Broeils \(1992\)](#). Therefore, we could indirectly deduce that the slope of the TFr line for our LSBG subsample is also in good agreement with the slope of the TFr line for HSBGs, albeit our LSBG sample has a larger scatter than the HSBGs ( $\sigma=1.14$  mag v.s. 0.77 mag) in *B* band.

Besides, Ponomareva et al. (2017) has reported TFr for 32 large and relatively nearby galaxies which are generally HSBGs in  $g$  and  $r$  bands. So we also expect to compare the TFr of our LSBG subsample with the TFr of the HSBGs from Ponomareva et al. (2017) in  $g$  and  $r$  bands. We made the Galactic and internal extinction correction for the absolute magnitudes in  $g$  and  $r$  bands for the LSBG subsample, using the same prescription as was used by Ponomareva et al. (2017). According to Ponomareva et al. (2017), the Galactic extinction correction was obtained using the “Galactic dust reddening and extinction” tool provided by the NASA/IPAC infrared science archive which estimates the Galactic dust extinction from Schlafly & Finkbeiner (2011). For  $g$ -band magnitude, the internal extinction correction,  $A_g^i$ , was assumed to be 0.6 mag which is an average internal extinction of spiral galaxies from face-on to edge-on. For  $r$ -band magnitude, the internal extinction correction,  $A_r^i$ , can be expressed as:

$$A_r^i = \gamma_r \log(a/b) \quad (5)$$

$$\gamma_r = 1.15 + 1.88(\log W_{50}^i - 2.5) \quad (6)$$

where  $a/b$  is the major-to-minor axis ratio of the galaxy and  $\gamma_r$  is an extinction amplitude parameter which was calibrated by Tully et al. (1998) as a function of the width of the HI line profile corrected for inclination. After correcting the Galactic and internal extinction for the absolute magnitude in  $g$  and  $r$  bands using the prescription described above which was used in Ponomareva et al. (2017), we plot our LSBG subsample (black filled circles) and the regression TFr lines (black solid lines fitted by MPFITEXY function in IDL) in  $g$ - and  $r$ -band TFr planes in Figures 4 (b) and (c). The confidence bands of the fit were shown as black dashed hyperbolae. For comparison, the  $g$ - and  $r$ -band TFr lines for the Ponomareva et al. (2017) sample (HSBGs) were also over-plotted as blue lines in Figures 4 (b) and (c). The coefficients, confidence intervals, scatter and tightness of the TFr fit in  $g$  and  $r$  bands are also listed in Table 3. Within the uncertainties of the value of the TFr slope (listed in Table 3), the TFr slopes for our LSBG subsample are generally in agreement with the TFr slopes for the HSBGs from Ponomareva et al. (2017) in  $g$  and  $r$  bands, although the scatter ( $\sigma \sim 1.17$  mag) and tightness ( $\sim 0.17$  mag) of the TFr fit for our LSBGs is not so good as the scatter ( $\sigma=0.27$ ) and tightness (0.068 mag) of the TFr fit for the HSBGs from Ponomareva et al. (2017).

Conclusively, in the optical  $B$ ,  $g$  and  $r$  bands, the TFr lines for our LSBG subsample agree with the TFr lines for HSBGs in slope. This result is consistent with the previous optical TFr results for LSBGs from Zwaan et al. (1995) and Sprayberry, Bernstein & Impey (1995), which confirmed that the LSBGs follow the same TFr as the normal spiral galaxies (HSBGs) in the optical bands. However, compared with the HSBGs in Figure 4, our LSBGs have relatively larger scatter and are less tight around our TFr lines, which might be due to the variations in mass-to-light ratio among our LSBGs.

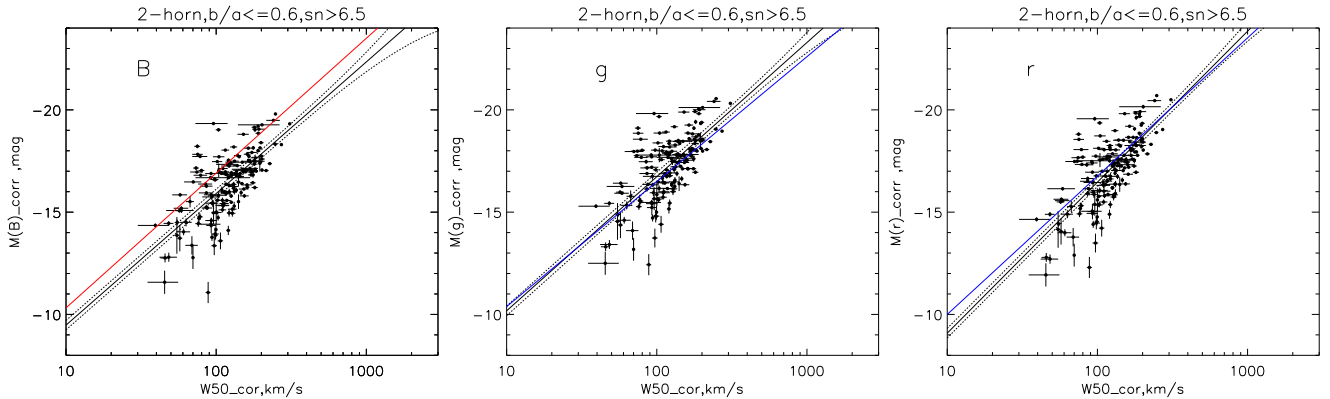


**Figure 4.** Tully-Fisher diagrams in  $B$ (left),  $g$ (middle) and  $r$ (right) bands for our LSBG subsample. We show the linear fit (black solid line) and the corresponding 95% confidence bands (black dashed hyperbolae) of the fit for the LSBG subsample. The error bars along both coordinates for each of our data points are shown. The TFr line followed by the Broeil sample of HSB spiral galaxies and also followed by a small sample of LSBGs from Zwaan et al. (1995) is overlaid as the red line in Figure 4(a). Besides, the  $g$ - and  $r$ -band TFr lines which are followed by a sample of 32 large and relatively nearby galaxies from Ponomareva et al. (2017) are also over-plotted as blue lines in Figures 4(b) and (c).

### 5.2. NIR TFr

In the subsample of 173 LSBGs which are appropriate for studying TFr, 99 galaxies have been observed in  $J$ ,  $H$  and  $K$  bands by the Large Area Survey (LAS) of UKIRT Infrared Deep Sky Survey (UKIDSS). In this subsection, we investigate the TFr for these 99 LSBGs in  $J$ ,  $H$  and  $K$  bands.

First of all, we subtracted the sky background for NIR band images of galaxies in  $J$ ,  $H$  and  $K$  bands, using the same method as described in Zheng et al. (1999), Wu et al. (2002) and Du et al. (2015). Then, the magnitudes were measured on the sky-subtracted images within the AUTO aperture by SExtractor. The measured magnitudes were then corrected for Galactic extinction using the prescription of Schlafly & Finkbeiner (2011). The internal extinction of LSBGs is very difficult to estimate. Tully et al. (1998) found that the internal extinction was unmeasurably small for faint galaxies with  $M_B \geq 17$  mag which is the case for most of the galaxies in our LSBG subsample (see Figure 4(a)). Most LSBGs are thought to be poor in dust based on the statistically inferred low internal extinction (e.g., Tully et al. (1998); Masters et al. (2008)). Therefore, we did not make any internal extinction correction for the NIR-band magnitudes of our LSBG subsample so as to avoid large uncertainties that might be introduced in the magnitudes due to internal correction. The details on data reduction including sky subtraction and surface photometry in the NIR bands will be reported in our forthcoming paper which will be on spectral energy distributions (SED) of our entire LSBG sample. Then, the NIR-band magnitudes were converted to absolute magnitude by using the distance from the ALFALFA catalogue.

Based on the corrected W50 of HI and the absolute magnitudes without internal extinction correction, we show these 99 LSBGs (black dots) in the TFr planes in  $J$ ,  $H$  and  $K$  bands, respectively, and the corresponding regression TFr lines (black solid lines; by the MPFITEXY function in IDL) in Figure 5. The coefficients, confidence bands, scatter and tightness of the regression lines (black lines in Figure 5) for  $J$ ,  $H$  and  $K$  bands were tabulated in the middle three lines in Table 3. For comparison, we overplotted the TFr lines of the three NIR bands for the HSBGs of Ponomareva et al. (2017) as the blue solid lines in Figure 5.

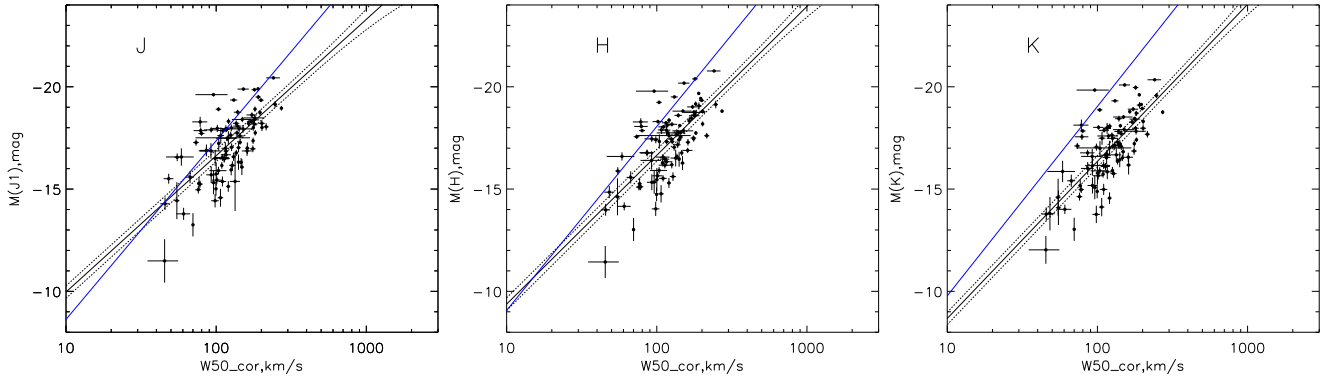


**Figure 5.** Tully-Fisher relation diagrams in the NIR  $J$  (left),  $H$  (middle) and  $K$  (right) bands for the LSBG subsample (black dots), based on magnitudes without internal extinction correction. We show the regression TFr lines (black solid lines) and the corresponding 95% confidence bands (black dashed hyperbolic curves) of the black regression lines for the LSBG subsample in each band. The error bars along both coordinates for our data points are also shown. For a comparison, the TFr lines which are followed by the sample of 32 large and relatively nearby galaxies from Ponomareva et al. (2017) in 2MASS  $J$ - ,  $H$ - and  $K$ s bands are also overplotted as blue lines.

Compared with optical bands, the slopes of the NIR-band TFr lines (black solid lines) for our LSBG subsample do not appear to be well consistent with the slopes of the NIR-band TFr lines (blue solid lines) for the HSBGs of Ponomareva et al. (2017). In each panel of Figure 5, the offset in magnitude between the two TFr lines for LSBGs (black solid line) and HSBGs (blue solid line) increases with the line width. We think this might be caused by the effect of internal extinction correction for magnitudes. As LSBGs are well known to have little internal extinction, especially in the NIR bands, we did not do any internal extinction correction for magnitudes in  $J$ ,  $H$  and  $K$  bands for our LSBGs to avoid large uncertainties that might be introduced into the magnitudes. However, the internal

extinction is a significant effect on magnitudes for HSBGs, so Ponomareva et al. (2017) corrected the magnitudes in  $J$ ,  $H$  and  $K$  bands for internal extinction for their HSBGs. The prescription they used for correcting internal extinction was from Tully et al. (1998) and Sorce et al. (2012) (Ponomareva et al. 2017), which calibrated the internal extinction value as an increasing function of the width of the HI line. This may account for the increasing magnitude offset between the TFr lines of our LSBGs (black solid lines in Figure 5) and the HSBGs (blue solid lines in Figure 5) from Ponomareva et al. (2017) with increasing line width. To check the effect of the internal extinction correction, we attempted to correct the internal extinction for  $J$ -,  $H$ - and  $K$ -band absolute magnitudes for our LSBG subsample, using the same prescription as was used by Ponomareva et al. (2017) and detailedly listed in Ponomareva et al. (2017). Based on the corrected absolute magnitudes, we further studied the NIR-band TFr regressions (black solid lines) in Figure 6. The coefficients of the new TFr lines based on the corrected magnitudes in  $J$ ,  $H$  and  $K$  bands are tabulated in the last three lines in Table 3. In order to better compare the NIR TFr lines based on magnitudes before and after internal extinction correction, the TFr lines which was previously regressed before the internal extinction correction for NIR-band magnitudes were overplotted as the green lines in Figure 6 which are exactly the black solid lines in Figure 5. By comparison, no big difference was found between the TFr lines regressed before and after correcting the internal extinction for the magnitudes in  $J$ ,  $H$  and  $K$  bands, suggesting that the internal extinction correction is not an important factor which caused the difference between the TFr lines of LSBGs and HSBGs. This result further strengthens that the dust internal extinction is very little for LSBGs.

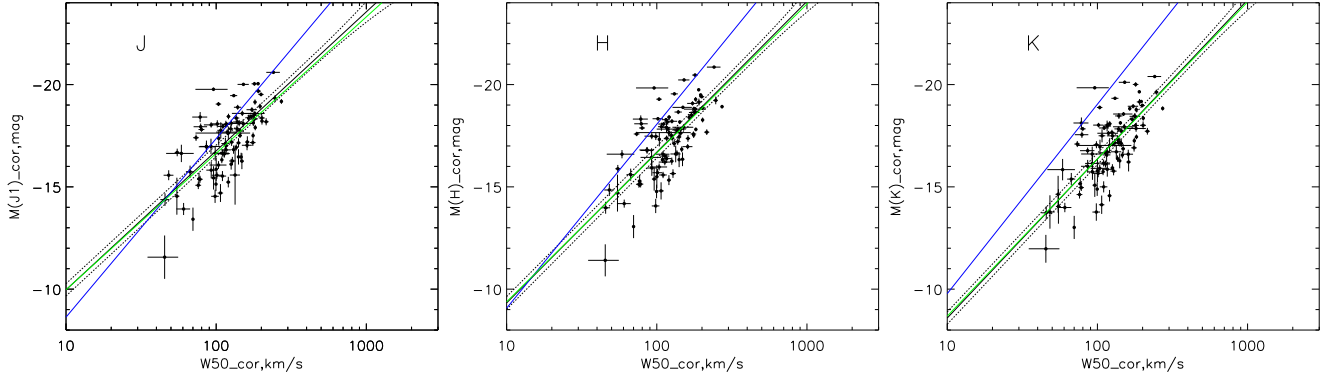


**Figure 6.** Tully-Fisher diagrams in the NIR  $J$  (left),  $H$  (middle) and  $K$  (right) bands for the LSBG subsample (black dots), based on the magnitudes corrected for internal extinction. The error bars along both coordinates for the data points are shown. The black solid lines are the linear regression lines (by the MPFITEXY function in IDL) based on the corrected magnitudes and the black dashed hyperbolic curves show the corresponding 95% confidence bands of the black regression lines. The blue solid lines represent the TFr lines for the Ponomareva et al. (2017) sample which is composed of 32 large and relatively nearby galaxies in  $J$ - ,  $H$ - and  $K$ s bands based on the 2MASS data. For comparison, the TFr lines which was previously regressed based on the magnitudes without internal extinction were also overplotted as the green lines (Note: The green lines are exactly the black solid lines in Figure 5).

Then, we have to find other possible reasons which might cause the difference between the TFr lines of our LSBGs and the HSBGs from Ponomareva et al. (2017). Compared with the bright disk of HSBGs, the outer disk of LSBGs are fainter and thus more difficult to be detected in NIR bands than HSBGs. Generally, the surface brightness profiles of LSBGs are systematically 3.5 mag fainter than normal HSBGs in  $J$  band (Galaz et al. 2002). Therefore, with the shallow surface brightness limiting of UKIDSS, the disk of the extended LSBG could only be detected out to a small radius in NIR bands, compared to the outmost edge of the optical disk. However, for HSBGs in ?, even although their NIR-band magnitudes are measured on 2MASS images which are even shallower than UKIDSS, the HSBG disks can still be detected out to a larger radius close to the outmost edge of the optical disk. So this would cause more serious underestimation of the total disk luminosity for LSBGs than for HSBGs in NIR bands, which can then cause the magnitude offset between the TFr lines for LSBGs and HSBGs. This might be one possible reason for the difference between the TFr lines of LSBGs and HSBGs in NIR bands, and more possible reasons needs to be explored in the further work.

**Table 3.** Regression coefficients for our LSBG sample in Tully-Fisher diagram in optical  $B$ ,  $g$ ,  $r$ , NIR  $J$ ,  $H$ , and  $K$  bands, and for different luminosity types and morphological types in  $B$  band.

Band	k	b	95% CI for k	95% CI for b	scatter	tightness
$B$	-6.43 $\pm$ 0.51	-3.04 $\pm$ 1.07	[-7.48, -5.41]	[-5.26, -0.77]	1.14	0.18
$g$	-6.56 $\pm$ 0.53	-3.62 $\pm$ 1.11	[-7.55, -5.55]	[-5.82, -1.47]	1.18	0.18
$r$	-7.38 $\pm$ 0.54	-1.70 $\pm$ 1.12	[-8.45, -6.35]	[-3.88, 0.61]	1.17	0.16
$J$	-6.67 $\pm$ 0.72	-3.30 $\pm$ 1.50	[-8.12, -5.18]	[-6.55, -0.17]	1.17	0.17
$H$	-7.28 $\pm$ 0.74	-2.10 $\pm$ 1.55	[-8.71, -5.76]	[-5.34, 0.93]	1.19	0.16
$K$	-7.68 $\pm$ 0.74	-1.00 $\pm$ 1.55	[-9.08, -6.35]	[-4.05, 2.01]	1.16	0.15
$J$	-6.79 $\pm$ 0.71	-3.17 $\pm$ 1.49	[-8.29, -5.25]	[-6.56, 0.11]	1.17	0.17
$H$	-7.37 $\pm$ 0.74	-1.96 $\pm$ 1.55	[-8.65, -5.83]	[-5.20, 0.80]	1.19	0.16
$K$	-7.77 $\pm$ 0.74	-0.81 $\pm$ 1.55	[-9.03, -6.41]	[-3.69, 1.84]	1.16	0.15

NOTE—The regression line can be expressed as  $y=kb+b$ , where  $x$  represents  $W50_{corr}$  in logarithm,  $y$  represents absolute magnitude in  $B$ ,  $g$ ,  $r$ ,  $J$ ,  $H$ , or  $K$  bands,  $k$  is the slope, and  $b$  is the intercept. CI represents Confidence Interval.

## 6. DISCUSSION

### 6.1. Strength and weakness of our LSBG sample

As for strength, firstly, we need the redshift information to correct the cosmological dimming of the central surface brightnesses of galaxies. However, SDSS has spectroscopic redshifts only for those galaxies which are brighter than 17.77 mag in  $r$  band and called the Main Galaxy Sample of the SDSS survey. As most of LSBGs are fainter in optical band, it means that a large fraction of true LSBGs could not be defined by only using the optical survey of SDSS due to the lack of accurate redshifts from spectroscopy. For example, as shown in Figure 3 (b), 31% of galaxies in our LSBG sample are fainter than 17.77 mag in  $r$  band. So if we were selecting our LSBG sample only on the basis of the optical SDSS survey, those 31% faint LSBGs would have been lost from our final sample. However, our LSBG sample is an HI-selected sample the radial velocities of which, especially the faint LSBGs, are all available from the  $\alpha.40$  HI catalogue. So our HI-selected LSBG sample does not limited by the magnitude of the SDSS Main Galaxy Sample. Instead, it includes more faint LSBGs (31% fainter than  $r=17.77$  mag) which could reach down to the surface brightness depth of the SDSS photometric survey but could not be confirmed by only using the SDSS data due to lack of the spectroscopic redshift.

Secondly, LSBG selections are very sensitive to the subtraction of sky background of images. However, as explained detailedly in Section 3.1 in Du et al. (2015), the SDSS photometric pipeline has a high risk of considering the large extended outskirts of the objects as part of the sky background , and thus overestimated the sky background of galaxies which further leads to the underestimation of the luminosity of galaxies. The underestimation in luminosity is  $\sim 0.2$  mag for bright galaxies with extend outskirts and is up to  $\sim 0.5$  mag for LSBGs. Therefore, we reconstructed the sky background map for all galaxy images, using a more precise method which were described and testified in detail in Section 3.1 in Du et al. (2015). Thus, we corrected the underestimation of luminosity for galaxies in our LSBG sample.

As for the weakness, on one hand, our LSBG sample was selected basing on the central disk surface brightness which was derived by fitting the galaxy image with a single exponential profile model with Galfit. So for galaxies which have light concentration or bulges in the centers, the central disk surface brightnesses of the disk must have been overestimated (bias to brighter values). However, we made some tests in Du et al. (2015) by fitting the LSBGs with two components (Sersic+Exponential) and found that the overestimation for the disk central surface brightness were systematically very small and less than 0.2 mag/arcsec $^2$ . Additionally, the part of bulge-dominated galaxies (only 5.8%) is not dominant in our LSBG sample. In the case of overestimation, the true central disk surface brightnesses for those galaxies should be even fainter than currently, so these galaxies currently in our LSBG sample should still be members of the LSBG sample. However, it is poor in bulge-dominated LSB galaxies due to our fitting method

of only using a single exponential profile precluding the detection of LSBGs with bulges. But this fitting method is fast and valid for the fast majority of the LSBGs. On the other hand, as selected from the HI survey, our LSBG sample is composed of more gas-rich galaxies, but should have been deficient in the true gas-poor LSBGs. If there was no such effects explained above, our LSBG sample would on one hand include more galaxies with large central light concentration or bulges. These galaxies would have large rotational velocities and bright luminosities so that our LSBG sample would be enlarged and stretched to the ends of larger W50 and brighter absolute magnitude in the TF plane in Section 5. On the other hand, our LSBG sample would have more gas-poor galaxies which would be more likely to enlarge or stretch our sample to the end of smaller W50 and lower absolute magnitude in the TF plane in Section 5. With those possibly-added LSBGs in the TF plane, the TFr fit in Section 5 would probably be better constrained.

### 6.2. Mass-to-light ratios

Theoretically for a spiral galaxy, the mass  $M$  is proportional to  $V_{max}^2 h$  and the total luminosity  $L$  is proportional to  $\Sigma_0 h$ , where  $V_{max}$  is the maximal rotational velocity,  $h$  is the disk scale length and  $\Sigma_0$  is the central surface brightness. From these two relations, a simple relation between the luminosity ( $L$ ), the maximal rotational velocity ( $V_{max}$ ), central surface brightness ( $\Sigma_0$ ), and mass-to-light ratio ( $M/L$ ) follows that

$$L \propto \frac{V_{max}^4}{\Sigma_0(M/L)^2} \quad (7)$$

The slope  $\alpha$  of the TFr in the form of  $L \propto V_{max}^\alpha$  generally changes with the observed band and gradually increases from  $\alpha \sim 2.5$  in the optical  $B$  band to  $\alpha \sim 4$  in the NIR  $K$  band (e.g. [Aaronsen & Mould. (1983); Giovanelli et al. (1997); Courteau et al. (2007)]). In Equation (7),  $L \propto V_{max}^4$  is recognized as the universal TFr.

As we concluded in Section 5 that our LSBG subsample follows a normal TFr that is followed by the normal HSBGs, we could attempt to explore the clues for the total mass-to-light ratio  $M/L$  of these LSBGs by statistically comparing with the  $M/L$  of the Broeil's HSBGs below, following the comparison method of Zwaan et al. (1995). In Figure 4 (a), the  $B$ -band slope of TFr (black solid line) for our LSBG subsample is  $-6.43 \pm 0.51$  (Table 3), which is in good agreement with the  $B$ -band slope of TFr (red line) for the HSB spiral galaxy sample of Broeils (1992) (hereafter Broeils spiral sample), which is found to be  $-6.59$ . The intercept of the black line and red line are, respectively,  $-3.04 \pm 1.07$  (Table 3) and  $-3.73 \pm 0.77$  for the Broeils spiral sample (O'Neil et al. 2000). So albeit the consistent slope, there is a systematical offset of  $\sim 0.7$  mag in absolute magnitude between the two TFr lines. This means that our LSBGs are systematically  $\sim 0.7$  mag fainter than the Broeils HSBGs in  $B$  band magnitude, which can be expressed as  $M_{LSBG} - M_{HSBG} = 0.7$  mag. As  $L_{LSBG}/L_{HSBG} = 10.0^{-0.4 \times (M_{LSBG} - M_{HSBG})}$ , the luminosity of our LSBGs is then systematically  $\sim 0.5$  times ( $= 10.0^{-0.4 \times 0.7}$ ) the luminosity of the Broeils HSBG sample in  $B$  band at a fixed HI line width. As for central surface brightness, the mean  $B$ -band central surface brightness is  $23.1$  mag arcsec $^{-2}$  for our LSBG subsample and  $21.6$  mag arcsec $^{-2}$  for the Broeils HSBGs, so our LSBG subsample is  $1.5$  mag fainter than, or  $1/4$  ( $= 10^{-0.4 \times 1.5}$ ) times, the typical central surface brightness value of the Broeils HSBGs. Therefore, according to Equation (7), in order to account for the factors of differences in  $\Sigma_0$  and  $L$  at the fixed line velocity, it can be deduced that  $M/L$  of our LSBGs must be  $\sim 2.8$  times of the  $M/L$  of Broeils HSB spiral galaxy sample.

However, although the NIR  $K$ -band slope of  $\sim 4$  ( $L \propto V_{max}^4$ ) is recognized as the universal TFr (The slope  $k$  is corresponding to  $\sim 10$  when the luminosity is expressed in absolute magnitudes,  $M$ , and the TFr is in the form of  $M = -k \log(V_{max}) + b$ ). it should be noticed that the derivation of the TFr has been questioned by recent papers (e.g. Courteau et al. (2007); Ponomareva et al. (2017)), which obtained shallower slopes ( $\alpha \leq 4$ ) in agreement with their own data in NIR  $K$  band. For our LSBG subsample, we also obtained a shallower TFr. So, insisting on using the theoretical Equation (7) which reflects a universal TFr ( $L \propto V_{max}^4$ ), we might have overestimated the luminosity,  $L$ , of our LSBG subsample and thus overestimated the luminosity ratios between our LSBG subsample and the Broeils HSBG sample at a fixed rotational velocity, and finally underestimated the  $M/L$  of our LSBG subsample. So the ratio between the total  $M/L$  of our LSBG subsample and the Broeils HSBG sample should be larger than  $\sim 2.8$  that was deduced above based on a universal TFr of the slope of 4.

### 6.3. Disk scale lengths

Since  $M/L \propto V_{max}^2 h/L$ , where  $h$  is the disk scale length,  $M/L$  depends on  $h/L$  at a fixed line width. In § 6.2, using Equation (7), we derived that the  $M/L$  of our LSBG subsample was 2.8 times the  $M/L$  of the Broeils HSB spiral

galaxy sample, and  $L$  (luminosity) of our LSBG subsample was 0.5 times the luminosity of the Broeils HSB spiral galaxy sample at a fixed line width. So, the disk scale length of our LSBG subsample should be 1.4 times of the disk scale length of the Broeils HSB spiral galaxy sample.

In Figure 7, we plot the disk scale length versus the corrected HI line width for our LSBG subsample in  $g$  band. For comparison, HSBGs of the Broeils sample are over-plotted in Figure 7. It is worth noting that the disk scale length for HSBGs of the Broeils sample in Figure 7 are in  $B$  band because only the  $B$ -band the disk scale lengths are available for Broeils sample. This would not seriously affect the results about disk scale length later since galaxy size in the  $B$ -band image appears very similar to that in  $g$  band.

Apparently in Figure 7, a trend exists between disk scale length and line width for both the LSBGs and the HSBGs. To make the trend as clear as possible, we made a linear regression between line width and disk scale length for both the LSBG subsample (black solid line) and the Broeils's HSBG sample (red dashed line). It obviously appears that our LSBG subsample is systematically larger than the HSBG sample in disk scale length. Observationally, a minor difference between the slopes (1.05 for LSBGs v.s. 0.81 for Broeils's HSBGs) of both lines is present, and the offset between the two fitting lines is 0.24 dex at  $W_{50} \sim 40$  km/s (the minimal corrected  $W_{50}$  for our LSBG subsample) and 0.45 dex at  $W_{50} \sim 300$  km/s (the maximal corrected  $W_{50}$  for our LSBG subsample). The offsets implies that our LSBGs have disk scale lengths that are  $1.75 (=10^{0.24})$  times larger than the HSBGs of Broeils sample at the minimal corrected  $W_{50}$  and  $2.82 (=10^{0.45})$  times larger than the HSBGs of Broeils sample at the maximal corrected  $W_{50}$ . Therefore, our LSBGs are  $1.75 \sim 2.54$  times larger in size than the HSBGs from the Broeils sample at the fixed line width. This factor range from observation is slightly higher than the factor of 1.4 deduced from the M/L above using Equation (7). This discrepancy might be because that our LSBG subsample observationally follows a shallower TFr so that the M/L of our LSBGs has been underestimated by Equation (7) which is based on a universal TFr.

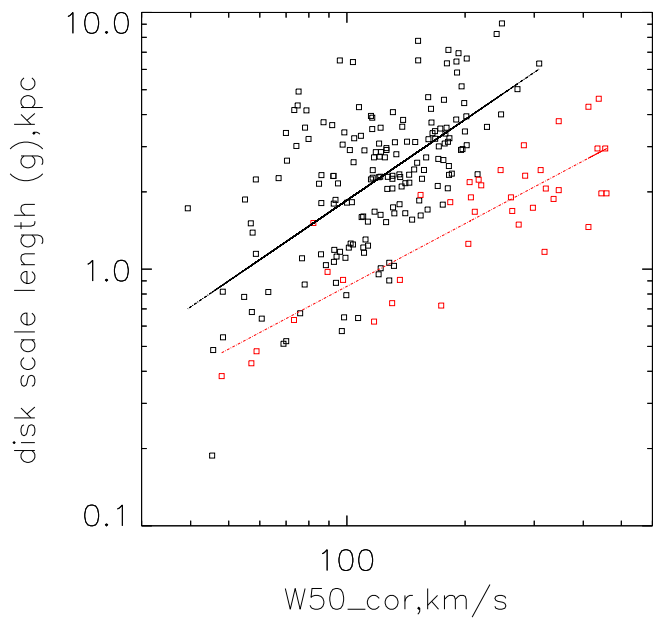


**Figure 7.** Corrected HI line width vs. disk scale length. Black open squares are LSBGs of our subsample and the black line is the linear regression for our LSBG subsample. Red open squares are spiral galaxies from the Broeils sample used in ? and the red line is the linear regression for Broeils sample.

#### 6.4. Mass surface density

From a universal TFr, it follows that  $L \propto V_{max}^4$  and  $V_{max}^4 \propto M^2/h^2$ . So, we can derive that  $L \propto M^2/h^2$  or that

$$\frac{M}{L} \propto \frac{h^2}{M} = \frac{1}{\bar{\sigma}} \quad (8)$$

where  $h$  is the disk scale length and  $\bar{\sigma}$  is the average mass surface density. This relation declares that galaxies with similar mass surface densities have similar  $M/L$  while galaxies with higher  $M/L$  have lower  $\bar{\sigma}$ . As derived in § 6.2, for LSBGs of our subsample, the  $M/L$  is 2.8 times the  $M/L$  of spiral galaxies of the Broeils sample, so the  $\bar{\sigma}$  for the subsample of our LSBGs is  $\sim 1/2.8 \simeq 0.4$  times the mass surface density of the spiral galaxies of the Broeils sample. As discussed in Section 6.2, the  $M/L$  might have been underestimated for our LSBGs by a universal TFr of slope  $\sim 4$ , so the  $\bar{\sigma}$  might have been overestimated here for our LSBG subsample. Any way, this result proves that LSBGs have lower mass surface densities than the HSBGs (the Broeils spiral sample) with the same rotational velocity.

## 7. SUMMARY

We present a catalogue of our LSBG sample which is selected from the  $\alpha.40$ -SDSS DR7 survey combination and extends the parameter space of the previous LSBG samples. This sample is an HI-selected sample which is composed of 1129 LSBGs of various types of luminosity and morphology.

Based on the width of the HI line and the absolute magnitude, we investigate the Tully-Fisher relations (TFr) for a subsample from our entire LSBG sample in the optical  $B$ ,  $g$  and  $r$  and NIR  $J$ ,  $H$  and  $K$  bands. The TFrs in the NIR bands are tighter than those in the optical bands for our LSBG subsample. This is because NIR magnitudes are less affected by internal attenuation and recent episodes of star formation than optical bands. In the optical bands, the LSBG subsample follows the fundamental TFr which was defined for the normal spiral galaxies. In the NIR bands, the slopes of the TFr lines for our LSBG subsample are slightly different from those for the bright and nearby galaxies, but are generally consistent with the TFrs for the bright and nearby galaxies within the uncertainties. This conclusions agree with those from the previous TFr studies for LSBGs (Sprayberry, Bernstein & Impey 1995; Zwaan et al. 1995; Verheijen 1997).

On the basis of the optical TFr results for our subsample, we further estimated the mass-to-light ratio, disk scale length and mass surface density of our LSBG subsample. Compared with the normal spiral galaxies with the same HI line width, the LSBGs have higher mass-to-light ratio, higher disk scale length, and lower mass surface brightness than the HSB spiral galaxies, implying that LSBGs are mostly dominated by dark matter and they have low star formation at present.

We appreciate the anonymous referee for his/her constructive comments, which helped us strengthen this paper. We would like to gratefully thank Prof. Albert Bosma from Aix Marseille University, France, who had face-to-face discussions with us to give us very helpful and suggestive comments on the Tully-Fisher relation part of this paper. We thank Dr. Tao Hong from National Astronomical Observatories, CAS for helpful and constructive discussions and comments. We thank Dr. Anastasis Ponomareva from Australian National University who had private communications, shared her method of intrinsic extinction correction and also PhD thesis with us which is very helpful for us. We also thank Prof. Galaz Gaspar from Pontificia Universidad Católica de Chile, who also gave us suggestive comments to help us improve this paper.

DW and WH is supported by the National Natural Science Foundation of China (NSFC) grant Nos.11733006 and 11403037, and the National Key R&D Program of China grant No. 2017YFA0402704. CC is supported by the NSFC grant No. 11803044 and is also supported in part by the Chinese Academy of Sciences (CAS), through a grant to the CAS South America Center for Astronomy (CASSACA) in Santiago, Chile. ZM is supported by the the National Key R&D Program of China grant No. 2017YFA0402600, NSFC grant No. U1531246 and the Major Applied Basic Research Program of Guizhou Province (No. JZ[2014]2001-05). WY is supported by the NSFC grant Nos. 11390372 and 11773034. Both DW and CC are also supported by the Young Researcher Grant of National Astronomical Observatories, Chinese Academy of Sciences (NAOC) and the Key Laboratory of Optical Astronomy, NAOC

*Facilities:*

*Software:*

## APPENDIX

**Table 4.** A subset of the catalogue of our LSBG sample from the  $\alpha$ .40–SDSS DR7.

AGC	W50	g	r	B	b/a	h(g)	$R_{eff}(g)$	$\mu_{0,g}$	$\mu_{0,B}$	$\mu_{0,B}$	$\mu_{0,B}$	$\mu_{0,B}$	T1	T2
	(km s <sup>-1</sup> )	(mag)	(mag)	(mag)		(kpc)	(kpc)	(AUTO)	( AUTO)	ISO	ISOCOR	PETRO	AVE	
7200	77± 2	14.45±0.003	14.10±0.003	14.78±0.005	0.62	1.42	1.80	22.17	22.53	23.32	22.86	22.49	22.80	S D
7223	80± 1	14.87±0.004	14.48±0.005	15.22±0.007	0.90	1.09	1.79	22.39	22.84	23.96	23.32	22.81	23.23	S D
7236	55± 2	17.01±0.010	16.72±0.012	17.32±0.016	0.91	0.70	0.65	24.38	24.63	26.96	26.39	24.51	25.62	L D
7239	111± 2	13.58±0.003	13.20±0.003	13.92±0.004	0.84	2.10	3.00	22.47	22.86	23.74	23.12	22.83	23.14	S M
7254	96± 1	14.39±0.004	14.00±0.004	14.74±0.006	0.70	1.85	2.28	22.80	23.15	24.13	23.35	23.10	23.43	S D
7307	52± 0	16.52±0.010	16.19±0.011	16.84±0.015	0.36	1.93	1.31	24.29	24.59	27.39	25.88	24.61	25.62	L D
7424	38± 1	14.61±0.004	14.15±0.004	15.00±0.007	0.79	1.33	1.73	22.48	22.89	23.60	22.87	22.80	23.04	S D
7547	71± 1	15.18±0.008	14.89±0.008	15.49±0.013	0.60	1.78	2.04	23.33	23.29	24.99	24.54	23.23	24.01	S D
7737	103± 1	15.03±0.005	14.75±0.007	15.34±0.009	0.37	1.59	1.54	22.44	22.75	23.77	23.34	22.74	23.15	S D
7739	104± 9	14.31±0.005	13.88±0.004	14.68±0.008	0.70	1.52	2.00	22.32	22.61	23.37	22.96	22.59	22.89	S D
7781	44± 2	13.98±0.003	13.76±0.004	14.26±0.006	0.67	1.66	2.43	22.15	22.53	23.86	23.54	22.41	23.08	S D
7795	58± 3	15.26±0.005	15.25±0.007	15.44±0.008	0.53	1.58	1.87	23.09	23.26	25.50	24.94	23.19	24.22	L D
7852	410± 7	15.37±0.002	14.78±0.001	15.82±0.003	0.34	5.79	2.19	22.31	22.82	23.23	23.20	22.55	22.95	S M
7906	104± 1	15.68±0.008	15.39±0.010	15.99±0.013	0.65	1.31	1.51	23.25	23.50	25.50	24.68	23.49	24.29	L D
8030	53± 2	15.68±0.010	15.30±0.009	16.03±0.016	0.42	0.68	0.70	23.01	23.27	24.48	23.81	23.19	23.69	L D
8055	89± 2	15.82±0.010	15.55±0.009	16.12±0.015	0.49	1.81	1.47	23.80	24.10	25.81	25.25	23.99	24.79	L D
8061	56± 6	16.17±0.008	15.81±0.010	16.51±0.013	0.86	1.02	1.39	23.51	23.86	26.66	25.35	23.90	24.94	L D
8091	28± 1	16.54±0.006	16.30±0.008	16.82±0.010	0.58	0.16	0.06	24.01	24.26	25.20	25.07	24.06	24.65	L D
8253	156± 1	15.22±0.006	15.01±0.008	15.48±0.010	0.78	5.12	5.97	23.53	23.91	26.08	24.85	23.87	24.68	S M
8276	68± 2	16.15±0.010	15.94±0.013	16.42±0.016	0.49	1.10	1.08	23.02	23.25	24.62	23.56	23.19	23.66	L D
8450	52± 1	15.09±0.006	14.71±0.006	15.44±0.009	0.70	0.99	1.29	22.20	22.51	23.13	22.60	22.52	22.69	S D
8567	129± 7	16.18±0.010	15.84±0.009	16.51±0.016	0.79	4.31	6.24	22.31	22.72	23.59	23.18	22.71	23.05	L M
8762	152± 3	15.05±0.005	14.66±0.006	15.40±0.009	0.53	4.56	5.75	22.63	23.01	24.24	23.53	22.99	23.44	S M
8915	158± 2	15.85±0.007	15.55±0.008	16.16±0.012	0.47	2.66	3.03	22.84	23.25	24.44	23.84	23.25	23.69	L D
8957	151± 4	15.98±0.008	15.54±0.008	16.36±0.012	0.73	3.67	4.53	22.69	23.07	23.86	23.20	23.08	23.30	L M
9002	96± 4	14.83±0.003	14.63±0.004	15.09±0.005	0.41	6.40	3.91	22.51	22.93	23.48	23.29	22.83	23.13	S M
9007	37± 3	15.55±0.008	15.16±0.008	15.90±0.012	0.69	3.94	5.17	22.46	22.83	23.86	23.16	22.84	23.17	L M
9063	176± 3	15.89±0.010	15.43±0.008	16.27±0.016	0.30	7.14	5.50	22.65	23.04	23.71	23.26	23.05	23.27	S M
9380	95± 2	15.01±0.005	14.74±0.006	15.31±0.009	0.44	2.60	2.61	22.59	22.82	23.88	23.46	22.82	23.25	S D
9385	91± 2	15.21±0.007	14.84±0.007	15.55±0.011	0.84	2.26	3.02	23.21	23.57	25.35	24.48	23.46	24.22	S D
9500	24± 2	16.62±0.010	16.19±0.011	16.99±0.015	0.37	2.76	1.99	24.10	24.33	26.58	25.83	24.25	25.25	L D
9614	134± 2	15.23±0.005	14.81±0.006	15.59±0.009	0.75	3.60	4.85	22.91	23.23	24.56	23.81	23.22	23.70	S M
9821	102± 3	13.76±0.002	13.23±0.002	14.18±0.003	0.82	17.27	19.61	22.01	22.78	23.29	22.94	22.72	22.93	S G
9941	150± 2	14.83±0.005	14.52±0.006	15.15±0.008	0.74	2.65	3.80	22.74	23.24	24.80	23.68	23.16	23.72	S M

Table 4 continued on next page

**Table 4** (*continued*)

AGC	W50	g	r	B	b/a	h(g)	$R_{eff}(g)$	$\mu_{0,g}$	$\mu_{0,B}$	$\mu_{0,B}$	$\mu_{0,B}$	$\mu_{0,B}$	T1	T2
	(km s <sup>-1</sup> )	(mag)	(mag)	(mag)		(kpc)	(kpc)	(AUTO)	( AUTO)	ISO	ISOCOR	PETRO	AVE	
10009	124± 4	16.04±0.012	15.62±0.012	16.41±0.019	0.36	2.24	2.00	22.67	23.06	24.16	22.22	23.05	23.12	L D
10014	109± 2	15.16±0.006	14.79±0.007	15.51±0.010	0.72	3.97	4.05	23.40	23.63	25.11	23.86	23.56	24.04	S M
10058	119± 2	15.77±0.007	15.56±0.008	16.04±0.011	0.77	3.62	4.88	22.62	23.02	24.25	23.68	22.96	23.48	L M
10146	143± 8	15.51±0.007	15.05±0.007	15.90±0.011	0.79	5.67	7.34	22.12	22.59	23.18	22.39	22.55	22.68	S G
10419	87± 2	17.29±0.012	16.90±0.013	17.64±0.019	0.88	3.69	2.20	25.38	25.47	27.50	26.97	25.33	26.32	L D
12212	99± 2	14.42±0.003	14.13±0.004	14.73±0.005	0.76	2.44	2.92	22.69	23.04	23.94	23.46	22.93	23.34	S M
12289	217± 12	14.55±0.007	13.97±0.004	15.00±0.010	0.89	9.06	13.68	21.91	22.65	23.39	22.59	22.46	22.77	S G
12845	233± 3	13.83±0.002	13.26±0.002	14.27±0.004	0.64	8.48	9.46	22.30	22.79	23.20	22.46	22.81	22.82	S G
100037	63± 1	15.80±0.008	15.37±0.008	16.18±0.013	0.93	2.03	2.86	22.54	22.92	23.66	22.72	22.97	23.07	L M
100350	107± 13	17.70±0.021	17.37±0.023	18.02±0.033	0.51	2.85	2.85	23.69	23.97	26.76	22.50	23.98	24.30	U D
101191	88± 6	17.53±0.020	17.27±0.023	17.83±0.031	0.62	2.21	2.76	22.87	23.22	24.80	23.75	23.19	23.74	L D
101812	93± 3	17.90±0.029	17.64±0.027	18.19±0.045	0.39	1.10	0.88	23.49	23.66	26.17	24.69	23.64	24.54	L D
101877	185± 4	16.88±0.016	16.52±0.017	17.23±0.025	0.44	3.03	3.51	22.59	23.07	24.49	22.92	23.05	23.38	L M
101942	76± 8	17.87±0.029	17.54±0.029	18.19±0.045	0.59	1.80	2.32	22.56	22.90	24.29	22.33	22.89	23.10	L D
101986	51± 3	16.83±0.012	16.65±0.016	17.09±0.020	0.79	3.20	4.16	22.48	22.80	23.88	23.41	22.71	23.20	L M
102098	196± 16	17.80±0.026	17.35±0.024	18.19±0.040	0.52	3.81	4.60	22.20	22.60	23.53	21.93	22.50	22.64	L M
102101	113± 4	16.74±0.015	16.29±0.016	17.12±0.024	0.78	2.64	3.57	22.68	23.07	24.38	21.70	23.00	23.04	L M
102229	82± 8	17.55±0.018	17.35±0.020	17.82±0.028	0.52	1.11	1.37	22.30	22.58	23.73	23.25	22.49	23.01	L D
102243	139± 12	16.29±0.014	15.86±0.010	16.66±0.021	0.89	2.51	4.28	21.89	22.50	23.41	22.79	22.39	22.77	L M
102302	100± 2	17.00±0.017	16.64±0.018	17.34±0.027	0.62	0.88	1.08	22.73	22.96	24.20	23.03	22.92	23.28	L D
102558	48± 2	17.95±0.026	17.60±0.026	18.29±0.040	0.77	0.85	1.28	22.75	23.01	24.40	22.89	22.89	23.30	L D
102630	96± 16	18.03±0.020	17.82±0.023	18.30±0.032	0.65	4.14	3.25	24.40	24.67	26.69	25.92	24.56	25.46	L D
102635	94± 12	16.47±0.008	16.15±0.010	16.79±0.013	0.87	3.98	5.79	22.17	22.57	23.25	22.74	22.53	22.77	L M
102672	170± 40	17.08±0.011	16.83±0.014	17.37±0.018	0.75	1.79	2.42	22.19	22.57	23.28	22.95	22.51	22.83	L D
102674	131± 24	17.37±0.015	17.13±0.016	17.65±0.023	0.98	4.98	7.95	22.78	23.32	24.89	24.20	23.22	23.91	L M
102684	33± 6	17.62±0.019	17.36±0.020	17.92±0.029	0.50	4.61	4.02	23.64	23.93	25.36	24.52	23.77	24.40	L M
102728	21± 6	19.02±0.037	18.80±0.047	19.29±0.059	0.88	0.10	0.17	22.79	22.85	24.49	23.71	22.77	23.45	L D
102729	53± 6	18.24±0.016	18.33±0.027	18.36±0.027	0.43	1.38	1.86	22.46	22.59	25.05	24.71	22.55	23.72	L D
102730	79± 23	17.62±0.016	17.29±0.017	17.95±0.025	0.88	2.96	5.37	22.01	22.68	23.82	23.10	22.62	23.06	L M
102900	133± 4	18.96±0.023	19.10±0.035	19.06±0.037	0.51	7.75	3.08	24.94	25.04	28.24	26.47	24.86	26.15	L M
102981	65± 15	15.37±0.004	15.01±0.004	15.71±0.007	0.89	2.61	3.94	21.78	22.54	23.35	23.07	22.53	22.87	S M
110150	108± 1	15.60±0.007	15.21±0.007	15.95±0.011	0.69	2.71	3.67	22.42	22.75	23.60	22.87	22.74	22.99	L M
110319	21± 3	18.00±0.023	17.62±0.024	18.35±0.036	0.81	2.83	2.73	24.31	24.67	27.13	22.85	24.60	24.81	L D
110379	121± 2	16.65±0.012	16.38±0.015	16.95±0.019	0.66	1.57	1.86	23.13	23.51	25.18	24.21	23.39	24.08	L D
110398	176± 7	16.01±0.008	15.69±0.010	16.33±0.013	0.49	4.43	5.05	22.13	22.52	23.23	22.60	22.51	22.71	L M
112503	43± 9	16.82±0.014	16.33±0.014	17.23±0.021	0.71	0.29	0.44	22.34	22.56	23.69	22.95	22.49	22.92	U D

Table 4 continued on next page

**Table 4** (*continued*)

AGC	W50	g	r	B	b/a	h(g)	$R_{eff}(g)$	$\mu_{0,g}$	$\mu_{0,B}$	$\mu_{0,B}$	$\mu_{0,B}$	$\mu_{0,B}$	T1	T2
		(km s <sup>-1</sup> )	(mag)	(mag)		(kpc)	(kpc)	(AUTO)	( AUTO)	ISO	ISOCOR	PETRO	AVE	
112892	76± 8	17.59±0.021	17.24±0.024	17.93±0.033	0.72	3.27	4.61	22.29	22.57	24.07	23.41	22.54	23.15	L M
113200	101± 40	17.83±0.022	17.59±0.029	18.11±0.035	0.57	2.28	2.92	22.42	22.73	24.09	23.34	22.71	23.22	L D
113752	91± 7	18.76±0.028	18.64±0.038	18.99±0.045	0.57	3.30	4.06	22.95	23.17	24.79	24.18	23.08	23.80	L M
113790	31± 10	20.46±0.050	20.23±0.060	20.74±0.079	0.42	0.69	0.81	23.07	23.22	26.49	22.27	23.29	23.82	L D
113825	107± 9	18.15±0.027	17.89±0.030	18.44±0.042	0.34	1.30	1.30	22.47	22.80	23.79	23.01	22.72	23.08	L D
113845	82± 17	18.47±0.024	18.21±0.028	18.77±0.038	0.90	1.40	2.32	22.29	22.74	23.86	23.28	22.62	23.12	L D
113907	36± 5	17.12±0.013	16.72±0.012	17.49±0.020	0.74	3.51	4.36	22.19	22.69	23.21	22.76	22.54	22.80	L M
113918	46± 7	17.85±0.019	17.56±0.021	18.16±0.031	0.80	2.92	4.39	22.51	22.83	23.96	23.33	22.70	23.20	L M
113923	83± 4	17.88±0.026	17.69±0.024	18.14±0.040	0.70	1.43	2.15	22.99	23.22	25.62	24.78	23.21	24.21	L D
114040	130± 17	17.17±0.013	16.90±0.016	17.47±0.021	0.88	2.47	3.87	22.30	22.68	23.59	23.05	22.56	22.97	L M
121174	79± 3	18.02±0.020	17.60±0.021	18.39±0.031	0.48	1.03	0.28	25.93	26.30	29.27	26.81	26.31	27.17	L D
122138	74± 2	20.08±0.044	19.82±0.055	20.37±0.070	0.97	0.62	0.16	26.88	27.18	30.58	26.35	27.18	27.82	L D
122210	84± 7	16.85±0.016	16.53±0.017	17.17±0.026	0.76	2.57	3.31	23.14	23.33	25.23	23.28	23.29	23.78	L D
122211	29± 1	17.15±0.016	16.82±0.016	17.48±0.025	0.99	1.94	2.30	23.62	23.95	26.70	22.38	23.97	24.25	L D
122218	98± 2	17.70±0.019	17.43±0.023	17.99±0.030	0.36	1.82	1.30	23.65	24.35	28.39	24.14	26.35	25.81	L D
122341	171± 4	17.19±0.018	16.89±0.021	17.50±0.028	0.51	5.15	5.39	22.47	22.82	24.16	23.14	22.82	23.24	L M
122874	135± 10	17.83±0.026	17.36±0.023	18.22±0.039	0.50	1.85	2.19	22.18	22.61	23.45	21.79	22.45	22.58	L D
122877	81± 5	17.14±0.016	16.88±0.017	17.43±0.025	0.58	3.05	3.80	22.81	24.18	26.72	22.35	24.11	24.34	L M
122884	119± 2	16.99±0.020	16.77±0.023	17.26±0.031	0.78	1.07	1.40	22.86	23.13	25.02	22.69	23.11	23.49	L D
122924	78± 6	20.60±0.092	20.50±0.094	20.81±0.143	0.81	1.42	1.11	23.94	24.06	26.26	25.62	23.92	24.96	U D
123046	125± 8	18.32±0.042	17.84±0.038	18.72±0.065	0.64	1.22	1.58	22.70	23.02	24.95	20.68	23.07	22.93	U D
123047	61± 8	18.30±0.033	18.18±0.044	18.53±0.053	0.52	2.64	3.12	22.37	23.03	24.70	23.02	22.86	23.40	L M
123170	48± 3	16.58±0.017	16.20±0.017	16.92±0.027	0.46	0.58	0.53	22.74	22.88	24.09	22.40	22.80	23.04	L D
123172	160± 3	16.77±0.021	16.47±0.019	17.08±0.032	0.40	3.00	2.84	22.31	22.59	23.57	22.73	22.58	22.87	L M
171467	126± 8	17.56±0.014	17.26±0.018	17.87±0.023	0.81	1.39	2.29	22.46	22.97	24.33	23.83	22.87	23.50	L D
171585	126± 8	17.03±0.013	16.73±0.015	17.35±0.021	0.51	2.33	2.44	22.45	22.83	23.60	23.08	22.77	23.07	L D
171643	179± 33	17.15±0.014	16.86±0.015	17.46±0.022	0.78	2.99	3.41	22.57	22.87	23.71	23.27	22.72	23.15	L M
171782	65± 3	17.01±0.016	16.68±0.016	17.34±0.025	0.88	2.72	4.01	22.43	22.81	23.70	22.71	22.77	23.00	L M
171838	26± 2	16.89±0.015	16.55±0.017	17.22±0.024	0.74	2.13	3.10	22.47	22.70	23.98	22.72	22.71	23.03	L M
172071	78± 3	16.94±0.016	16.54±0.015	17.30±0.025	0.69	2.29	2.68	22.69	22.92	23.80	23.14	22.95	23.20	L D
172073	132± 5	16.20±0.010	15.79±0.010	16.56±0.016	0.83	2.41	3.75	22.26	22.74	23.75	22.79	22.69	22.99	L M
172086	119± 5	17.09±0.014	16.89±0.016	17.35±0.022	0.67	1.77	2.24	22.22	22.56	23.32	22.80	22.52	22.80	L D
174501	32± 10	17.61±0.016	17.30±0.019	17.92±0.026	0.48	5.68	6.13	22.25	22.70	23.68	23.21	22.68	23.07	L M
174513	119± 5	16.87±0.010	16.66±0.013	17.14±0.016	0.76	3.48	4.11	22.18	22.55	23.05	22.72	22.50	22.70	L M
174601	173± 3	16.11±0.007	15.69±0.008	16.48±0.011	0.45	3.82	3.60	22.35	22.63	23.18	22.78	22.58	22.79	L M
174610	95± 13	17.10±0.012	16.81±0.015	17.41±0.019	0.68	5.79	5.15	23.14	23.53	24.56	24.09	23.32	23.87	L M

Table 4 continued on next page

**Table 4** (*continued*)

AGC	W50	g	r	B	b/a	h(g)	$R_{eff}(g)$	$\mu_{0,g}$	$\mu_{0,B}$	$\mu_{0,B}$	$\mu_{0,B}$	$\mu_{0,B}$	T1	T2
	(km s <sup>-1</sup> )	(mag)	(mag)	(mag)		(kpc)	(kpc)	(AUTO)	( AUTO)	ISO	ISOCOR	PETRO	AVE	
174612	221± 5	16.47±0.008	16.12±0.009	16.81±0.013	0.60	5.86	5.37	22.55	23.40	24.09	23.67	23.27	23.61	L M
180686	120± 3	16.43±0.010	15.97±0.010	16.82±0.016	0.94	3.08	5.08	22.53	23.06	24.14	23.27	23.04	23.38	L M
180737	16± 5	18.21±0.023	17.89±0.024	18.52±0.036	0.46	0.87	0.98	22.95	23.33	27.43	23.30	23.40	24.36	L D
181471	91± 5	17.04±0.014	16.60±0.016	17.41±0.023	0.34	2.15	1.57	23.68	24.05	25.60	24.49	24.06	24.55	L D
181566	20± 3	16.79±0.013	16.48±0.014	17.11±0.020	0.58	1.10	1.32	22.36	22.67	23.39	22.75	22.61	22.85	L D
181571	69± 3	16.79±0.013	16.45±0.014	17.13±0.021	0.39	4.16	3.87	23.41	23.92	26.04	24.82	23.83	24.65	L D
181610	157± 8	17.44±0.019	17.02±0.019	17.81±0.029	0.74	5.44	7.89	22.21	22.69	23.77	22.92	22.54	22.98	S G
181620	92± 10	16.64±0.009	16.44±0.012	16.90±0.015	0.77	5.79	7.60	22.10	22.64	23.45	23.14	22.57	22.95	L G
181685	116± 33	16.97±0.013	16.64±0.015	17.30±0.021	0.62	5.61	5.77	23.13	23.29	24.65	24.02	23.18	23.78	L M
181730	111± 13	16.38±0.009	16.07±0.011	16.69±0.014	0.60	2.50	3.22	22.18	22.51	23.36	22.59	22.31	22.69	L M
181762	212± 22	16.59±0.009	16.23±0.011	16.93±0.015	0.50	8.24	8.49	22.39	22.88	23.68	23.09	22.85	23.12	L G
181830	105± 10	17.36±0.017	16.97±0.018	17.71±0.026	0.74	1.41	1.99	22.12	22.50	23.24	22.72	22.41	22.72	L D
181843	150± 61	18.59±0.019	18.30±0.023	18.90±0.030	0.92	3.00	4.74	22.88	23.44	25.49	24.90	23.16	24.25	L M
181949	61± 2	16.98±0.013	16.75±0.021	17.26±0.022	0.80	1.06	1.32	23.09	23.30	25.01	23.91	23.21	23.86	L D
182462	76± 2	16.84±0.013	16.50±0.014	17.17±0.021	0.60	0.82	0.97	22.51	22.76	23.56	22.92	22.76	23.00	L D
182466	80± 2	18.22±0.023	17.98±0.027	18.51±0.037	0.54	0.88	0.93	23.49	23.86	25.74	24.35	23.76	24.42	L D
182467	34± 8	19.16±0.031	19.05±0.041	19.38±0.050	0.53	1.72	1.13	24.29	24.57	27.69	25.06	24.58	25.47	L D
182477	84± 3	18.08±0.018	18.23±0.035	18.18±0.032	0.59	1.25	1.42	22.55	22.77	24.53	24.27	22.68	23.56	L D
182491	106± 7	16.95±0.013	16.64±0.018	17.26±0.021	0.61	1.99	2.66	22.50	22.69	23.99	23.28	22.65	23.15	L D
182545	49± 2	16.81±0.012	16.59±0.015	17.09±0.019	0.91	0.86	1.33	22.44	22.81	23.86	23.38	22.72	23.19	L D
182608	109± 4	17.67±0.022	17.27±0.024	18.03±0.035	0.39	2.27	2.38	22.78	23.26	24.67	23.10	23.26	23.57	L D
182871	108± 32	17.24±0.014	16.98±0.019	17.53±0.022	0.79	3.57	5.14	22.14	22.51	23.53	23.09	22.52	22.91	L M
182924	223± 7	17.64±0.016	17.53±0.023	17.87±0.027	0.46	4.00	4.89	22.11	22.54	23.62	23.18	22.47	22.95	L M
182966	49± 4	17.44±0.018	17.07±0.021	17.78±0.028	0.79	3.80	4.72	23.35	23.57	25.60	23.80	23.55	24.13	L M
183068	165± 7	16.98±0.012	16.70±0.013	17.28±0.019	0.43	6.33	7.29	22.16	22.79	23.68	23.26	22.61	23.09	L G
183138	128± 11	16.86±0.011	16.47±0.013	17.21±0.018	0.56	6.50	6.92	22.53	22.97	23.96	23.43	22.92	23.32	L M
183216	89± 16	17.27±0.016	16.83±0.017	17.65±0.025	0.75	2.25	3.12	22.45	22.86	23.70	22.97	22.86	23.10	L M
183311	185± 9	17.11±0.013	16.75±0.014	17.45±0.020	0.35	7.81	5.94	22.39	22.60	23.09	22.56	22.59	22.71	L M
183314	162± 23	17.74±0.021	17.27±0.020	18.13±0.032	0.65	1.91	2.68	22.47	22.84	23.86	23.18	22.86	23.19	L D
183372	310± 68	17.26±0.013	16.99±0.016	17.55±0.021	0.75	2.19	3.04	22.15	22.53	23.30	22.87	22.47	22.79	L M
183465	229± 86	17.95±0.008	17.47±0.007	18.35±0.012	0.67	0.56	1.39	17.79	22.90	22.97	22.91	22.88	22.91	S M
183594	93± 41	17.47±0.016	17.10±0.017	17.82±0.026	0.39	2.41	2.63	22.15	22.61	23.35	22.55	22.57	22.77	L D
183691	152± 12	17.23±0.014	16.99±0.017	17.51±0.022	0.50	3.53	4.14	22.20	22.62	23.48	22.99	22.59	22.92	L M
183924	175± 44	17.12±0.017	16.74±0.018	17.47±0.026	0.69	9.13	7.08	23.50	24.44	25.70	24.64	24.34	24.78	S M
184304	165± 7	17.92±0.024	17.46±0.025	18.30±0.038	0.38	1.78	1.86	22.17	22.51	23.30	22.56	22.48	22.71	L D
184458	129± 7	17.23±0.013	16.92±0.015	17.54±0.021	0.74	2.20	3.08	22.19	22.59	23.26	22.66	22.60	22.78	L M

Table 4 continued on next page

**Table 4** (*continued*)

AGC	W50	g	r	B	b/a	h(g)	$R_{eff}(g)$	$\mu_{0,g}$	$\mu_{0,B}$	$\mu_{0,B}$	$\mu_{0,B}$	$\mu_{0,B}$	T1	T2
		(km s <sup>-1</sup> )	(mag)	(mag)	(mag)	(kpc)	(kpc)	(AUTO)	( AUTO)	ISO	ISOCOR	PETRO	AVE	
184599	143± 4	16.81±0.014	16.64±0.019	17.06±0.022	0.79	4.15	5.72	22.70	23.04	24.76	24.12	22.99	23.73	U M
188737	134± 12	17.71±0.016	17.38±0.020	18.03±0.026	0.62	4.53	5.54	22.16	22.55	23.35	22.85	22.51	22.81	L M
188739	113± 11	19.00±0.026	18.83±0.036	19.25±0.041	0.82	1.67	1.61	24.13	24.27	27.77	26.81	24.36	25.80	L D
188750	155± 41	17.51±0.017	17.19±0.021	17.83±0.027	0.68	3.16	3.95	22.40	22.71	23.72	23.05	22.78	23.06	L M
188768	40± 17	19.30±0.038	19.04±0.047	19.59±0.061	0.44	1.90	1.73	23.60	23.87	26.25	23.34	23.74	24.30	L D
188781	25± 3	17.14±0.013	16.70±0.012	17.52±0.020	0.81	2.74	4.22	22.87	23.43	24.87	23.95	23.24	23.87	L M
188785	101± 24	17.83±0.021	17.59±0.029	18.12±0.034	0.37	3.85	4.25	22.54	22.85	24.43	23.30	22.78	23.34	L M
188788	53± 10	16.92±0.012	16.59±0.015	17.24±0.020	0.70	4.55	6.14	22.69	23.10	24.45	23.84	23.09	23.62	L M
188845	79± 7	16.62±0.012	16.25±0.015	16.96±0.020	0.99	2.36	3.41	22.68	23.05	24.25	23.32	23.06	23.42	S M
188851	192± 7	18.53±0.025	18.08±0.026	18.91±0.039	0.65	4.52	4.17	23.84	24.18	25.74	24.67	24.04	24.66	L M
188869	30± 3	19.11±0.027	19.18±0.045	19.25±0.046	0.31	1.02	0.69	23.60	23.74	26.96	26.14	23.77	25.15	L D
188881	102± 3	17.61±0.019	17.26±0.020	17.94±0.030	0.86	3.90	5.70	22.32	22.82	23.65	22.73	22.71	22.98	L M
188937	280± 85	17.81±0.022	17.39±0.022	18.17±0.033	0.71	1.54	2.21	22.74	23.04	24.34	23.57	23.01	23.49	L D
188957	42± 5	18.51±0.022	18.38±0.029	18.75±0.036	0.70	0.62	0.90	23.03	23.19	25.94	24.76	23.16	24.26	L D
188963	93± 9	18.00±0.022	17.73±0.024	18.29±0.035	0.60	6.51	7.38	23.55	24.03	26.09	23.83	23.97	24.48	L M
188993	62± 13	18.96±0.028	18.39±0.025	19.40±0.043	0.83	3.25	3.01	23.97	24.41	26.00	25.35	23.95	24.93	S D
189000	60± 4	17.79±0.022	17.51±0.024	18.09±0.034	0.86	1.08	1.53	23.07	23.29	25.47	24.53	23.28	24.14	L D
190796	123± 4	15.69±0.006	15.36±0.006	16.02±0.009	0.70	8.69	9.06	22.86	23.82	24.92	24.39	23.63	24.19	L G
191707	32± 2	17.44±0.012	17.17±0.018	17.74±0.020	0.37	1.22	1.08	23.38	23.51	25.43	25.01	23.33	24.32	L D
191737	110± 2	15.59±0.006	15.17±0.008	15.95±0.010	0.70	3.79	4.35	22.71	23.13	24.05	23.24	22.95	23.34	S M
191791	47± 19	19.68±0.035	19.26±0.041	20.04±0.055	0.57	0.12	0.13	23.24	23.13	26.62	22.49	24.93	24.29	L D
191817	124± 2	16.74±0.012	16.44±0.016	17.05±0.019	0.45	1.79	1.94	22.63	22.95	24.23	23.41	22.86	23.36	L D
191818	25± 7	18.17±0.024	17.80±0.029	18.51±0.039	0.87	1.16	1.33	23.88	24.04	26.62	22.37	24.00	24.26	L D
191819	135± 4	17.46±0.019	17.13±0.023	17.78±0.031	0.34	2.96	3.34	23.02	23.35	25.68	22.85	23.35	23.81	L D
191849	62± 3	16.43±0.011	16.06±0.012	16.77±0.018	0.61	1.15	1.34	22.88	23.21	24.13	23.42	23.21	23.49	L D
191871	108± 7	17.00±0.017	16.69±0.015	17.32±0.027	0.76	2.13	2.99	22.42	22.75	23.69	23.28	22.78	23.13	L M
191873	83± 9	17.68±0.024	17.36±0.021	18.00±0.037	0.68	1.55	2.08	22.28	22.59	23.44	23.05	22.67	22.94	L D
191879	112± 28	17.08±0.013	16.78±0.018	17.39±0.021	0.57	3.39	4.06	22.72	23.12	24.71	23.75	23.06	23.66	L M
191906	119± 3	17.70±0.019	17.41±0.023	18.00±0.030	0.37	1.52	1.62	22.64	22.95	23.92	23.17	22.89	23.23	L D
191917	180± 8	17.75±0.020	17.35±0.020	18.11±0.031	0.47	3.61	4.58	22.11	22.58	23.54	22.81	22.54	22.87	L M
191952	142± 8	17.75±0.020	17.36±0.021	18.11±0.032	0.71	2.36	3.37	22.08	22.51	23.40	22.63	22.44	22.74	L M
191970	66± 12	17.54±0.016	17.15±0.018	17.90±0.026	0.84	4.89	6.55	22.52	22.90	23.72	22.92	22.84	23.09	S M
191989	109± 5	16.53±0.012	16.13±0.013	16.89±0.019	0.57	2.06	2.70	22.58	22.94	24.04	23.22	22.98	23.29	L D
192039	36± 7	17.83±0.020	17.54±0.026	18.14±0.032	0.33	1.31	1.40	22.40	22.77	23.98	23.06	22.73	23.13	L D
192118	160± 3	17.15±0.013	16.84±0.014	17.46±0.020	0.50	2.32	2.83	22.14	22.57	23.46	22.94	22.48	22.86	L M
192165	111± 6	16.86±0.011	16.56±0.013	17.17±0.017	0.55	4.08	5.19	22.28	22.69	23.67	23.19	22.68	23.06	L M

Table 4 continued on next page

**Table 4** (*continued*)

AGC	W50	g	r	B	b/a	h(g)	$R_{eff}(g)$	$\mu_{0,g}$	$\mu_{0,B}$	$\mu_{0,B}$	$\mu_{0,B}$	$\mu_{0,B}$	T1	T2
	(km s <sup>-1</sup> )	(mag)	(mag)	(mag)		(kpc)	(kpc)	(AUTO)	( AUTO)	ISO	ISOCOR	PETRO	AVE	
192225	175± 4	17.55±0.018	17.15±0.018	17.91±0.028	0.73	4.07	6.26	22.28	22.78	23.83	22.72	22.77	23.02	S M
192254	154± 6	17.79±0.016	17.37±0.018	18.16±0.025	0.69	2.25	3.33	21.99	22.50	23.32	22.83	22.42	22.77	L M
192364	121± 4	17.35±0.015	17.00±0.019	17.69±0.024	0.87	1.74	2.64	22.32	22.63	23.72	23.10	22.56	23.00	L D
192424	236± 27	17.55±0.017	17.13±0.018	17.91±0.027	0.51	4.09	4.61	22.38	22.78	23.43	22.62	22.72	22.89	L M
192510	37± 20	17.02±0.019	16.66±0.016	17.36±0.029	0.59	1.56	2.14	22.43	22.79	23.84	23.26	22.86	23.19	L D
192669	136± 7	17.22±0.013	16.76±0.015	17.60±0.021	0.86	4.02	5.73	22.19	22.66	23.47	22.82	22.63	22.89	L M
192735	98± 4	17.32±0.014	17.00±0.017	17.64±0.023	0.91	1.69	2.54	22.51	23.06	24.26	23.63	22.98	23.48	L D
192739	193± 8	16.03±0.008	15.46±0.007	16.48±0.012	0.81	6.01	7.56	22.05	22.57	22.92	22.33	22.52	22.58	S G
192776	133± 3	16.70±0.012	16.31±0.014	17.05±0.020	0.73	2.32	3.00	22.86	23.24	24.58	23.26	23.23	23.58	L D
193780	86± 7	16.52±0.012	16.19±0.014	16.84±0.019	0.73	1.87	2.63	22.44	22.80	24.05	23.16	22.72	23.18	L D
193781	152± 4	17.96±0.032	17.64±0.031	18.28±0.050	0.54	3.08	3.84	22.77	23.09	24.90	23.45	23.01	23.61	L M
193782	138± 3	16.15±0.009	15.88±0.011	16.44±0.015	0.63	2.79	3.55	22.96	23.38	24.83	23.86	23.37	23.86	L M
193790	57± 13	19.99±0.053	19.78±0.067	20.26±0.085	0.76	1.15	0.98	24.00	24.23	25.76	25.35	23.98	24.83	L D
193791	155± 3	16.85±0.010	16.61±0.012	17.14±0.016	0.71	5.35	5.90	22.98	23.27	24.25	23.94	23.19	23.66	L M
193792	83± 12	18.12±0.017	17.88±0.022	18.39±0.028	0.58	2.08	2.67	23.27	23.56	25.64	25.04	23.48	24.43	L D
193800	98± 18	19.58±0.041	19.29±0.049	19.88±0.065	0.84	1.35	1.32	24.13	24.43	27.83	23.63	24.41	25.08	L D
193802	43± 3	19.13±0.028	18.87±0.033	19.42±0.044	0.38	0.48	0.50	23.21	22.91	26.38	24.79	22.98	24.27	L D
193813	87± 6	16.33±0.013	15.85±0.010	16.73±0.020	0.76	1.00	1.33	22.18	22.56	23.14	22.61	22.52	22.71	L D
193816	56± 3	15.97±0.008	15.75±0.013	16.25±0.014	0.61	1.15	1.39	22.58	22.85	24.36	23.78	22.80	23.45	L D
193818	151± 8	21.03±0.085	19.45±0.031	21.94±0.126	0.70	1.16	0.81	24.43	25.74	26.87	24.18	25.21	25.50	S D
193819	33± 2	17.39±0.015	17.10±0.019	17.70±0.024	0.78	1.94	2.91	22.30	22.67	23.91	23.32	22.69	23.15	L M
193824	126± 15	16.99±0.012	16.62±0.013	17.34±0.019	0.92	2.59	4.45	22.19	22.62	23.56	23.00	22.57	22.94	S M
193833	44± 3	18.24±0.024	17.91±0.027	18.57±0.038	0.82	1.42	1.72	23.76	24.00	26.14	24.94	23.96	24.76	L D
193841	51± 5	20.16±0.050	19.95±0.061	20.43±0.079	0.74	1.40	1.06	24.55	24.97	27.92	23.75	24.95	25.40	L D
193846	120± 5	17.25±0.015	16.88±0.017	17.59±0.023	0.85	1.51	2.42	22.39	22.90	24.20	23.45	22.81	23.34	S D
193862	168± 8	17.45±0.017	17.10±0.020	17.78±0.027	0.41	2.06	2.17	22.81	23.14	24.29	22.85	23.12	23.35	L D
193866	45± 7	17.95±0.020	17.71±0.027	18.23±0.033	0.72	1.99	2.45	23.56	23.84	26.14	24.43	23.79	24.55	L D
193877	117± 8	19.03±0.042	18.74±0.038	19.33±0.064	0.88	1.76	2.93	22.43	22.65	24.07	23.68	22.59	23.25	L D
193881	66± 11	17.67±0.019	17.40±0.023	17.97±0.030	0.97	2.72	4.28	22.30	22.69	23.97	23.26	22.70	23.15	L M
193883	133± 13	17.18±0.014	16.98±0.016	17.45±0.022	0.71	5.64	7.91	22.29	22.72	23.74	22.99	22.66	23.03	L G
193888	46± 11	17.69±0.018	17.41±0.020	17.98±0.028	0.83	2.32	3.48	22.49	22.91	23.89	23.17	22.85	23.21	L M
193891	127± 7	16.92±0.011	16.56±0.013	17.27±0.018	0.86	2.86	4.18	22.35	22.73	23.46	22.95	22.74	22.97	S M
193893	53± 2	18.32±0.026	18.12±0.033	18.58±0.041	0.99	1.13	1.79	22.89	23.16	24.50	23.72	23.09	23.62	L D
193894	90± 6	17.96±0.028	17.74±0.027	18.24±0.043	0.36	3.08	3.18	23.04	23.39	24.97	24.27	23.37	24.00	L D
193905	82± 7	18.15±0.021	17.91±0.027	18.43±0.034	0.49	2.30	2.95	22.34	22.71	23.87	23.33	22.58	23.12	L D
193919	124± 7	18.34±0.026	18.05±0.029	18.65±0.042	0.82	0.92	1.34	22.69	23.00	24.12	23.31	22.97	23.35	U D

Table 4 continued on next page

**Table 4** (*continued*)

AGC	W50	g	r	B	b/a	h(g)	$R_{eff}(g)$	$\mu_{0,g}$	$\mu_{0,B}$	$\mu_{0,B}$	$\mu_{0,B}$	$\mu_{0,B}$	T1	T2
		(km s <sup>-1</sup> )	(mag)	(mag)		(kpc)	(kpc)	(AUTO)	( AUTO)	ISO	ISOCOR	PETRO	AVE	
193921	$39 \pm 5$	$19.37 \pm 0.032$	$19.18 \pm 0.044$	$19.63 \pm 0.052$	0.50	0.60	0.40	24.23	24.40	27.40	25.03	24.44	25.32	L D
193923	$183 \pm 2$	$16.60 \pm 0.011$	$16.24 \pm 0.011$	$16.93 \pm 0.017$	0.95	3.54	5.68	22.52	23.11	24.16	23.28	22.99	23.39	L M
194002	$77 \pm 3$	$17.35 \pm 0.016$	$17.00 \pm 0.020$	$17.68 \pm 0.026$	0.47	1.14	1.40	22.46	22.79	24.06	23.04	22.76	23.16	L D
194300	$117 \pm 27$	$17.37 \pm 0.017$	$16.98 \pm 0.017$	$17.73 \pm 0.026$	0.89	4.38	6.31	22.33	22.76	23.63	22.74	22.74	22.97	S M
194441	$123 \pm 8$	$16.20 \pm 0.007$	$15.72 \pm 0.007$	$16.59 \pm 0.012$	0.71	7.84	8.99	22.18	22.75	23.31	22.82	22.65	22.88	L G
194549	$179 \pm 10$	$17.03 \pm 0.013$	$16.64 \pm 0.015$	$17.39 \pm 0.021$	0.67	3.40	4.56	22.40	22.81	23.73	23.08	22.81	23.11	L M
194618	$126 \pm 12$	$17.75 \pm 0.024$	$17.26 \pm 0.024$	$18.15 \pm 0.037$	0.39	2.90	3.24	22.32	22.59	23.44	22.69	22.59	22.83	S M
194718	$152 \pm 8$	$16.76 \pm 0.012$	$16.42 \pm 0.014$	$17.09 \pm 0.020$	0.66	3.06	3.87	22.28	22.69	23.54	22.82	22.68	22.93	L M
195255	$96 \pm 9$	$17.97 \pm 0.021$	$17.66 \pm 0.028$	$18.28 \pm 0.034$	0.85	2.03	2.93	22.33	22.68	23.71	22.89	22.69	22.99	L M
198336	$87 \pm 7$	$16.89 \pm 0.013$	$16.57 \pm 0.016$	$17.21 \pm 0.021$	0.71	1.61	2.08	22.68	23.26	24.64	23.59	23.14	23.66	L D
198344	$106 \pm 15$	$16.70 \pm 0.014$	$16.30 \pm 0.014$	$17.06 \pm 0.021$	0.78	1.67	2.83	22.57	22.98	24.33	22.89	22.82	23.25	L D
198350	$232 \pm 10$	$18.18 \pm 0.030$	$17.83 \pm 0.033$	$18.52 \pm 0.047$	0.92	2.92	3.92	23.23	23.57	25.00	22.75	23.56	23.72	L M
198353	$140 \pm 5$	$19.07 \pm 0.033$	$18.85 \pm 0.041$	$19.34 \pm 0.053$	0.81	2.26	3.41	22.36	22.74	23.99	23.48	22.59	23.20	L M
198354	$27 \pm 8$	$18.36 \pm 0.028$	$17.99 \pm 0.030$	$18.71 \pm 0.045$	0.54	0.40	0.49	22.68	22.93	24.10	23.36	22.92	23.33	U D
198430	$46 \pm 9$	$17.92 \pm 0.023$	$17.68 \pm 0.027$	$18.20 \pm 0.036$	0.75	0.65	0.83	22.73	23.04	24.20	23.36	22.99	23.40	L D
198434	$100 \pm 23$	$17.96 \pm 0.023$	$17.49 \pm 0.022$	$18.35 \pm 0.035$	0.72	2.64	2.94	23.86	24.18	26.16	23.70	24.11	24.54	L D
198452	$63 \pm 21$	$20.83 \pm 0.062$	$20.64 \pm 0.099$	$21.09 \pm 0.103$	0.47	3.39	0.59	26.56	26.94	28.89	28.35	26.85	27.76	U D
198453	$117 \pm 6$	$17.47 \pm 0.016$	$17.20 \pm 0.021$	$17.77 \pm 0.026$	0.80	2.60	3.87	22.29	22.62	23.73	23.11	22.56	23.00	L M
198454	$45 \pm 6$	$18.88 \pm 0.028$	$18.84 \pm 0.043$	$19.06 \pm 0.046$	0.41	0.54	0.44	23.42	23.59	25.36	24.99	23.35	24.32	L D
198456	$57 \pm 6$	$18.42 \pm 0.025$	$18.32 \pm 0.037$	$18.63 \pm 0.041$	0.39	0.64	0.71	22.62	22.93	24.31	23.64	22.85	23.43	L D
200571	$84 \pm 9$	$18.54 \pm 0.027$	$18.41 \pm 0.038$	$18.78 \pm 0.043$	0.65	2.02	2.67	23.13	23.51	25.60	24.54	23.46	24.28	L D
201989	$77 \pm 2$	$16.75 \pm 0.011$	$16.37 \pm 0.013$	$17.10 \pm 0.017$	0.81	1.31	1.51	23.91	24.30	26.45	24.91	24.25	24.98	L D
201993	$94 \pm 4$	$18.89 \pm 0.028$	$18.69 \pm 0.035$	$19.16 \pm 0.044$	0.33	2.13	0.61	25.84	26.08	28.36	27.89	26.07	27.10	L D
202015	$48 \pm 8$	$18.80 \pm 0.029$	$18.52 \pm 0.037$	$19.10 \pm 0.046$	0.64	1.18	1.09	24.04	24.41	26.81	24.72	24.38	25.08	L D
202024	$24 \pm 6$	$17.49 \pm 0.018$	$17.11 \pm 0.022$	$17.83 \pm 0.029$	0.51	0.33	0.40	22.71	22.90	24.37	23.43	22.85	23.39	L D
202040	$96 \pm 4$	$17.33 \pm 0.018$	$17.02 \pm 0.019$	$17.65 \pm 0.028$	0.47	0.64	0.74	22.90	23.24	24.54	23.58	23.23	23.65	L D
202043	$36 \pm 2$	$16.34 \pm 0.010$	$15.98 \pm 0.011$	$16.68 \pm 0.016$	0.99	1.50	2.23	22.63	22.95	23.92	23.15	22.92	23.23	L D
202138	$88 \pm 8$	$16.31 \pm 0.008$	$16.00 \pm 0.010$	$16.63 \pm 0.014$	0.61	0.89	0.99	22.39	22.73	23.36	22.93	22.71	22.93	L D
202141	$205 \pm 33$	$17.38 \pm 0.017$	$17.08 \pm 0.016$	$17.69 \pm 0.026$	0.41	3.29	3.40	22.35	22.68	23.24	22.85	22.67	22.86	L M
202142	$146 \pm 9$	$16.09 \pm 0.008$	$15.76 \pm 0.009$	$16.41 \pm 0.012$	0.83	3.67	5.47	22.26	22.70	23.65	23.14	22.74	23.06	L M
202143	$71 \pm 3$	$18.32 \pm 0.027$	$18.04 \pm 0.034$	$18.61 \pm 0.043$	0.82	2.14	3.03	22.89	23.22	24.67	23.55	23.10	23.63	L D
202201	$45 \pm 4$	$17.29 \pm 0.015$	$16.98 \pm 0.018$	$17.60 \pm 0.024$	0.99	3.66	5.93	22.74	23.22	24.74	23.94	23.18	23.77	L M
202210	$162 \pm 5$	$17.33 \pm 0.013$	$17.27 \pm 0.019$	$17.53 \pm 0.021$	0.72	2.94	4.17	22.33	22.93	24.17	23.83	22.89	23.46	L M
202221	$38 \pm 2$	$16.92 \pm 0.017$	$16.58 \pm 0.014$	$17.26 \pm 0.026$	0.95	2.61	2.71	24.08	24.41	26.09	25.44	24.33	25.07	L D
202230	$66 \pm 8$	$17.23 \pm 0.016$	$16.84 \pm 0.017$	$17.58 \pm 0.025$	0.84	2.05	3.09	22.58	22.88	24.05	23.37	22.88	23.29	L D
202237	$128 \pm 13$	$17.73 \pm 0.020$	$17.42 \pm 0.022$	$18.05 \pm 0.032$	0.49	3.90	4.73	22.66	23.12	24.54	23.76	23.04	23.62	L M

Table 4 continued on next page

**Table 4** (*continued*)

AGC	W50	g	r	B	b/a	h(g)	$R_{eff}(g)$	$\mu_{0,g}$	$\mu_{0,B}$	$\mu_{0,B}$	$\mu_{0,B}$	$\mu_{0,B}$	T1	T2
	(km s <sup>-1</sup> )	(mag)	(mag)	(mag)		(kpc)	(kpc)	(AUTO)	( AUTO)	ISO	ISOCOR	PETRO	AVE	
202250	122± 4	16.58±0.010	16.37±0.014	16.84±0.017	0.60	1.89	2.09	22.65	22.98	23.81	23.25	22.97	23.25	L D
202257	51± 2	16.18±0.010	15.84±0.011	16.51±0.016	0.40	0.77	0.73	23.07	23.40	24.68	23.97	23.30	23.84	L D
202264	107± 4	17.68±0.017	17.41±0.020	17.99±0.027	0.94	3.83	4.08	23.50	23.80	25.07	24.60	23.63	24.28	L M
202270	191± 10	17.08±0.013	16.71±0.014	17.43±0.020	0.65	2.56	3.42	22.14	22.54	23.21	22.76	22.55	22.76	L M
202282	66± 5	17.94±0.022	17.60±0.029	18.27±0.036	0.81	2.03	2.96	22.71	23.01	24.65	23.80	22.99	23.61	L D
202328	253± 12	16.68±0.011	16.31±0.012	17.02±0.017	0.76	3.63	4.22	22.38	22.72	23.47	23.07	22.63	22.97	L M
202422	85± 10	17.79±0.017	17.69±0.027	18.00±0.028	0.59	4.81	5.12	22.40	22.68	23.86	23.49	22.57	23.15	L M
202704	89± 7	17.15±0.012	16.88±0.015	17.44±0.019	0.51	2.91	2.84	22.24	22.54	23.17	22.88	22.46	22.76	L M
202771	97± 15	17.73±0.016	17.29±0.018	18.10±0.026	0.84	3.61	6.73	22.17	22.63	23.97	23.35	22.51	23.11	S M
202854	173± 10	17.59±0.017	17.18±0.020	17.95±0.026	0.79	3.12	4.47	22.11	22.57	23.42	22.62	22.63	22.81	S M
202915	99± 12	17.11±0.013	16.88±0.018	17.39±0.021	0.93	2.28	3.59	22.32	22.75	24.05	23.31	22.72	23.21	L M
203000	128± 8	17.01±0.011	16.79±0.015	17.28±0.018	0.78	4.62	6.53	22.15	22.56	23.50	23.08	22.50	22.91	L G
203020	172± 7	17.41±0.015	17.21±0.021	17.67±0.025	0.70	4.19	5.32	22.86	23.24	24.89	23.68	23.14	23.74	L M
203082	41± 4	16.74±0.012	16.32±0.013	17.11±0.018	0.42	0.69	0.86	22.35	22.66	23.63	23.02	22.62	22.98	L D
203174	176± 7	17.01±0.013	16.61±0.013	17.37±0.020	0.89	5.15	7.61	22.09	22.53	23.34	22.57	22.33	22.69	S G
203364	73± 2	16.96±0.014	16.59±0.015	17.30±0.022	0.88	0.94	1.35	22.28	22.61	23.28	22.76	22.62	22.82	L D
203405	38± 10	17.58±0.020	17.31±0.021	17.87±0.031	0.51	5.11	6.41	22.17	22.59	23.69	23.24	22.59	23.03	L M
203515	186± 6	17.14±0.015	16.88±0.018	17.44±0.024	0.59	3.58	4.42	22.81	23.27	24.73	23.74	23.21	23.74	L M
203521	114± 9	17.35±0.014	17.04±0.015	17.67±0.022	0.44	4.98	5.06	22.37	22.73	23.32	22.83	22.77	22.91	L M
203527	87± 28	18.20±0.024	17.90±0.028	18.52±0.038	0.56	1.10	1.24	22.55	22.88	23.69	22.99	23.57	23.28	L D
203581	184± 13	17.12±0.013	16.64±0.012	17.52±0.021	0.70	4.73	7.79	21.82	22.53	23.30	22.43	22.57	22.71	S G
203647	90± 11	17.93±0.016	17.49±0.017	18.30±0.025	0.99	1.66	2.57	22.12	22.57	23.12	22.57	22.53	22.70	S M
203667	72± 7	17.17±0.012	17.11±0.017	17.36±0.019	0.57	2.32	2.59	23.14	23.40	25.47	25.19	23.34	24.35	L D
203854	98± 10	17.34±0.016	16.95±0.017	17.69±0.025	0.79	2.70	3.86	22.78	23.16	24.34	23.66	23.13	23.57	S M
203860	154± 9	17.50±0.019	16.97±0.016	17.92±0.029	0.80	1.70	2.61	23.03	23.28	24.80	23.16	23.24	23.62	L D
203874	52± 6	16.94±0.011	16.82±0.015	17.17±0.018	0.75	4.20	5.53	22.97	23.41	25.10	24.50	23.36	24.09	L M
203952	98± 6	16.93±0.012	16.47±0.011	17.32±0.019	0.92	2.79	4.57	22.03	22.51	23.18	22.54	22.55	22.70	L M
204082	59± 22	16.44±0.008	15.95±0.008	16.84±0.013	0.91	6.41	8.75	22.06	22.54	22.99	22.49	22.53	22.64	S G
204096	76± 16	17.32±0.015	16.97±0.016	17.65±0.024	0.92	2.96	5.34	22.21	22.69	23.83	23.21	22.65	23.10	L M
204112	91± 22	17.10±0.012	16.84±0.014	17.40±0.019	0.36	6.50	6.54	22.13	22.57	23.38	23.01	22.47	22.86	L M
205061	51± 11	20.65±0.055	20.34±0.064	20.97±0.087	0.43	1.63	0.38	26.26	26.77	30.12	25.77	26.81	27.37	L D
205062	54± 6	19.63±0.047	19.31±0.055	19.95±0.074	0.43	2.23	1.46	23.95	24.19	26.75	24.46	24.18	24.90	L D
205072	26± 6	18.95±0.030	18.72±0.039	19.23±0.048	0.78	0.95	1.09	23.86	24.14	26.22	25.18	24.09	24.91	L D
205078	32± 6	19.59±0.033	19.61±0.051	19.74±0.055	0.52	0.52	0.28	24.60	24.76	28.45	26.53	24.85	26.15	L D
205097	73± 8	17.91±0.019	17.41±0.020	18.32±0.030	0.63	0.72	1.18	22.48	22.88	24.46	23.00	22.76	23.28	L D
205104	43± 8	18.01±0.030	17.75±0.030	18.30±0.047	0.92	0.70	1.05	22.98	23.29	25.06	24.26	23.29	23.97	L D

Table 4 continued on next page

**Table 4** (*continued*)

AGC	W50	g	r	B	b/a	h(g)	$R_{eff}(g)$	$\mu_{0,g}$	$\mu_{0,B}$	$\mu_{0,B}$	$\mu_{0,B}$	$\mu_{0,B}$	T1	T2
		(km s <sup>-1</sup> )	(mag)	(mag)		(kpc)	(kpc)	(AUTO)	( AUTO)	ISO	ISOCOR	PETRO	AVE	
205108	26± 5	19.00±0.035	18.75±0.044	19.28±0.056	0.45	0.42	0.41	22.92	23.03	24.14	23.29	22.93	23.35	L D
205112	62± 11	18.29±0.023	17.87±0.024	18.66±0.036	0.78	1.98	2.87	22.26	22.67	23.44	22.62	22.79	22.88	L M
205148	30± 7	18.27±0.028	17.80±0.028	18.66±0.043	0.70	1.25	1.20	23.53	23.69	24.73	23.73	23.68	23.96	L D
205170	118± 11	18.39±0.026	17.99±0.029	18.75±0.041	0.83	2.01	2.95	23.02	23.34	24.87	23.75	23.29	23.81	L D
205172	153± 39	18.74±0.025	18.65±0.038	18.95±0.041	0.51	3.55	2.57	23.41	23.62	25.09	24.80	23.49	24.25	L D
205195	156± 6	17.84±0.019	17.65±0.025	18.10±0.031	0.62	2.70	3.89	22.18	22.55	23.91	23.52	22.49	23.12	L M
205197	42± 6	19.40±0.040	19.11±0.052	19.71±0.064	0.80	0.14	0.23	22.36	22.58	23.74	23.19	22.51	23.00	L D
205205	103± 6	18.09±0.027	17.83±0.033	18.39±0.043	0.39	1.21	1.26	22.84	23.17	24.53	22.25	23.05	23.25	L D
205216	40± 3	18.54±0.023	18.39±0.033	18.79±0.038	0.58	0.81	1.07	22.66	23.07	24.49	23.81	22.89	23.56	L D
205222	104± 6	17.40±0.013	16.99±0.016	17.76±0.021	0.64	3.88	5.57	22.42	22.86	24.14	23.54	22.87	23.35	S M
205260	329± 9	17.49±0.016	17.36±0.021	17.71±0.025	0.56	5.27	6.14	22.40	22.67	23.64	23.14	22.58	23.01	L M
205336	77± 12	21.21±0.092	21.05±0.117	21.46±0.146	0.57	2.30	1.25	24.84	25.35	28.25	23.90	25.35	25.71	U D
205347	139± 8	17.24±0.014	16.90±0.014	17.56±0.021	0.69	2.90	3.28	22.61	22.99	23.62	23.06	22.94	23.15	L M
205413	184± 4	16.31±0.009	15.87±0.010	16.69±0.015	0.65	3.47	4.70	22.36	22.71	23.75	23.12	22.65	23.06	L M
206787	269± 5	16.33±0.007	15.87±0.008	16.71±0.012	0.52	6.32	7.69	21.96	22.51	23.10	22.57	22.45	22.66	L G
207024	58± 6	17.86±0.018	17.52±0.021	18.18±0.029	0.70	1.71	2.26	22.66	22.99	24.26	23.43	22.83	23.38	L D
207028	139± 14	17.65±0.023	17.34±0.022	17.97±0.036	0.66	1.96	3.59	22.05	22.58	24.18	23.43	22.59	23.19	L M
207036	35± 5	18.88±0.033	18.65±0.038	19.16±0.052	0.79	1.22	1.34	23.92	24.37	26.48	23.21	24.30	24.59	L D
208307	67± 8	18.28±0.025	18.02±0.028	18.58±0.039	0.68	2.99	3.44	23.26	23.75	25.32	24.25	23.57	24.22	L D
208309	55± 6	18.66±0.029	18.23±0.033	19.03±0.045	0.91	2.47	3.34	23.51	24.01	26.28	21.90	23.99	24.05	U D
208313	81± 24	18.01±0.026	17.61±0.025	18.37±0.040	0.82	3.15	4.30	23.05	23.23	24.77	23.02	23.16	23.54	S M
208359	102± 9	17.93±0.023	17.75±0.027	18.19±0.036	0.82	2.99	4.40	22.47	22.76	23.91	23.10	22.72	23.12	L M
208364	97± 3	16.93±0.012	16.58±0.014	17.26±0.020	0.86	2.36	3.65	22.23	22.70	23.58	23.00	22.63	22.97	L M
208368	63± 10	19.39±0.051	19.00±0.052	19.74±0.079	0.39	1.65	1.88	23.10	23.29	25.68	21.48	23.25	23.43	S D
208385	113± 2	17.10±0.014	16.89±0.018	17.38±0.022	0.53	1.74	2.23	22.44	22.67	23.83	23.18	22.62	23.07	L D
208395	26± 10	18.62±0.041	18.36±0.037	18.91±0.063	0.80	2.04	2.84	22.63	22.94	23.84	23.39	22.88	23.26	L D
208397	33± 8	19.09±0.038	18.90±0.044	19.35±0.060	0.71	0.13	0.18	22.89	23.15	25.11	24.36	23.14	23.94	L D
208434	60± 13	18.83±0.030	18.56±0.033	19.12±0.047	0.55	0.46	0.63	22.14	22.56	23.39	22.93	22.54	22.86	L D
208435	105± 8	18.40±0.027	18.13±0.029	18.69±0.042	0.64	1.02	1.43	22.68	22.97	24.28	23.32	22.92	23.37	L D
210111	60± 3	18.19±0.014	18.06±0.017	18.42±0.022	0.55	0.79	0.18	24.37	24.48	24.83	24.74	24.06	24.53	L D
210861	79± 2	15.78±0.009	15.43±0.008	16.12±0.014	0.71	0.82	0.96	22.31	22.65	23.14	22.77	22.63	22.80	L D
212837	22± 3	16.87±0.011	16.57±0.014	17.19±0.017	0.77	0.64	0.63	24.03	24.27	26.61	25.51	24.21	25.15	L D
212838	22± 2	17.18±0.012	17.00±0.018	17.44±0.020	0.48	0.52	0.41	23.49	23.54	25.29	25.07	23.46	24.34	L D
212839	85± 2	16.17±0.011	15.80±0.012	16.52±0.017	0.61	1.02	1.21	23.19	23.44	25.24	23.48	23.42	23.90	L D
213086	62± 3	17.65±0.024	17.39±0.027	17.94±0.037	0.71	1.92	2.57	22.34	22.69	24.08	23.52	22.60	23.22	L D
213283	149± 15	17.59±0.018	17.22±0.021	17.93±0.028	0.62	2.14	2.64	22.34	22.54	23.30	22.57	22.53	22.74	L D

Table 4 continued on next page

**Table 4** (*continued*)

AGC	W50	g	r	B	b/a	h(g)	$R_{eff}(g)$	$\mu_{0,g}$	$\mu_{0,B}$	$\mu_{0,B}$	$\mu_{0,B}$	$\mu_{0,B}$	T1	T2
	(km s <sup>-1</sup> )	(mag)	(mag)	(mag)		(kpc)	(kpc)	(AUTO)	( AUTO)	ISO	ISOCOR	PETRO	AVE	
213316	187± 4	17.44±0.019	17.07±0.020	17.78±0.030	0.66	3.45	4.57	22.38	22.81	23.88	23.05	22.84	23.15	L M
213404	119± 12	17.57±0.016	17.23±0.019	17.90±0.026	0.90	3.77	5.81	22.22	22.71	23.69	23.14	22.59	23.03	L M
213423	86± 12	17.47±0.017	17.18±0.022	17.78±0.028	0.76	2.38	3.21	22.81	23.15	24.51	23.65	23.11	23.60	L D
213473	246± 88	17.54±0.016	17.22±0.018	17.85±0.026	0.90	3.31	4.81	22.06	22.51	23.16	22.50	22.43	22.65	L M
213482	70± 13	17.89±0.023	17.53±0.024	18.23±0.035	0.97	3.82	5.74	22.14	22.52	23.31	22.75	22.45	22.76	L M
213516	350± 9	16.76±0.011	16.28±0.011	17.16±0.017	0.82	4.20	6.61	21.97	22.52	23.29	22.69	22.42	22.73	S M
213828	101± 7	17.61±0.021	17.41±0.025	17.88±0.033	0.85	1.73	2.66	22.55	22.85	24.27	23.41	22.80	23.33	L D
213845	132± 5	17.07±0.015	16.76±0.017	17.38±0.024	0.70	3.39	4.24	22.87	24.14	25.63	24.85	24.09	24.68	L M
213932	136± 10	17.77±0.020	17.32±0.018	18.16±0.031	0.77	3.82	5.61	22.57	23.12	24.43	23.66	22.90	23.52	L M
214042	43± 7	17.22±0.019	16.78±0.019	17.60±0.029	0.92	4.71	7.23	22.46	22.92	24.22	21.90	22.88	22.98	S M
214098	142± 3	17.01±0.014	16.70±0.017	17.32±0.022	0.53	3.72	4.63	22.72	23.08	24.62	23.73	23.04	23.62	L M
214132	107± 8	17.16±0.013	16.84±0.016	17.48±0.021	0.80	4.17	5.89	22.23	22.71	23.68	23.06	22.68	23.03	L M
214172	213± 79	17.79±0.023	17.46±0.023	18.11±0.035	0.83	1.81	2.79	22.33	22.75	23.74	22.83	22.66	22.99	L D
214194	85± 31	17.54±0.021	17.17±0.021	17.89±0.033	0.79	2.04	2.88	22.48	22.78	23.78	22.83	22.77	23.04	L D
214276	89± 29	17.55±0.019	17.28±0.023	17.84±0.030	0.47	2.80	3.22	22.30	22.65	23.77	22.98	22.58	23.00	L M
214281	67± 10	17.51±0.021	17.04±0.020	17.91±0.033	0.84	5.18	7.56	22.82	23.22	24.72	23.09	23.20	23.56	S M
214282	20± 5	17.75±0.020	17.49±0.023	18.05±0.031	0.78	0.72	1.07	22.32	22.66	23.74	23.03	22.61	23.01	L D
214358	145± 4	16.91±0.011	16.64±0.014	17.21±0.018	0.77	2.48	4.05	22.28	22.72	24.03	23.54	22.62	23.23	L M
214562	105± 15	17.43±0.022	17.06±0.018	17.78±0.034	0.85	3.01	5.20	22.12	22.59	23.69	23.02	22.49	22.95	S M
215135	102± 2	17.69±0.022	17.27±0.021	18.06±0.035	0.62	1.41	2.09	22.68	22.96	24.44	22.91	22.93	23.31	L D
215138	102± 7	19.04±0.029	18.90±0.041	19.27±0.047	0.63	2.45	2.31	23.75	23.83	26.14	25.20	23.77	24.74	L D
215143	108± 6	17.23±0.022	17.13±0.024	17.45±0.034	0.56	2.11	2.20	22.33	22.56	23.54	23.16	22.52	22.95	L D
215146	122± 10	17.37±0.017	17.34±0.025	17.56±0.028	0.60	2.97	3.51	22.93	23.26	25.09	24.42	23.21	24.00	L M
215147	157± 4	15.44±0.005	14.85±0.004	15.89±0.008	0.51	14.51	12.73	22.14	23.27	23.83	23.39	23.17	23.42	S G
215151	73± 4	18.39±0.036	18.01±0.033	18.74±0.056	0.62	1.26	1.45	23.32	23.58	25.36	24.26	23.47	24.17	S D
215197	100± 7	17.67±0.019	17.24±0.020	18.05±0.029	0.50	1.23	1.57	22.38	22.72	23.77	23.13	22.68	23.08	L D
215198	337± 23	18.41±0.025	18.32±0.037	18.63±0.041	0.42	3.34	3.83	22.31	22.55	23.81	23.33	22.50	23.05	L M
215213	68± 1	17.24±0.017	16.86±0.020	17.58±0.028	0.30	0.52	0.43	23.34	23.69	25.25	22.65	23.70	23.82	L D
215222	154± 8	17.12±0.016	16.77±0.018	17.46±0.025	0.54	3.55	4.29	22.74	23.16	24.56	23.57	23.19	23.62	L M
215227	276± 11	19.05±0.039	18.67±0.045	19.40±0.062	0.39	0.71	0.82	22.43	22.59	23.90	23.14	22.59	23.05	L D
215237	151± 4	18.52±0.028	18.21±0.036	18.84±0.044	0.73	3.31	3.50	23.54	23.96	25.99	24.68	23.93	24.64	L D
215239	122± 2	17.91±0.020	17.85±0.026	18.11±0.032	0.60	3.66	4.89	22.36	22.91	24.19	23.57	22.82	23.37	L M
215246	43± 8	17.75±0.024	17.32±0.024	18.12±0.037	0.80	1.30	1.76	23.29	23.68	25.41	21.75	23.67	23.63	L D
215256	105± 11	16.26±0.010	15.71±0.010	16.69±0.016	0.36	1.15	1.15	22.43	22.74	23.53	22.52	22.78	22.89	L D
215259	163± 8	19.12±0.044	18.48±0.041	19.60±0.068	0.93	1.52	1.99	23.62	24.15	26.45	22.19	24.10	24.22	S D
215262	63± 6	17.72±0.020	17.40±0.024	18.04±0.032	0.44	0.51	0.55	22.71	22.90	24.08	23.56	22.92	23.36	U D

Table 4 continued on next page

**Table 4** (*continued*)

AGC	W50	g	r	B	b/a	h(g)	$R_{eff}(g)$	$\mu_{0,g}$	$\mu_{0,B}$	$\mu_{0,B}$	$\mu_{0,B}$	$\mu_{0,B}$	T1	T2
		(km s <sup>-1</sup> )	(mag)	(mag)	(mag)	(kpc)	(kpc)	(AUTO)	( AUTO)	ISO	ISOCOR	PETRO	AVE	
215265	$125 \pm 7$	$17.82 \pm 0.019$	$17.59 \pm 0.025$	$18.09 \pm 0.031$	0.47	3.81	5.27	22.61	23.02	25.04	24.06	22.96	23.77	L M
215280	$93 \pm 4$	$18.06 \pm 0.018$	$17.80 \pm 0.024$	$18.36 \pm 0.030$	0.34	0.57	0.59	23.03	23.52	25.33	24.92	23.44	24.30	L D
215283	$109 \pm 3$	$18.98 \pm 0.030$	$18.69 \pm 0.038$	$19.29 \pm 0.048$	0.53	2.96	2.17	24.34	24.54	27.31	25.69	24.53	25.52	L D
215290	$42 \pm 3$	$17.31 \pm 0.014$	$17.05 \pm 0.017$	$17.60 \pm 0.023$	0.62	0.82	0.83	23.71	24.27	27.83	25.86	24.36	25.58	L D
215315	$114 \pm 12$	$17.69 \pm 0.017$	$17.61 \pm 0.023$	$17.90 \pm 0.028$	0.51	5.28	5.86	22.66	23.07	24.52	24.12	23.01	23.68	L M
215420	$116 \pm 6$	$18.07 \pm 0.024$	$17.86 \pm 0.029$	$18.34 \pm 0.038$	0.84	2.35	2.97	23.48	23.81	26.08	24.40	23.80	24.52	L D
215425	$53 \pm 10$	$17.13 \pm 0.017$	$16.88 \pm 0.016$	$17.42 \pm 0.027$	0.61	3.42	4.84	22.91	23.32	25.50	24.78	23.30	24.23	L M
215428	$55 \pm 11$	$19.30 \pm 0.053$	$18.93 \pm 0.044$	$19.65 \pm 0.081$	0.94	1.74	1.94	24.18	24.52	26.99	25.52	24.42	25.36	S D
215630	$113 \pm 5$	$17.55 \pm 0.017$	$17.30 \pm 0.019$	$17.84 \pm 0.026$	0.59	2.09	2.66	22.30	22.65	23.46	22.83	22.62	22.89	L D
215716	$100 \pm 13$	$17.34 \pm 0.016$	$16.96 \pm 0.017$	$17.69 \pm 0.025$	0.32	1.24	1.27	22.22	22.57	23.25	22.58	22.55	22.74	L D
217459	$158 \pm 45$	$18.65 \pm 0.035$	$18.23 \pm 0.035$	$19.02 \pm 0.054$	0.90	2.50	2.56	23.87	24.24	25.63	24.12	24.03	24.50	L D
219093	$67 \pm 7$	$17.89 \pm 0.023$	$17.66 \pm 0.026$	$18.17 \pm 0.037$	0.66	3.16	4.15	23.39	24.00	27.00	22.74	24.01	24.44	L D
219128	$36 \pm 8$	$19.12 \pm 0.040$	$18.80 \pm 0.042$	$19.44 \pm 0.062$	0.85	1.86	3.11	22.38	22.95	24.42	23.50	22.86	23.43	L D
219195	$95 \pm 6$	$17.73 \pm 0.020$	$17.50 \pm 0.024$	$18.01 \pm 0.032$	0.53	2.91	3.12	22.47	22.75	23.77	23.14	22.72	23.09	L M
219198	$67 \pm 8$	$18.80 \pm 0.034$	$18.46 \pm 0.040$	$19.12 \pm 0.054$	0.77	0.83	0.90	23.74	24.22	26.75	22.40	24.11	24.37	L D
219201	$24 \pm 8$	$18.58 \pm 0.029$	$18.45 \pm 0.037$	$18.80 \pm 0.046$	0.89	0.40	0.61	23.00	23.18	25.23	23.82	23.14	23.84	L D
219203	$28 \pm 7$	$18.05 \pm 0.025$	$17.77 \pm 0.028$	$18.36 \pm 0.040$	0.52	0.58	0.72	22.74	23.33	24.81	23.75	23.19	23.77	L D
219206	$138 \pm 4$	$18.45 \pm 0.032$	$18.13 \pm 0.037$	$18.77 \pm 0.051$	0.41	2.44	2.20	22.96	23.39	24.53	23.75	23.33	23.75	L D
219209	$130 \pm 9$	$18.57 \pm 0.028$	$18.15 \pm 0.030$	$18.94 \pm 0.043$	0.64	0.95	1.27	22.21	22.57	23.22	21.97	22.57	22.58	L D
219212	$44 \pm 4$	$18.32 \pm 0.025$	$18.07 \pm 0.033$	$18.61 \pm 0.041$	0.49	1.81	2.49	22.64	22.96	24.65	23.33	22.87	23.45	L D
219232	$48 \pm 10$	$20.14 \pm 0.074$	$19.61 \pm 0.069$	$20.56 \pm 0.114$	0.59	1.14	1.57	22.47	22.86	24.06	22.65	22.86	23.11	L D
219237	$94 \pm 20$	$16.90 \pm 0.013$	$16.60 \pm 0.014$	$17.21 \pm 0.021$	0.74	2.66	3.24	22.35	22.53	23.61	23.25	22.48	22.97	L M
219238	$150 \pm 16$	$18.28 \pm 0.026$	$18.19 \pm 0.035$	$18.49 \pm 0.042$	0.76	1.79	2.85	22.39	22.82	24.20	23.59	22.75	23.34	L D
219240	$30 \pm 5$	$18.65 \pm 0.032$	$18.48 \pm 0.038$	$18.91 \pm 0.050$	0.75	4.07	5.21	23.07	23.49	25.32	24.47	23.37	24.16	L M
219244	$26 \pm 5$	$18.82 \pm 0.034$	$18.39 \pm 0.033$	$19.20 \pm 0.053$	0.91	3.88	3.78	24.18	24.46	26.13	24.86	24.31	24.94	L D
219245	$85 \pm 25$	$17.92 \pm 0.022$	$17.64 \pm 0.025$	$18.22 \pm 0.034$	0.35	1.25	1.28	22.51	22.77	23.75	23.16	22.69	23.09	L D
219246	$94 \pm 6$	$18.77 \pm 0.032$	$18.49 \pm 0.038$	$19.07 \pm 0.051$	0.43	1.29	1.42	22.52	22.79	23.97	23.52	22.74	23.25	L D
219247	$215 \pm 6$	$18.94 \pm 0.031$	$18.85 \pm 0.042$	$19.15 \pm 0.050$	0.36	1.73	1.65	22.97	23.14	25.35	24.46	23.07	24.00	L D
219253	$289 \pm 76$	$18.23 \pm 0.026$	$17.91 \pm 0.029$	$18.55 \pm 0.041$	0.52	2.59	2.84	23.16	23.58	25.25	24.24	23.51	24.14	L D
219307	$48 \pm 8$	$19.33 \pm 0.049$	$19.19 \pm 0.058$	$19.56 \pm 0.077$	0.87	0.68	1.12	23.02	23.39	25.41	24.41	23.28	24.12	L D
219355	$71 \pm 10$	$19.09 \pm 0.039$	$18.86 \pm 0.053$	$19.36 \pm 0.063$	0.67	1.19	1.37	23.04	23.61	25.49	23.52	23.49	24.03	L D
220005	$75 \pm 0$	$17.92 \pm 0.020$	$17.66 \pm 0.024$	$18.21 \pm 0.031$	0.59	3.64	3.85	23.55	23.92	26.07	24.77	23.87	24.66	L D
220006	$133 \pm 39$	$17.47 \pm 0.018$	$17.14 \pm 0.020$	$17.80 \pm 0.028$	0.65	4.46	6.00	22.43	23.02	24.22	23.47	22.92	23.41	L M
220025	$38 \pm 4$	$16.79 \pm 0.013$	$16.31 \pm 0.012$	$17.19 \pm 0.020$	0.68	2.61	5.46	21.89	22.86	24.48	23.28	22.78	23.35	S M
220172	$40 \pm 3$	$17.67 \pm 0.019$	$17.33 \pm 0.023$	$18.01 \pm 0.030$	0.66	0.36	0.44	22.49	22.72	23.49	22.89	22.75	22.96	L D
220195	$25 \pm 13$	$17.58 \pm 0.021$	$17.15 \pm 0.022$	$17.94 \pm 0.033$	0.87	0.47	0.77	22.42	22.69	23.74	23.05	22.62	23.02	L D

Table 4 continued on next page

**Table 4** (*continued*)

AGC	W50	g	r	B	b/a	h(g)	$R_{eff}(g)$	$\mu_{0,g}$	$\mu_{0,B}$	$\mu_{0,B}$	$\mu_{0,B}$	$\mu_{0,B}$	T1	T2
	(km s <sup>-1</sup> )	(mag)	(mag)	(mag)		(kpc)	(kpc)	(AUTO)	( AUTO)	ISO	ISOCOR	PETRO	AVE	
220237	101± 1	16.42±0.011	15.97±0.011	16.80±0.018	0.67	4.07	4.34	22.78	23.07	23.79	22.82	23.03	23.18	L M
220242	26± 1	16.85±0.013	16.56±0.015	17.16±0.021	0.52	1.59	1.93	23.31	24.03	26.30	24.09	23.99	24.60	L D
220257	60± 3	16.84±0.018	16.45±0.016	17.19±0.027	0.62	0.68	0.80	22.96	23.27	24.67	23.76	23.21	23.73	U D
220261	21± 8	20.14±0.040	20.00±0.053	20.37±0.065	0.74	0.77	0.21	26.74	26.83	30.13	28.25	26.91	28.03	L D
220299	93± 4	17.54±0.021	17.31±0.021	17.81±0.033	0.37	3.41	3.01	23.64	23.87	26.06	25.32	23.78	24.76	L D
220304	39± 6	16.59±0.013	16.22±0.014	16.93±0.020	0.82	1.10	1.39	23.22	23.52	25.01	23.64	23.45	23.91	L D
220319	158± 72	17.68±0.027	17.39±0.024	17.99±0.041	0.75	2.58	3.58	22.54	22.88	23.99	23.38	22.93	23.30	L M
220320	154± 3	16.15±0.009	15.81±0.011	16.48±0.014	0.80	4.08	5.64	22.70	23.16	24.84	24.04	23.08	23.78	L M
220336	37± 1	16.26±0.009	16.00±0.011	16.55±0.014	0.67	0.70	1.01	22.52	22.79	24.19	23.74	22.70	23.35	L D
220351	72± 3	16.14±0.010	15.77±0.010	16.48±0.016	0.42	0.87	0.86	22.34	22.58	23.29	22.88	22.55	22.83	L D
220352	73± 22	17.86±0.024	17.62±0.031	18.14±0.039	0.70	0.76	0.81	23.63	23.90	26.58	23.31	23.94	24.43	L D
220366	29± 1	17.79±0.017	17.66±0.020	18.02±0.026	0.52	0.45	0.57	22.84	22.97	26.13	24.82	23.04	24.24	L D
220435	24± 9	20.23±0.046	19.98±0.059	20.51±0.073	0.75	0.60	0.20	26.27	26.55	28.65	27.88	27.09	27.55	L D
220450	25± 6	16.46±0.009	16.22±0.011	16.74±0.014	0.81	1.32	1.14	24.29	24.15	26.77	25.65	24.13	25.18	L D
220460	28± 7	16.62±0.014	16.15±0.015	17.02±0.022	0.53	0.78	0.93	22.91	23.23	24.58	23.46	23.23	23.63	L D
220478	43± 3	16.65±0.014	16.32±0.015	16.98±0.022	0.44	0.73	0.74	22.52	22.76	23.67	23.02	22.84	23.07	L D
220483	40± 16	21.08±0.116	20.13±0.074	21.69±0.175	0.78	0.64	0.27	27.35	27.97	30.95	26.51	27.79	28.30	S D
220509	55± 12	17.25±0.017	16.92±0.019	17.57±0.027	0.48	3.60	4.26	22.57	22.89	23.94	23.13	22.80	23.19	L M
220561	33± 2	18.73±0.032	18.26±0.031	19.12±0.050	0.86	0.42	0.41	24.21	24.56	27.75	23.43	24.57	25.08	L D
220580	115± 18	16.86±0.014	16.42±0.014	17.24±0.022	0.30	2.85	2.65	22.42	22.77	23.64	22.70	22.75	22.96	L D
220597	48± 2	16.83±0.013	16.44±0.015	17.18±0.020	0.69	0.59	0.76	22.72	22.99	24.09	23.32	22.92	23.33	L D
220603	24± 12	16.38±0.011	16.02±0.012	16.71±0.017	0.98	0.70	1.05	22.35	22.60	23.27	22.77	22.59	22.81	L D
220609	20± 7	16.75±0.014	16.28±0.013	17.14±0.021	0.76	0.58	0.91	22.78	23.05	24.38	23.71	23.00	23.54	L D
220762	88± 3	16.04±0.009	15.77±0.011	16.33±0.015	0.44	1.16	1.22	22.93	23.19	24.78	24.02	23.14	23.78	L D
220767	98± 5	16.60±0.010	16.28±0.011	16.92±0.015	0.80	3.34	5.26	22.24	22.64	23.70	23.28	22.58	23.05	L M
220780	80± 3	15.30±0.008	14.78±0.006	15.71±0.012	0.63	0.99	1.21	22.24	22.62	23.16	22.65	22.60	22.76	S D
220812	80± 11	17.47±0.017	17.14±0.019	17.79±0.027	0.52	0.40	0.49	22.29	22.50	23.19	22.75	22.45	22.72	L D
220863	50± 2	17.64±0.032	15.99±0.011	18.59±0.047	0.36	0.79	0.65	23.49	24.44	25.57	23.73	24.46	24.55	S D
220939	68± 3	16.42±0.010	16.17±0.011	16.72±0.015	0.48	0.67	0.72	22.24	22.51	23.24	22.77	22.37	22.72	L D
220944	58± 9	16.36±0.010	16.10±0.013	16.65±0.017	0.71	0.99	1.08	23.43	23.69	25.48	24.30	23.63	24.28	L D
220956	50± 9	16.11±0.010	15.87±0.012	16.39±0.016	0.55	0.89	0.99	22.69	22.96	23.96	23.46	22.91	23.32	L D
221078	107± 6	17.21±0.015	16.97±0.017	17.50±0.024	0.86	2.86	4.64	22.37	23.05	24.26	23.41	22.93	23.41	L M
221085	89± 1	16.67±0.012	16.37±0.015	16.98±0.019	0.48	0.79	0.98	22.83	23.11	24.58	23.77	23.04	23.62	L D
222021	27± 8	21.04±0.078	20.82±0.077	21.31±0.120	0.34	0.14	0.13	23.10	23.38	26.07	25.84	23.47	24.69	L D
222099	92± 7	17.58±0.019	17.22±0.021	17.91±0.030	0.67	2.02	2.23	23.57	23.86	25.85	24.29	23.80	24.45	L D
222857	102± 10	19.30±0.039	18.82±0.037	19.69±0.060	0.57	0.53	0.39	24.76	25.34	27.89	23.50	25.27	25.50	L D

Table 4 continued on next page

**Table 4** (*continued*)

AGC	W50	g	r	B	b/a	h(g)	$R_{eff}(g)$	$\mu_{0,g}$	$\mu_{0,B}$	$\mu_{0,B}$	$\mu_{0,B}$	$\mu_{0,B}$	T1	T2
	(km s <sup>-1</sup> )	(mag)	(mag)	(mag)		(kpc)	(kpc)	(AUTO)	( AUTO)	ISO	ISOCOR	PETRO	AVE	
222966	40± 12	19.15±0.028	18.98±0.037	19.39±0.046	0.98	2.52	2.39	24.35	24.63	26.83	26.53	24.54	25.63	L D
223205	40± 1	17.19±0.016	16.87±0.019	17.52±0.026	0.70	0.52	0.62	22.92	23.26	24.32	23.37	23.22	23.54	L D
223219	49± 5	16.72±0.010	16.34±0.011	17.07±0.016	0.63	1.32	1.67	23.17	23.47	25.24	24.51	23.36	24.15	L D
223247	48± 2	18.72±0.023	18.53±0.028	18.98±0.037	0.56	0.27	0.35	22.80	22.96	26.93	25.30	23.09	24.57	L D
223279	121± 5	17.66±0.021	17.57±0.024	17.88±0.033	0.31	2.72	2.51	22.32	22.61	23.71	23.42	22.54	23.07	L D
223295	151± 16	18.22±0.027	18.08±0.034	18.45±0.043	0.36	2.72	3.10	22.63	23.04	24.64	23.45	23.01	23.53	L D
223372	157± 2	17.80±0.019	17.39±0.020	18.16±0.030	0.66	2.36	3.49	22.68	23.07	24.62	23.78	23.09	23.64	L D
223392	83± 6	17.33±0.017	16.96±0.018	17.68±0.026	0.47	1.06	1.14	22.74	23.13	23.97	22.76	23.04	23.23	L D
223437	35± 2	17.74±0.023	17.44±0.025	18.06±0.037	0.97	2.26	3.48	22.79	23.23	24.77	23.63	23.18	23.70	L M
223445	111± 16	17.30±0.019	16.75±0.018	17.74±0.030	0.86	0.66	0.81	23.68	24.01	25.75	22.17	23.98	23.98	L D
223470	35± 16	19.60±0.053	19.30±0.049	19.91±0.081	0.96	1.49	1.01	25.11	25.42	28.66	24.51	25.37	25.99	L D
223471	126± 7	18.88±0.033	18.66±0.040	19.15±0.052	0.49	2.22	2.32	23.41	23.81	26.03	24.13	23.78	24.44	L D
223555	80± 8	18.09±0.024	17.69±0.027	18.45±0.038	0.96	1.86	2.42	23.95	24.38	27.14	22.95	24.34	24.70	L D
223760	108± 25	19.63±0.048	19.11±0.041	20.05±0.074	0.62	1.40	1.21	24.29	24.65	27.31	23.08	24.68	24.93	L D
223805	89± 18	18.08±0.031	17.79±0.029	18.38±0.048	0.88	2.07	3.12	23.08	23.46	25.07	24.23	23.39	24.04	L D
223819	42± 9	19.97±0.042	19.66±0.049	20.29±0.066	0.63	0.16	0.21	23.05	22.82	25.98	24.16	22.93	23.97	L D
223873	21± 3	20.61±0.067	20.28±0.077	20.93±0.105	0.56	0.10	0.17	22.66	23.06	24.70	24.00	22.74	23.63	L D
223965	120± 9	18.07±0.026	17.66±0.027	18.44±0.041	0.59	2.60	3.25	22.93	23.21	24.85	23.48	23.19	23.68	L D
224073	128± 25	18.04±0.027	17.65±0.027	18.40±0.041	0.78	2.78	3.40	23.26	23.61	25.20	22.15	23.56	23.63	S D
224075	139± 22	17.68±0.021	17.33±0.023	18.02±0.033	0.43	2.59	2.91	22.37	22.72	23.76	22.94	22.72	23.04	L D
224094	106± 5	16.98±0.012	16.74±0.015	17.27±0.019	0.58	0.90	1.33	22.33	22.63	23.89	23.47	22.59	23.14	L D
224296	39± 6	17.24±0.017	16.95±0.019	17.55±0.027	0.41	0.54	0.56	22.56	22.82	23.61	22.76	22.77	22.99	L D
224304	105± 2	15.93±0.009	15.54±0.009	16.29±0.014	0.67	2.20	3.19	22.75	23.09	24.48	23.62	23.05	23.56	S D
224335	121± 4	17.49±0.017	17.11±0.018	17.84±0.027	0.97	2.17	3.65	22.56	22.96	24.19	23.45	22.93	23.39	S M
224354	62± 8	17.30±0.015	17.04±0.018	17.59±0.024	0.69	3.67	5.15	23.00	23.48	25.19	24.32	23.46	24.11	L M
224387	39± 2	17.37±0.017	16.99±0.021	17.72±0.027	0.89	1.77	2.93	22.09	22.61	23.71	22.96	22.57	22.96	L M
224402	126± 17	16.99±0.013	16.79±0.016	17.26±0.021	0.40	4.04	4.22	22.41	22.71	23.59	23.09	22.65	23.01	L M
224414	129± 16	17.11±0.016	16.75±0.020	17.46±0.025	0.89	1.57	2.35	22.27	22.69	23.73	22.86	22.67	22.99	L D
224454	68± 2	17.52±0.015	17.33±0.020	17.78±0.025	0.92	2.12	3.35	22.32	22.78	23.83	23.32	22.69	23.16	L M
224531	118± 5	16.46±0.005	15.91±0.006	16.89±0.009	0.96	7.89	3.88	22.71	23.14	23.49	23.27	23.05	23.24	S G
224599	84± 14	17.63±0.020	17.30±0.025	17.96±0.031	0.80	2.46	3.62	22.09	22.51	23.52	22.81	22.37	22.80	L M
224877	206± 34	17.48±0.016	17.12±0.019	17.81±0.025	0.42	3.46	3.98	22.35	22.82	23.99	23.28	22.84	23.23	L M
225041	207± 53	17.29±0.013	16.86±0.013	17.67±0.020	0.38	4.68	4.31	22.22	22.63	23.11	22.61	22.61	22.74	L M
225072	318± 51	16.00±0.008	15.47±0.007	16.42±0.012	0.82	3.68	5.02	22.32	22.77	23.23	22.40	22.72	22.78	S M
225257	39± 9	18.01±0.021	17.72±0.026	18.32±0.034	0.71	4.42	6.25	22.63	23.08	24.56	23.46	23.00	23.53	L M
225297	126± 6	17.60±0.019	17.34±0.023	17.89±0.031	0.41	2.34	2.64	22.50	22.85	24.13	23.25	22.85	23.27	L D

Table 4 continued on next page

**Table 4** (*continued*)

AGC	W50	g	r	B	b/a	h(g)	$R_{eff}(g)$	$\mu_{0,g}$	$\mu_{0,B}$	$\mu_{0,B}$	$\mu_{0,B}$	$\mu_{0,B}$	T1	T2
	(km s <sup>-1</sup> )	(mag)	(mag)	(mag)		(kpc)	(kpc)	(AUTO)	( AUTO)	ISO	ISOCOR	PETRO	AVE	
225849	86± 5	16.85±0.012	16.64±0.015	17.12±0.020	0.51	0.64	0.71	22.67	22.98	23.83	23.28	22.95	23.26	L D
225873	134± 19	18.25±0.025	17.91±0.027	18.58±0.039	0.87	2.14	2.76	23.06	23.56	25.11	24.27	23.33	24.07	L D
225876	39± 9	19.21±0.038	19.05±0.054	19.45±0.062	0.53	0.18	0.22	22.37	22.58	23.52	22.97	22.51	22.90	L D
225878	37± 4	20.32±0.055	20.25±0.085	20.52±0.091	0.38	0.15	0.15	22.79	22.99	24.97	24.35	22.88	23.80	L D
225882	24± 2	17.36±0.014	17.12±0.018	17.65±0.023	0.75	1.10	1.00	23.95	24.23	25.96	25.61	24.15	24.99	U D
225945	141± 2	17.76±0.026	17.33±0.021	18.14±0.040	0.82	4.12	6.78	22.11	22.57	23.72	23.14	22.47	22.98	S M
225992	145± 11	18.30±0.026	18.16±0.030	18.54±0.041	0.46	1.70	2.22	22.32	23.04	24.43	24.05	22.97	23.62	L D
226026	133± 14	17.91±0.020	17.71±0.026	18.17±0.032	0.77	3.59	4.98	22.32	22.66	23.83	23.28	22.70	23.12	L M
226030	22± 5	18.05±0.025	17.73±0.029	18.37±0.039	0.54	1.03	1.29	23.21	23.48	25.07	24.20	23.34	24.02	L D
226069	96± 4	15.36±0.005	14.83±0.005	15.77±0.008	0.90	6.74	10.77	22.79	24.26	25.62	24.98	24.08	24.74	S G
226076	242± 34	18.03±0.019	17.75±0.024	18.34±0.031	0.68	1.84	2.50	22.20	22.55	23.37	22.98	22.58	22.87	L D
226082	123± 6	18.17±0.021	17.95±0.027	18.44±0.034	0.65	1.70	2.41	22.18	22.52	23.61	23.20	22.36	22.92	L D
226096	143± 8	17.83±0.018	17.64±0.026	18.09±0.030	0.55	3.80	4.74	22.32	22.75	23.89	23.29	22.67	23.15	L M
226122	53± 3	17.68±0.022	17.49±0.026	17.94±0.034	0.34	0.70	0.62	23.21	23.44	25.27	23.84	23.37	23.98	L D
226125	145± 12	18.29±0.035	18.02±0.033	18.59±0.054	0.39	2.07	2.44	22.44	22.76	24.05	23.42	22.74	23.24	L D
226131	37± 3	18.67±0.030	18.52±0.037	18.90±0.047	0.44	0.83	1.08	22.91	22.99	25.61	22.47	22.98	23.51	L D
226136	60± 7	18.20±0.023	18.10±0.031	18.41±0.037	0.68	2.16	2.89	22.76	22.76	24.43	23.47	22.68	23.34	L D
226138	66± 2	17.01±0.014	16.52±0.014	17.41±0.022	0.90	3.70	6.12	22.11	22.53	23.47	22.65	22.53	22.79	S M
226141	60± 17	17.39±0.019	17.04±0.021	17.73±0.030	0.95	3.58	5.24	22.71	23.08	24.46	22.88	23.04	23.37	L M
226152	74± 13	17.23±0.013	16.96±0.016	17.53±0.020	0.90	2.28	3.57	22.23	22.65	23.56	23.06	22.59	22.96	L M
226182	249± 16	17.81±0.020	17.46±0.023	18.15±0.031	0.69	1.88	2.48	22.29	22.61	23.43	22.73	22.59	22.84	L D
226360	119± 40	17.26±0.016	16.94±0.018	17.58±0.025	0.97	2.36	3.45	22.28	22.61	23.32	22.81	22.62	22.84	L M
226406	128± 16	17.54±0.019	17.11±0.020	17.91±0.030	0.37	3.23	2.95	22.93	23.27	24.49	23.56	23.23	23.64	L D
226891	67± 17	17.06±0.005	16.63±0.005	17.43±0.008	0.85	3.10	1.64	22.51	22.88	23.10	23.05	22.60	22.91	S M
227878	48± 12	20.00±0.048	19.91±0.065	20.21±0.077	0.39	2.64	1.64	24.36	24.57	27.80	23.45	24.49	25.08	L D
227882	98± 3	19.08±0.036	18.91±0.055	19.34±0.060	0.58	1.17	1.52	22.47	22.72	24.44	24.05	22.67	23.47	L D
227884	34± 16	18.61±0.039	18.35±0.037	18.90±0.061	0.72	2.28	2.87	23.04	23.33	24.91	24.25	23.22	23.93	L D
227889	20± 11	18.44±0.029	18.16±0.036	18.74±0.046	0.98	0.22	0.34	22.64	22.96	24.10	23.26	22.84	23.29	L D
227895	104± 21	20.46±0.086	19.40±0.049	21.12±0.129	0.83	0.21	0.32	23.06	23.78	24.44	20.00	23.73	22.99	S D
227896	59± 7	16.61±0.011	16.32±0.012	16.91±0.017	0.37	0.71	0.83	22.28	22.60	23.51	22.99	22.51	22.90	L D
227917	333± 7	20.53±0.085	19.91±0.076	20.99±0.130	0.85	1.55	2.65	22.76	23.10	24.98	20.77	22.99	22.96	S D
227936	81± 6	18.71±0.023	18.48±0.029	19.00±0.036	0.72	3.00	2.82	24.04	24.33	27.08	26.21	24.36	25.49	U D
227957	55± 16	19.13±0.035	19.04±0.053	19.34±0.057	0.74	1.22	1.49	23.30	23.71	25.88	24.50	23.61	24.42	L D
227962	65± 8	18.03±0.022	17.74±0.027	18.33±0.036	0.98	1.81	2.60	23.28	23.70	25.65	24.24	23.62	24.30	L D
227965	48± 6	20.91±0.067	20.37±0.063	21.33±0.103	0.99	0.98	0.64	25.31	25.71	28.77	24.51	25.79	26.19	L D
227974	31± 2	20.91±0.060	20.66±0.069	21.20±0.094	0.66	1.05	0.14	28.04	28.33	32.60	28.30	28.45	29.42	L D

Table 4 continued on next page

**Table 4** (*continued*)

AGC	W50	g	r	B	b/a	h(g)	$R_{eff}(g)$	$\mu_{0,g}$	$\mu_{0,B}$	$\mu_{0,B}$	$\mu_{0,B}$	$\mu_{0,B}$	T1	T2
	(km s <sup>-1</sup> )	(mag)	(mag)	(mag)		(kpc)	(kpc)	(AUTO)	( AUTO)	ISO	ISOCOR	PETRO	AVE	
227975	28± 5	18.88±0.035	18.80±0.050	19.09±0.057	0.91	0.18	0.27	22.56	22.74	24.25	23.80	22.64	23.36	L D
228096	136± 8	17.98±0.017	17.80±0.024	18.23±0.028	0.79	2.43	2.68	23.65	23.99	26.06	25.39	23.91	24.84	L D
228097	68± 7	17.66±0.016	17.40±0.022	17.94±0.026	0.53	4.15	4.57	23.81	24.20	26.39	25.25	24.11	24.99	L D
229034	131± 7	18.01±0.025	17.83±0.026	18.27±0.038	0.60	4.57	4.88	23.02	23.40	24.84	24.45	23.29	24.00	L M
229036	168± 6	17.94±0.020	17.80±0.026	18.18±0.032	0.63	2.86	3.80	22.24	22.52	23.77	23.41	22.43	23.03	L M
229050	25± 6	19.76±0.055	19.56±0.068	20.03±0.087	0.40	0.46	0.48	22.62	22.59	24.17	22.83	22.48	23.02	L D
229053	40± 4	18.07±0.018	17.96±0.025	18.29±0.030	0.54	0.34	0.26	24.08	24.26	27.52	25.33	24.28	25.35	L D
230077	46± 1	15.38±0.006	15.03±0.007	15.71±0.010	0.60	1.03	1.13	22.36	22.65	23.30	22.83	22.67	22.86	S D
231980	19± 2	16.79±0.012	16.52±0.015	17.09±0.019	0.69	0.13	0.15	23.55	23.85	27.11	24.16	23.89	24.75	L D
231989	86± 3	16.80±0.009	16.59±0.013	17.07±0.015	0.65	1.98	2.12	23.89	24.41	27.19	26.04	24.41	25.51	L D
232008	30± 3	20.58±0.058	20.13±0.057	20.96±0.090	0.36	0.94	0.77	23.82	24.24	28.28	24.09	24.31	25.23	L D
232025	45± 4	15.62±0.010	15.18±0.008	15.99±0.015	0.52	0.88	1.14	22.35	22.63	23.83	23.32	22.59	23.09	L D
232147	69± 7	16.75±0.011	16.42±0.013	17.08±0.017	0.87	1.92	2.78	22.46	22.82	23.69	23.19	22.82	23.13	L D
232158	70± 14	16.91±0.012	16.86±0.018	17.11±0.020	0.60	3.35	3.73	22.41	22.67	23.60	23.06	22.57	22.98	L M
232235	87± 6	16.48±0.011	16.07±0.012	16.85±0.017	0.74	3.62	5.28	22.35	22.67	23.71	23.14	22.69	23.05	S M
232247	95± 6	17.11±0.013	16.74±0.015	17.45±0.021	0.99	2.13	3.35	22.21	22.57	23.21	22.81	22.47	22.77	S M
232337	130± 25	16.77±0.010	16.47±0.013	17.09±0.016	0.94	3.89	5.57	22.24	22.52	23.05	22.53	22.52	22.66	L M
232380	88± 2	16.60±0.010	16.28±0.011	16.92±0.016	0.96	1.72	2.60	22.26	22.69	23.51	23.15	22.68	23.01	L M
232412	48± 10	17.18±0.015	16.82±0.016	17.52±0.023	0.92	2.20	3.39	22.20	22.61	23.41	22.69	22.57	22.82	L M
232735	124± 2	17.23±0.016	16.92±0.018	17.54±0.025	0.69	1.52	1.84	22.62	22.80	23.69	23.12	22.93	23.14	L D
232746	89± 9	17.83±0.020	17.58±0.023	18.12±0.032	0.69	2.01	3.14	22.31	22.63	23.90	23.43	22.57	23.13	L D
232871	180± 7	17.81±0.019	17.62±0.024	18.07±0.030	0.57	2.34	3.03	22.25	22.71	23.80	23.18	22.71	23.10	L M
232879	148± 12	16.74±0.012	16.45±0.015	17.04±0.020	0.58	3.37	4.10	22.53	22.87	24.04	23.17	22.82	23.23	L M
232892	148± 11	16.97±0.013	16.69±0.016	17.27±0.021	0.99	2.54	3.75	22.36	22.72	23.68	23.12	22.71	23.06	L M
232898	34± 5	17.09±0.017	16.59±0.016	17.49±0.026	0.84	2.61	3.80	22.54	22.92	23.92	22.78	23.03	23.16	S M
232903	173± 21	17.91±0.023	17.59±0.027	18.23±0.037	0.85	4.02	5.70	22.97	23.49	25.14	22.91	23.44	23.75	L M
233559	36± 7	19.56±0.051	19.29±0.047	19.86±0.078	0.73	0.40	0.30	24.82	25.12	28.14	25.82	25.11	26.05	L D
233560	109± 7	17.83±0.021	17.65±0.026	18.09±0.033	0.59	1.69	1.85	22.92	23.14	24.52	23.67	23.07	23.60	L D
233571	110± 2	16.13±0.008	15.98±0.010	16.37±0.013	0.57	1.02	1.39	22.34	22.61	23.73	23.33	22.62	23.07	L D
233574	70± 1	17.01±0.015	16.63±0.016	17.36±0.023	0.60	1.50	1.79	23.44	23.81	25.91	22.56	23.79	24.02	L D
233583	119± 5	16.88±0.014	16.61±0.017	17.17±0.023	0.74	1.53	2.98	22.11	22.55	24.12	22.84	22.42	22.98	L D
233601	100± 3	17.12±0.015	16.88±0.018	17.41±0.024	0.58	0.95	1.03	23.24	23.60	25.51	24.44	23.53	24.27	L D
233605	119± 26	17.11±0.012	16.84±0.016	17.41±0.020	0.73	3.91	5.41	22.19	22.64	23.59	23.18	22.57	22.99	L M
233610	71± 20	18.64±0.028	18.62±0.040	18.83±0.046	0.42	2.70	2.56	23.09	23.27	25.42	24.84	23.21	24.19	L D
233611	151± 44	18.13±0.021	17.86±0.029	18.43±0.035	0.62	2.61	3.52	22.25	22.66	23.74	23.12	22.59	23.03	L M
233613	29± 1	18.67±0.034	18.27±0.037	19.04±0.054	0.80	1.26	1.79	22.45	22.71	23.56	22.65	22.84	22.94	L D

Table 4 continued on next page

**Table 4** (*continued*)

AGC	W50	g	r	B	b/a	h(g)	$R_{eff}(g)$	$\mu_{0,g}$	$\mu_{0,B}$	$\mu_{0,B}$	$\mu_{0,B}$	$\mu_{0,B}$	T1	T2
	(km s <sup>-1</sup> )	(mag)	(mag)	(mag)		(kpc)	(kpc)	(AUTO)	( AUTO)	ISO	ISOCOR	PETRO	AVE	
233615	93± 7	18.52±0.028	18.29±0.036	18.80±0.045	0.43	1.21	1.38	22.97	23.35	25.19	23.78	23.29	23.90	L D
233616	61± 3	18.38±0.026	18.11±0.029	18.68±0.041	0.79	2.78	3.45	23.31	23.73	25.59	24.34	23.62	24.32	L D
233624	116± 18	20.42±0.058	20.29±0.081	20.65±0.093	0.98	2.67	1.21	25.46	25.70	27.42	27.26	25.69	26.52	L D
233628	84± 3	17.21±0.016	17.06±0.019	17.45±0.025	0.73	3.01	4.14	22.72	22.72	24.17	23.94	22.63	23.37	L M
233629	137± 10	18.28±0.025	17.91±0.027	18.63±0.039	0.50	2.16	2.79	22.76	23.11	24.63	23.67	23.11	23.63	S D
233630	57± 1	18.01±0.024	17.82±0.031	18.27±0.039	0.96	3.43	5.18	22.90	23.28	25.12	23.54	23.26	23.80	L M
233633	67± 2	19.10±0.041	18.86±0.050	19.38±0.065	0.71	0.88	1.28	22.90	23.00	24.89	23.45	22.89	23.56	L D
233635	160± 4	17.64±0.018	17.30±0.018	17.96±0.028	0.31	3.38	3.32	22.39	22.85	23.64	22.93	22.72	23.04	L M
233638	62± 6	17.82±0.013	17.54±0.016	18.12±0.020	0.57	3.01	2.34	22.83	23.77	24.60	24.39	23.56	24.08	U M
233658	115± 12	17.62±0.024	17.31±0.022	17.93±0.036	0.68	2.10	3.03	22.24	22.68	23.82	23.31	22.67	23.12	L M
233659	129± 3	17.64±0.015	17.41±0.020	17.92±0.024	0.68	1.95	2.38	22.26	22.69	23.47	23.02	22.62	22.95	L D
233677	72± 2	16.48±0.010	16.17±0.011	16.79±0.016	0.95	3.84	6.58	22.51	22.91	24.18	23.44	22.87	23.35	L M
233681	36± 1	18.07±0.027	17.69±0.029	18.43±0.042	0.94	0.36	0.55	22.77	22.99	24.03	23.06	22.93	23.25	L D
233683	67± 3	17.48±0.018	17.22±0.021	17.77±0.029	0.56	3.21	3.83	22.95	23.36	24.73	23.66	23.31	23.76	L M
233684	114± 4	17.25±0.013	16.96±0.017	17.56±0.021	0.53	2.76	3.23	22.34	22.70	23.51	23.06	22.64	22.98	L M
233687	89± 11	19.43±0.038	19.33±0.054	19.65±0.062	0.51	1.40	1.51	22.85	23.09	24.77	23.93	22.97	23.69	U D
233693	108± 9	17.62±0.017	17.36±0.020	17.92±0.027	0.61	1.97	2.68	22.26	22.63	23.55	23.10	22.65	22.99	L D
233695	150± 4	17.35±0.013	17.10±0.018	17.63±0.021	0.78	3.47	5.08	22.16	22.51	23.48	23.17	22.53	22.92	L M
233706	106± 14	17.20±0.015	16.85±0.016	17.53±0.023	0.74	2.81	3.84	22.52	22.93	23.86	23.30	22.91	23.25	L M
233711	116± 4	17.71±0.015	17.49±0.020	17.98±0.025	0.44	2.05	2.75	22.26	22.70	23.92	23.40	22.59	23.15	L D
233758	64± 10	18.59±0.030	18.30±0.033	18.90±0.047	0.57	2.25	2.29	23.68	24.23	26.11	24.50	24.06	24.73	L D
233778	72± 5	19.53±0.039	19.30±0.048	19.81±0.062	0.66	5.41	1.93	26.05	26.55	30.98	26.73	26.59	27.71	L D
233781	49± 5	18.20±0.023	18.24±0.035	18.35±0.037	0.73	1.64	2.54	22.50	22.65	23.89	23.57	22.56	23.17	L D
233793	65± 4	18.14±0.026	17.85±0.030	18.44±0.041	0.71	5.21	5.85	23.28	23.72	25.18	24.04	23.56	24.12	L M
233807	198± 9	16.90±0.013	16.55±0.014	17.24±0.020	0.81	2.88	3.57	22.31	22.63	23.20	22.56	22.62	22.75	L M
233813	48± 6	17.24±0.017	16.92±0.019	17.56±0.027	0.99	2.73	3.97	22.75	23.10	24.30	23.22	23.05	23.42	L M
233815	166± 0	19.30±0.041	18.91±0.045	19.66±0.064	0.70	1.51	1.91	23.23	23.60	25.51	24.28	23.55	24.23	S D
233824	136± 17	17.56±0.018	17.24±0.021	17.88±0.028	0.60	2.51	3.42	22.25	22.67	23.83	23.27	22.67	23.11	L M
233835	82± 9	19.15±0.038	19.24±0.063	19.28±0.064	0.72	1.60	1.93	23.23	23.64	25.84	24.41	23.55	24.36	L D
233836	71± 11	18.84±0.034	18.58±0.040	19.13±0.054	0.98	1.49	2.32	23.08	23.50	25.35	23.75	23.48	24.02	L D
233852	120± 14	17.44±0.019	16.99±0.018	17.82±0.030	0.87	2.39	3.64	22.55	22.94	24.02	22.98	22.99	23.23	L M
234845	84± 10	17.56±0.025	17.13±0.020	17.94±0.038	0.88	2.92	4.40	22.95	23.42	25.06	23.98	23.43	23.97	S M
238611	106± 1	18.84±0.033	18.45±0.035	19.19±0.052	0.88	2.40	3.44	22.79	23.35	24.76	23.98	23.15	23.81	L M
238614	32± 8	18.26±0.026	17.93±0.029	18.59±0.041	0.62	1.58	2.02	22.18	22.56	23.25	22.64	22.55	22.75	L D
238633	110± 4	17.26±0.015	17.09±0.020	17.52±0.025	0.69	3.56	3.98	23.10	23.58	25.08	24.49	23.52	24.17	L M
238634	75± 5	16.87±0.012	16.62±0.015	17.15±0.019	0.85	2.79	4.47	22.45	22.87	24.26	23.69	22.79	23.40	L M

Table 4 continued on next page

**Table 4** (*continued*)

AGC	W50	g	r	B	b/a	h(g)	$R_{eff}(g)$	$\mu_{0,g}$	$\mu_{0,B}$	$\mu_{0,B}$	$\mu_{0,B}$	$\mu_{0,B}$	T1	T2
	(km s <sup>-1</sup> )	(mag)	(mag)	(mag)		(kpc)	(kpc)	(AUTO)	( AUTO)	ISO	ISOCOR	PETRO	AVE	
238636	45± 5	19.26±0.036	19.09±0.048	19.51±0.058	1.00	0.99	1.23	23.47	23.81	26.21	25.29	23.78	24.77	L D
238638	107± 7	18.16±0.024	17.98±0.033	18.41±0.039	0.45	4.53	4.82	22.64	22.92	24.55	23.75	22.94	23.54	L M
238640	150± 5	17.62±0.017	17.29±0.019	17.94±0.027	0.46	2.37	2.73	22.11	22.50	23.18	22.76	22.44	22.72	L M
238643	45± 7	17.85±0.021	17.43±0.022	18.22±0.033	0.64	0.85	0.87	23.84	24.14	26.81	22.42	24.05	24.35	L D
238682	108± 44	17.90±0.028	17.59±0.026	18.22±0.043	0.82	3.40	5.14	22.36	22.79	24.06	23.43	22.74	23.26	L M
238684	156± 6	17.37±0.016	17.07±0.018	17.68±0.025	0.49	6.16	7.63	22.29	22.74	23.98	23.22	22.70	23.16	L M
238687	83± 6	18.39±0.028	18.14±0.032	18.68±0.045	0.96	1.73	2.81	22.89	23.38	24.92	23.26	23.30	23.71	L D
238689	104± 8	17.65±0.020	17.37±0.023	17.94±0.032	0.48	2.43	2.41	23.49	23.78	25.72	24.04	23.72	24.31	L D
238690	133± 4	16.41±0.010	16.10±0.012	16.73±0.016	0.83	3.77	5.12	22.68	22.91	24.09	23.43	22.87	23.32	L M
238691	28± 7	17.20±0.018	16.78±0.017	17.56±0.027	0.50	0.57	0.66	22.69	22.98	23.96	22.84	22.91	23.17	L D
238692	83± 9	19.39±0.040	19.16±0.049	19.67±0.063	0.82	1.62	1.95	23.46	23.88	26.18	24.78	23.81	24.67	L D
238693	64± 12	18.42±0.028	18.21±0.034	18.70±0.044	0.49	1.14	1.40	22.67	23.00	24.30	23.40	22.95	23.41	L D
238694	18± 6	18.54±0.032	18.32±0.038	18.81±0.050	0.84	1.64	2.46	22.77	23.18	24.83	22.89	23.15	23.51	L D
238696	89± 4	17.00±0.019	16.47±0.014	17.42±0.029	0.98	3.93	6.67	22.26	22.80	23.77	23.06	22.90	23.13	S M
238697	118± 21	16.82±0.013	16.65±0.016	17.07±0.020	0.65	5.00	5.86	23.17	23.45	25.09	24.41	23.41	24.09	L M
238703	37± 6	17.94±0.020	17.81±0.027	18.18±0.032	0.99	1.79	2.86	22.63	22.97	24.53	24.02	22.92	23.61	L D
238704	24± 9	20.40±0.051	20.09±0.054	20.72±0.079	0.83	2.96	1.19	25.96	26.27	29.39	26.69	26.32	27.17	L D
238705	163± 6	18.81±0.034	18.51±0.039	19.12±0.054	0.82	3.58	4.23	23.63	24.14	26.52	22.14	24.10	24.22	L M
238708	62± 9	17.88±0.020	17.51±0.022	18.22±0.031	0.84	3.53	4.04	23.83	24.25	26.48	23.82	24.15	24.67	S D
238734	100± 15	17.32±0.021	16.94±0.019	17.67±0.033	0.97	2.08	3.55	22.19	22.57	23.65	23.00	22.51	22.93	L M
238737	41± 7	18.42±0.026	18.33±0.030	18.63±0.041	0.59	0.45	0.39	23.57	23.67	26.58	26.04	23.68	24.99	L D
238749	39± 4	17.99±0.022	17.58±0.024	18.35±0.034	0.96	2.68	3.28	23.51	23.95	25.74	24.55	23.76	24.50	L D
238751	108± 9	17.52±0.020	17.15±0.021	17.86±0.031	0.54	2.91	3.37	22.73	23.08	24.38	23.46	23.04	23.49	S M
238752	147± 25	18.09±0.023	17.89±0.030	18.35±0.036	0.31	4.83	4.84	22.34	22.64	23.91	23.22	22.55	23.08	L M
238754	64± 12	19.68±0.051	19.46±0.061	19.96±0.080	0.57	0.93	1.35	22.53	22.62	24.07	23.47	22.60	23.19	L D
238768	90± 5	18.78±0.029	18.68±0.040	18.99±0.046	0.85	1.51	2.40	22.91	23.24	25.90	24.07	23.19	24.10	L D
238769	85± 8	16.43±0.012	15.96±0.012	16.83±0.019	0.64	0.73	0.84	22.79	23.19	24.01	22.73	23.16	23.27	L D
238825	24± 5	19.40±0.046	19.08±0.055	19.72±0.073	0.87	2.26	2.93	23.31	23.72	26.34	23.69	23.69	24.36	L D
238827	37± 7	18.69±0.027	18.48±0.036	18.96±0.043	0.54	1.13	1.45	22.97	23.25	24.86	24.15	23.16	23.85	L D
238832	145± 3	17.15±0.013	16.96±0.018	17.41±0.022	0.69	2.01	2.80	22.48	22.74	23.95	23.53	22.63	23.21	L D
238834	55± 9	18.33±0.023	18.06±0.029	18.62±0.037	0.82	1.41	2.19	22.14	22.51	23.38	22.93	22.48	22.83	L D
238837	70± 23	17.46±0.014	17.06±0.016	17.81±0.022	0.89	4.06	6.79	22.31	22.76	24.00	23.33	22.73	23.20	S M
238838	187± 80	20.20±0.037	19.98±0.050	20.48±0.059	0.54	2.74	1.33	25.18	25.45	29.15	25.03	25.54	26.29	U D
238839	125± 9	19.50±0.040	19.30±0.052	19.76±0.064	0.69	2.98	3.10	23.91	24.33	27.20	22.93	24.33	24.70	L D
238840	57± 15	18.69±0.030	18.41±0.037	18.99±0.048	0.53	1.19	1.53	22.45	22.80	23.88	23.14	22.67	23.12	L D
238841	91± 11	19.04±0.032	18.67±0.039	19.39±0.050	0.45	0.61	0.71	22.33	22.67	23.49	22.76	22.66	22.90	L D

Table 4 continued on next page

**Table 4** (*continued*)

AGC	W50	g	r	B	b/a	h(g)	$R_{eff}(g)$	$\mu_{0,g}$	$\mu_{0,B}$	$\mu_{0,B}$	$\mu_{0,B}$	$\mu_{0,B}$	T1	T2
	(km s <sup>-1</sup> )	(mag)	(mag)	(mag)		(kpc)	(kpc)	(AUTO)	( AUTO)	ISO	ISOCOR	PETRO	AVE	
238842	118± 6	18.34±0.024	17.98±0.029	18.68±0.038	0.34	1.72	1.95	22.43	22.68	23.77	23.28	22.70	23.11	L D
238847	37± 6	18.22±0.034	17.99±0.033	18.50±0.053	0.53	0.34	0.39	23.03	23.23	24.68	24.04	23.19	23.78	L D
238849	89± 13	18.56±0.026	18.39±0.034	18.80±0.041	0.76	2.84	3.69	23.17	23.60	25.33	24.37	23.53	24.21	L D
238850	104± 6	18.51±0.026	18.32±0.033	18.77±0.041	0.39	3.14	3.92	22.65	22.89	24.33	23.69	22.84	23.44	L M
238874	171± 21	18.03±0.016	17.96±0.025	18.23±0.026	0.87	3.37	3.27	23.90	24.11	25.76	25.44	24.05	24.84	L D
238905	70± 3	20.87±0.066	20.75±0.075	21.09±0.103	0.97	3.77	0.71	27.87	27.95	31.63	29.52	27.94	29.26	L D
240523	121± 6	15.70±0.009	15.30±0.007	16.06±0.013	0.65	1.56	1.86	22.45	22.78	23.40	23.02	22.77	22.99	L D
241275	96± 10	16.75±0.013	16.40±0.014	17.08±0.020	0.51	1.60	1.85	22.93	23.21	24.43	23.68	23.19	23.63	L D
242011	69± 6	18.64±0.018	18.68±0.026	18.79±0.029	0.90	2.89	0.92	24.99	25.15	25.95	25.89	24.88	25.47	L D
242016	48± 2	16.78±0.009	16.52±0.011	17.08±0.015	0.43	2.92	2.08	24.41	24.60	27.61	26.26	24.58	25.76	L D
242042	124± 2	16.59±0.015	16.36±0.014	16.86±0.023	0.39	1.64	1.80	22.60	22.97	24.26	23.80	22.95	23.50	L D
242164	149± 4	18.10±0.019	17.67±0.023	18.47±0.031	0.88	2.24	3.36	23.08	23.50	24.91	24.08	23.41	23.97	S D
242166	106± 27	17.58±0.019	17.23±0.020	17.91±0.030	0.45	2.09	2.46	22.83	23.20	24.55	23.31	23.11	23.54	L D
242167	109± 2	16.01±0.009	15.72±0.010	16.32±0.014	0.86	3.17	4.31	22.83	23.22	24.34	23.44	23.17	23.55	L M
242173	104± 2	16.00±0.011	15.64±0.009	16.34±0.016	0.86	2.66	3.77	22.32	22.71	23.39	22.95	22.70	22.94	L M
242174	120± 2	18.12±0.016	17.83±0.018	18.43±0.025	0.95	1.38	1.75	23.25	23.58	25.16	24.76	23.15	24.16	L D
242175	144± 9	16.16±0.009	15.85±0.010	16.47±0.015	0.62	4.10	6.28	22.14	22.54	23.76	23.37	22.51	23.05	L M
242176	109± 10	16.91±0.011	16.62±0.014	17.22±0.018	0.79	2.66	3.75	22.45	22.95	23.89	23.04	23.02	23.22	L M
242246	101± 9	17.66±0.022	17.26±0.024	18.01±0.034	0.48	1.53	1.92	22.36	22.69	23.79	22.93	22.59	23.00	L D
242248	66± 3	16.54±0.010	16.23±0.011	16.86±0.016	0.50	4.34	5.89	22.31	22.74	24.26	23.51	22.63	23.28	L M
242284	132± 2	17.17±0.013	16.89±0.014	17.48±0.020	0.41	3.13	3.69	22.25	22.50	23.46	23.10	22.40	22.86	L M
242296	108± 3	16.23±0.012	15.95±0.011	16.53±0.018	0.48	3.08	3.66	22.35	22.71	23.79	23.46	22.66	23.15	L M
242351	46± 8	16.76±0.012	16.33±0.013	17.13±0.019	0.63	2.53	3.29	22.43	22.78	23.70	23.03	22.73	23.06	L M
242618	73± 3	15.86±0.008	15.46±0.009	16.22±0.013	0.89	1.16	1.69	22.41	22.80	23.70	22.76	22.82	23.02	S D
242684	48± 6	17.68±0.019	17.45±0.022	17.95±0.030	0.63	3.63	4.18	23.20	23.63	25.39	24.36	23.54	24.23	L M
243828	61± 6	17.45±0.018	17.11±0.019	17.77±0.028	0.84	1.78	2.69	22.66	23.10	24.34	23.31	23.06	23.45	L D
243830	22± 4	19.88±0.046	19.66±0.046	20.15±0.072	0.43	0.30	0.29	23.21	23.57	27.60	23.39	23.74	24.58	L D
243835	58± 4	20.18±0.044	19.84±0.050	20.51±0.070	0.66	1.42	1.17	24.22	25.13	28.42	24.18	25.21	25.74	L D
243843	81± 4	16.37±0.010	15.98±0.011	16.72±0.016	0.94	2.63	4.02	22.53	22.92	23.94	23.18	22.83	23.22	L M
243848	64± 3	16.70±0.011	16.41±0.012	17.00±0.017	0.82	3.20	4.30	22.26	22.67	23.48	23.10	22.59	22.96	L M
243859	85± 10	18.86±0.041	18.60±0.049	19.15±0.065	0.96	1.30	2.25	23.08	23.29	25.64	23.56	23.34	23.96	L D
243860	53± 3	17.64±0.018	17.51±0.025	17.87±0.030	0.65	2.22	2.93	22.81	23.38	25.01	24.32	23.34	24.02	L D
243901	37± 6	17.29±0.013	17.13±0.019	17.54±0.021	0.96	2.72	3.96	22.94	23.38	24.80	24.14	23.30	23.91	L M
243926	51± 41	17.81±0.027	17.35±0.022	18.19±0.042	0.84	1.54	2.12	22.33	22.76	23.52	22.98	22.63	22.97	L D
243979	122± 10	16.93±0.012	16.58±0.013	17.26±0.019	0.92	2.87	4.44	22.35	22.80	23.65	22.88	22.70	23.01	L M
243982	141± 36	17.29±0.015	16.99±0.017	17.60±0.024	0.95	2.20	3.64	22.23	22.69	23.68	23.03	22.59	23.00	L M

Table 4 continued on next page

**Table 4** (*continued*)

AGC	W50	g	r	B	b/a	h(g)	$R_{eff}(g)$	$\mu_{0,g}$	$\mu_{0,B}$	$\mu_{0,B}$	$\mu_{0,B}$	$\mu_{0,B}$	T1	T2
	(km s <sup>-1</sup> )	(mag)	(mag)	(mag)		(kpc)	(kpc)	(AUTO)	( AUTO)	ISO	ISOCOR	PETRO	AVE	
244001	53± 7	17.43±0.015	17.16±0.017	17.72±0.023	0.72	3.76	5.04	22.17	22.57	23.21	22.69	22.55	22.75	L M
244007	61± 9	17.93±0.019	17.68±0.023	18.22±0.031	0.47	1.81	2.16	22.87	23.08	24.54	24.18	22.89	23.67	L D
244102	94± 7	17.60±0.007	18.01±0.015	17.58±0.013	0.78	2.89	1.48	22.59	22.63	23.30	23.27	22.32	22.88	L M
244131	139± 43	17.31±0.014	16.91±0.015	17.66±0.022	0.80	1.64	2.31	22.27	22.69	23.17	22.46	22.73	22.76	L D
244245	130± 8	17.46±0.018	17.01±0.018	17.84±0.028	0.71	2.76	3.81	23.05	23.50	25.05	23.95	23.46	23.99	L D
244299	203± 18	17.72±0.020	17.46±0.023	18.01±0.031	0.83	2.25	3.37	22.70	23.13	24.53	23.58	23.06	23.58	L M
244402	239± 7	17.19±0.015	16.78±0.016	17.55±0.024	0.81	1.60	2.17	22.37	22.77	23.57	22.91	22.63	22.97	L D
244404	134± 17	17.28±0.013	17.17±0.018	17.50±0.022	0.52	3.44	3.79	22.27	22.58	23.46	23.21	22.55	22.95	L M
244419	134± 7	17.71±0.019	17.41±0.021	18.03±0.030	0.47	2.80	3.03	22.25	22.64	23.34	22.85	22.59	22.85	L M
244422	168± 29	17.34±0.017	17.07±0.020	17.63±0.027	0.77	3.24	4.58	22.71	22.96	24.33	23.60	22.74	23.41	L M
244512	28± 7	17.87±0.021	17.69±0.025	18.13±0.033	0.82	0.51	0.72	22.38	22.64	23.43	22.81	22.48	22.84	L D
244562	56± 7	17.85±0.023	17.44±0.021	18.22±0.035	0.57	0.67	0.75	22.48	22.79	23.44	22.80	23.03	23.02	L D
244875	106± 7	17.82±0.019	17.49±0.022	18.14±0.030	0.81	2.55	3.33	23.13	23.40	24.91	24.03	23.33	23.92	L D
244878	224± 10	17.02±0.012	16.77±0.016	17.30±0.020	0.78	4.03	5.49	22.27	22.59	23.33	22.90	22.59	22.85	L M
244912	53± 5	17.71±0.013	17.52±0.018	17.97±0.022	0.96	5.74	5.27	24.34	24.54	26.83	26.40	24.40	25.54	L M
244951	90± 5	17.10±0.013	16.88±0.017	17.37±0.021	0.85	4.33	5.42	23.06	23.46	24.87	24.22	23.40	23.98	L M
244953	166± 7	17.11±0.014	16.74±0.015	17.45±0.022	0.46	4.37	4.96	22.43	22.79	23.56	22.98	22.79	23.03	S M
245003	269± 18	17.26±0.010	16.84±0.010	17.63±0.016	0.57	7.15	4.20	23.29	23.79	24.56	24.27	23.66	24.07	L M
245576	44± 4	16.35±0.008	16.00±0.009	16.68±0.013	0.60	7.16	8.28	22.35	22.75	23.34	22.88	22.69	22.91	L G
248870	39± 9	18.03±0.021	17.62±0.022	18.39±0.032	0.82	1.11	1.73	22.14	22.56	23.35	22.66	22.53	22.78	L D
248874	145± 14	17.14±0.012	16.79±0.014	17.48±0.019	0.73	2.90	4.06	22.15	22.55	23.17	22.69	22.50	22.73	L M
248876	79± 8	17.63±0.020	17.36±0.017	17.93±0.031	0.85	2.09	3.64	22.31	22.77	23.91	23.63	22.66	23.24	L M
248884	26± 8	17.83±0.023	17.50±0.026	18.16±0.036	0.82	1.41	1.97	22.89	23.10	24.41	23.40	23.02	23.48	L D
248887	43± 8	19.13±0.036	18.93±0.047	19.40±0.058	0.67	1.14	1.46	23.30	23.46	25.42	24.40	23.40	24.17	L D
248896	73± 8	18.31±0.025	18.11±0.032	18.57±0.039	0.55	1.80	2.06	22.84	23.04	24.41	23.76	22.99	23.55	L D
248898	131± 8	18.31±0.034	17.90±0.028	18.67±0.053	0.87	3.37	4.45	22.99	23.37	24.94	24.13	23.35	23.95	S M
248906	52± 6	18.85±0.034	18.46±0.037	19.20±0.053	0.99	1.10	1.82	22.51	22.86	23.91	23.11	22.90	23.19	L D
248913	114± 7	18.31±0.024	18.10±0.032	18.58±0.038	0.65	2.88	3.58	22.65	22.99	24.15	23.35	22.98	23.37	L M
248914	92± 7	16.34±0.009	15.96±0.010	16.69±0.014	0.58	2.90	3.39	22.60	22.89	23.88	23.46	22.84	23.27	S M
248916	173± 8	18.55±0.028	18.29±0.033	18.84±0.044	0.96	1.81	2.92	23.02	23.42	25.37	24.22	23.40	24.10	L D
248928	23± 6	21.67±0.092	21.35±0.103	21.98±0.144	0.85	0.91	0.64	25.25	25.78	30.09	25.80	25.84	26.88	L D
248932	83± 6	18.16±0.024	17.75±0.024	18.53±0.037	0.50	0.79	0.93	22.67	22.99	23.94	23.10	23.04	23.27	L D
248937	40± 5	19.71±0.039	19.44±0.045	20.01±0.061	0.75	3.13	2.11	24.98	24.92	28.14	25.05	24.96	25.77	L D
248938	63± 6	18.54±0.024	18.47±0.036	18.75±0.040	0.39	0.86	0.75	23.19	23.36	25.07	24.61	23.28	24.08	L D
248940	73± 6	17.30±0.014	16.93±0.016	17.64±0.022	0.85	2.96	4.35	22.36	22.75	23.43	22.90	22.77	22.96	L M
248941	131± 4	16.04±0.007	15.62±0.008	16.40±0.012	0.76	3.36	4.52	22.14	22.55	23.16	22.48	22.54	22.68	S M

Table 4 continued on next page

**Table 4** (*continued*)

AGC	W50	g	r	B	b/a	h(g)	$R_{eff}(g)$	$\mu_{0,g}$	$\mu_{0,B}$	$\mu_{0,B}$	$\mu_{0,B}$	$\mu_{0,B}$	T1	T2
	(km s <sup>-1</sup> )	(mag)	(mag)	(mag)		(kpc)	(kpc)	(AUTO)	( AUTO)	ISO	ISOCOR	PETRO	AVE	
248945	70± 8	20.70±0.067	20.54±0.073	20.94±0.104	0.96	1.32	0.84	25.15	25.05	28.08	27.00	24.99	26.28	L D
248950	22± 6	17.91±0.018	17.67±0.022	18.19±0.029	0.90	3.48	5.84	22.28	22.71	23.84	23.32	22.62	23.12	L M
248953	202± 6	15.93±0.007	15.54±0.008	16.28±0.011	0.66	4.93	6.58	21.97	22.62	23.35	22.67	22.43	22.77	S G
248959	304± 93	18.39±0.021	18.19±0.031	18.66±0.035	0.70	2.05	2.90	22.24	22.68	23.87	23.35	22.61	23.13	L M
248970	137± 7	17.43±0.016	17.17±0.021	17.72±0.025	0.55	4.67	5.20	22.95	23.31	24.87	24.05	23.29	23.88	L M
248973	230± 7	18.45±0.024	18.12±0.026	18.77±0.038	0.75	2.10	3.20	22.14	22.61	23.61	23.08	22.38	22.92	L M
248981	66± 6	19.87±0.047	19.72±0.058	20.12±0.074	0.89	1.47	1.23	24.47	24.73	27.63	25.97	24.69	25.76	L D
248982	31± 5	20.67±0.053	20.64±0.077	20.86±0.086	0.66	1.86	1.14	24.40	24.54	26.68	26.36	24.48	25.51	L D
249023	102± 7	19.84±0.046	19.73±0.065	20.05±0.075	0.79	1.08	1.35	23.00	22.55	23.93	23.70	22.46	23.16	L D
249050	163± 10	17.61±0.022	17.34±0.020	17.91±0.033	0.72	3.15	4.19	22.32	22.68	23.59	23.20	22.73	23.05	L M
249095	64± 13	20.51±0.057	20.48±0.068	20.69±0.090	0.64	0.74	0.65	23.48	22.81	26.56	23.49	22.65	23.88	L D
249096	128± 8	18.34±0.025	18.18±0.033	18.58±0.040	0.99	1.37	2.50	22.50	22.86	24.31	23.53	22.77	23.37	L D
249099	43± 16	18.61±0.028	18.33±0.034	18.90±0.044	0.89	1.52	2.46	22.77	23.10	24.74	24.05	23.05	23.73	L D
249100	167± 3	16.65±0.009	16.50±0.012	16.89±0.015	0.50	6.43	6.35	22.28	22.60	23.25	22.97	22.55	22.84	U G
249108	50± 7	18.19±0.025	17.88±0.029	18.51±0.039	0.86	1.63	2.54	22.43	22.94	24.14	23.18	22.89	23.29	L D
249109	90± 7	19.18±0.032	19.07±0.045	19.39±0.052	0.34	2.24	1.86	23.55	23.84	26.13	25.33	23.80	24.78	L D
249110	204± 48	16.96±0.013	16.61±0.016	17.29±0.021	0.61	6.04	6.29	23.12	23.50	24.94	24.16	23.42	24.00	L M
249118	59± 10	20.17±0.041	20.17±0.065	20.34±0.068	0.74	1.93	1.01	24.72	25.06	27.07	26.91	24.94	26.00	U D
249120	84± 6	17.05±0.014	16.88±0.019	17.30±0.023	0.86	2.79	3.67	22.44	22.72	23.68	23.31	22.66	23.09	L M
249176	100± 6	18.22±0.025	18.22±0.035	18.39±0.041	0.87	2.63	3.74	22.77	23.10	24.48	23.80	23.07	23.61	L M
249178	40± 7	18.04±0.020	17.82±0.028	18.31±0.033	0.81	0.54	0.78	22.28	22.58	23.45	22.88	22.46	22.84	L D
249180	29± 8	18.83±0.029	18.55±0.034	19.13±0.046	0.75	0.82	0.84	23.89	24.12	26.75	25.52	24.15	25.13	L D
249188	110± 28	18.12±0.021	17.98±0.026	18.35±0.033	0.69	1.72	2.06	22.05	22.50	23.21	22.74	22.31	22.69	L D
249190	113± 27	18.49±0.039	18.15±0.034	18.82±0.060	0.99	1.75	3.03	22.47	22.73	24.09	23.52	22.59	23.23	U D
249195	89± 4	17.98±0.023	17.60±0.024	18.34±0.036	0.97	2.34	3.36	23.19	23.50	25.21	23.90	23.42	24.01	L D
249199	86± 5	16.71±0.014	16.47±0.017	17.00±0.022	0.66	5.94	6.75	22.65	22.94	23.91	23.37	22.85	23.27	L M
249256	112± 6	18.48±0.029	18.23±0.036	18.76±0.046	0.61	2.48	2.86	23.06	23.35	24.92	23.47	23.28	23.75	L D
249261	71± 21	18.30±0.024	17.96±0.029	18.63±0.038	0.48	2.74	3.31	22.21	22.62	23.59	23.00	22.46	22.91	L M
249264	34± 7	17.62±0.019	17.33±0.021	17.92±0.029	0.40	0.81	0.82	22.66	22.95	23.80	22.97	22.88	23.15	L D
249267	111± 4	17.48±0.023	17.23±0.022	17.77±0.036	0.86	2.25	3.34	22.67	23.02	24.31	23.75	23.01	23.52	L M
249302	226± 9	18.43±0.029	18.12±0.034	18.75±0.046	0.62	1.19	1.55	22.71	23.04	24.30	23.47	23.04	23.46	L D
249304	101± 6	17.80±0.020	17.55±0.024	18.08±0.031	0.51	2.23	2.73	22.22	22.70	23.64	23.14	22.54	23.01	L D
249306	34± 3	18.04±0.022	17.76±0.027	18.34±0.036	0.92	2.43	3.57	22.87	23.25	24.75	23.85	23.16	23.75	L M
249368	80± 3	19.38±0.032	19.25±0.044	19.61±0.051	0.75	2.55	2.37	23.75	23.94	26.85	26.20	24.02	25.25	L D
252520	29± 2	17.77±0.017	17.53±0.022	18.04±0.028	0.93	4.49	4.89	23.99	23.99	27.06	25.54	24.01	25.15	L M
252522	68± 2	16.06±0.009	15.86±0.012	16.32±0.015	0.77	4.79	2.30	25.46	26.33	28.83	24.56	26.27	26.50	L D

Table 4 continued on next page

**Table 4** (*continued*)

AGC	W50	g	r	B	b/a	h(g)	$R_{eff}(g)$	$\mu_{0,g}$	$\mu_{0,B}$	$\mu_{0,B}$	$\mu_{0,B}$	$\mu_{0,B}$	T1	T2
		(km s <sup>-1</sup> )	(mag)	(mag)	(mag)	(kpc)	(kpc)	(AUTO)	( AUTO)	ISO	ISOCOR	PETRO	AVE	
252648	59± 5	18.01±0.022	17.64±0.025	18.35±0.035	0.85	1.77	2.66	22.66	23.06	24.15	23.29	23.07	23.39	S D
252891	81± 11	16.30±0.012	16.04±0.015	16.60±0.020	0.52	1.86	1.84	23.04	23.33	24.93	24.00	23.28	23.89	L D
253921	109± 59	18.14±0.022	17.86±0.029	18.45±0.035	0.80	1.50	2.28	23.08	23.92	26.64	23.62	23.90	24.52	L D
253922	35± 9	18.59±0.028	18.47±0.039	18.82±0.045	0.54	0.76	1.01	22.58	22.78	24.08	23.56	22.71	23.28	L D
253923	17± 5	17.77±0.020	17.40±0.024	18.12±0.032	0.97	0.92	1.44	23.01	23.89	25.56	24.24	23.86	24.39	L D
253929	150± 8	16.26±0.008	15.90±0.010	16.60±0.014	0.80	4.45	6.78	22.48	22.96	24.28	23.67	22.97	23.47	L M
254033	137± 8	17.63±0.019	17.54±0.024	17.85±0.030	0.99	4.36	6.43	22.88	23.51	25.13	24.43	23.29	24.09	L M
257881	145± 5	18.10±0.021	17.95±0.029	18.33±0.034	0.61	2.60	3.16	22.77	23.18	24.73	24.27	23.00	23.79	U D
257889	73± 8	17.96±0.019	17.67±0.024	18.27±0.031	0.61	3.34	4.26	22.41	22.70	23.69	23.17	22.66	23.05	L M
257895	92± 20	17.67±0.018	17.41±0.024	17.96±0.029	0.98	2.95	4.65	22.53	22.77	23.95	23.27	22.72	23.17	L M
257907	55± 20	15.97±0.007	15.73±0.009	16.25±0.011	0.67	5.28	7.96	22.09	22.61	23.63	23.24	22.55	23.00	L G
257911	131± 3	17.29±0.015	17.00±0.018	17.60±0.024	0.62	1.35	2.57	22.12	22.60	24.30	23.23	22.54	23.17	L D
257918	36± 8	19.60±0.039	19.29±0.046	19.91±0.062	0.57	1.41	1.13	24.25	24.51	27.64	23.43	24.53	25.02	L D
257921	47± 4	16.71±0.011	16.33±0.011	17.05±0.017	0.40	1.21	1.26	22.30	22.55	23.04	22.50	22.51	22.65	L D
257923	62± 3	16.77±0.012	16.42±0.014	17.11±0.019	0.78	1.52	2.23	22.60	23.02	24.31	23.39	22.96	23.42	L D
257937	67± 3	17.38±0.015	17.10±0.018	17.68±0.024	0.91	1.57	2.30	23.55	24.54	26.50	25.30	24.46	25.20	U D
257939	68± 9	17.94±0.022	17.69±0.027	18.23±0.035	0.71	1.29	1.80	22.55	22.90	24.14	23.07	22.78	23.22	L D
257940	38± 7	18.45±0.021	18.23±0.030	18.72±0.035	0.90	1.94	3.10	22.25	22.75	24.03	23.46	22.66	23.23	L M
257944	167± 23	18.14±0.021	18.02±0.031	18.37±0.035	0.42	3.83	3.94	22.44	22.76	23.83	23.33	22.74	23.17	L M
257946	204± 6	17.57±0.017	17.32±0.021	17.86±0.027	0.66	3.52	4.57	22.36	22.76	23.83	23.19	22.69	23.12	L M
257950	49± 6	18.72±0.028	18.50±0.038	19.00±0.045	0.67	2.32	3.26	22.65	22.91	24.73	23.67	22.80	23.53	L D
257954	111± 7	18.89±0.032	18.71±0.041	19.15±0.051	0.38	1.67	1.65	23.03	23.60	25.25	24.07	23.53	24.11	L D
257955	103± 7	18.77±0.032	18.56±0.042	19.05±0.052	0.39	0.85	0.97	22.35	22.58	23.54	22.47	22.59	22.79	L D
257963	37± 8	20.10±0.044	19.64±0.042	20.48±0.067	0.91	0.64	0.55	23.97	24.93	26.58	25.53	24.58	25.41	L D
258008	89± 15	17.96±0.026	17.60±0.029	18.30±0.041	0.83	2.76	3.82	22.46	22.79	23.87	22.72	22.66	23.01	L M
258032	71± 13	17.06±0.014	16.69±0.014	17.40±0.022	0.91	3.85	5.87	22.29	22.68	23.50	22.66	22.66	22.87	S M
258106	98± 7	17.97±0.022	17.69±0.028	18.27±0.035	0.64	2.95	4.67	22.16	22.60	23.82	23.10	22.51	23.01	L M
258107	55± 2	16.84±0.014	16.49±0.014	17.17±0.021	0.51	4.84	5.14	22.98	23.23	24.47	23.79	23.05	23.64	L M
258110	27± 15	18.13±0.024	17.77±0.025	18.46±0.037	0.64	1.95	3.02	21.91	22.57	23.66	22.91	22.47	22.90	L M
258113	118± 6	17.35±0.016	16.92±0.017	17.72±0.026	0.61	6.81	7.66	23.10	23.57	25.26	24.02	23.50	24.09	S M
258118	70± 21	18.31±0.025	18.12±0.033	18.56±0.040	0.59	2.60	3.10	22.86	23.05	24.46	23.82	23.04	23.59	L D
258122	88± 9	18.92±0.027	18.89±0.041	19.10±0.045	0.72	2.56	2.87	23.29	23.25	24.84	24.65	23.15	23.97	L D
258123	38± 11	17.94±0.018	17.91±0.028	18.12±0.030	0.74	2.17	2.95	22.16	22.56	23.52	23.19	22.45	22.93	L M
258125	142± 4	17.27±0.012	16.93±0.015	17.61±0.020	0.65	2.72	4.35	22.32	22.80	24.13	23.59	22.62	23.29	L M
258128	95± 4	16.12±0.009	15.71±0.009	16.48±0.015	0.89	4.25	4.89	22.86	23.48	24.36	23.68	23.51	23.76	S M
258131	154± 13	17.58±0.019	17.34±0.022	17.86±0.030	0.59	3.47	4.75	22.37	22.75	24.06	23.43	22.69	23.23	L M

Table 4 continued on next page

**Table 4** (*continued*)

AGC	W50	g	r	B	b/a	h(g)	$R_{eff}(g)$	$\mu_{0,g}$	$\mu_{0,B}$	$\mu_{0,B}$	$\mu_{0,B}$	$\mu_{0,B}$	T1	T2
	(km s <sup>-1</sup> )	(mag)	(mag)	(mag)		(kpc)	(kpc)	(AUTO)	( AUTO)	ISO	ISOCOR	PETRO	AVE	
258132	204± 6	17.26±0.016	16.80±0.016	17.66±0.025	0.39	6.29	5.08	22.73	23.07	23.85	23.10	23.03	23.26	S M
258143	145± 9	16.69±0.012	16.47±0.015	16.96±0.020	0.61	2.41	2.69	22.67	23.00	24.14	23.61	23.06	23.45	L D
258154	88± 18	18.40±0.024	18.29±0.032	18.62±0.038	0.37	1.29	1.31	22.35	22.55	23.28	22.67	22.36	22.72	L D
258160	25± 11	18.16±0.023	17.93±0.026	18.44±0.037	0.76	5.08	6.07	23.50	24.70	27.75	23.49	24.75	25.17	L M
258165	137± 5	16.35±0.010	16.00±0.010	16.68±0.015	0.52	7.11	6.76	22.40	22.72	23.37	22.75	22.68	22.88	L G
258168	58± 11	17.12±0.014	16.71±0.016	17.49±0.022	0.81	3.35	5.36	22.11	22.58	23.68	22.96	22.53	22.94	L M
258173	118± 3	17.96±0.020	18.00±0.030	18.11±0.033	0.54	1.71	2.54	22.59	22.58	25.14	24.31	22.53	23.64	L D
258174	40± 8	19.36±0.036	19.34±0.052	19.54±0.059	0.65	1.17	1.24	23.37	23.54	26.58	25.27	23.58	24.74	L D
258216	52± 14	17.58±0.016	17.29±0.019	17.89±0.025	0.81	4.25	5.65	22.37	22.92	23.88	23.33	22.81	23.23	L M
258263	98± 5	19.00±0.026	19.06±0.042	19.14±0.043	0.44	4.27	3.01	23.71	23.71	26.75	25.48	23.76	24.92	L D
258268	70± 8	18.03±0.020	17.93±0.028	18.25±0.032	0.48	3.55	4.32	22.43	23.65	25.00	24.63	23.53	24.20	L M
258278	44± 13	18.04±0.021	17.81±0.025	18.32±0.033	0.69	0.49	0.62	22.69	22.91	24.22	23.80	22.79	23.43	L D
258289	58± 7	18.97±0.038	18.66±0.043	19.29±0.060	0.72	1.96	2.79	22.56	22.90	24.14	22.93	22.88	23.21	L D
258294	49± 14	18.60±0.027	18.24±0.029	18.94±0.042	0.88	2.99	4.02	23.48	23.92	26.50	22.13	23.89	24.11	L D
258300	61± 8	18.20±0.023	18.08±0.031	18.43±0.037	0.88	2.32	3.53	22.29	22.70	23.95	23.27	22.64	23.14	L M
258317	129± 4	17.13±0.014	16.85±0.017	17.43±0.023	0.50	5.88	6.30	22.75	23.07	24.42	23.79	23.03	23.58	L M
258324	105± 9	17.39±0.016	17.02±0.017	17.73±0.025	0.66	6.60	6.62	23.25	24.09	25.71	24.73	24.00	24.63	S M
258332	53± 7	17.17±0.014	16.83±0.017	17.50±0.022	0.87	0.68	0.88	22.25	22.54	23.07	22.50	22.57	22.67	L D
258342	34± 10	18.62±0.034	18.38±0.040	18.90±0.054	0.58	2.90	3.71	22.37	22.67	23.90	23.09	22.50	23.04	L M
258349	73± 2	16.45±0.012	16.27±0.015	16.70±0.019	0.34	1.69	1.79	22.59	22.77	24.08	23.48	22.61	23.24	L D
258366	316± 78	17.97±0.022	17.65±0.024	18.29±0.034	0.51	4.90	5.87	22.59	23.12	24.43	23.42	22.98	23.49	L M
258397	157± 8	17.73±0.022	17.59±0.023	17.96±0.034	0.34	7.80	7.28	22.93	23.22	24.94	24.64	23.12	23.98	L M
258407	254± 5	17.48±0.018	17.21±0.021	17.78±0.028	0.40	5.02	5.16	22.53	22.85	24.05	23.48	22.89	23.32	L M
258415	93± 15	18.02±0.020	17.74±0.024	18.32±0.032	0.88	2.66	4.22	22.53	23.12	24.60	23.85	23.00	23.64	L M
258422	201± 7	17.60±0.018	17.34±0.021	17.90±0.028	0.81	3.93	5.17	22.21	22.59	23.39	22.75	22.52	22.81	L M
258426	59± 6	17.32±0.017	17.03±0.018	17.62±0.027	0.46	6.16	6.58	22.55	22.93	24.07	23.37	22.93	23.33	L M
258428	78± 7	19.14±0.038	18.96±0.050	19.39±0.061	0.82	1.14	1.67	22.56	22.90	24.22	23.36	22.82	23.32	L D
258439	238± 65	17.50±0.017	17.19±0.019	17.81±0.027	0.73	6.26	7.87	23.04	23.39	25.44	23.76	23.37	23.99	L M
261166	42± 12	17.12±0.014	16.75±0.016	17.46±0.023	0.85	3.43	5.01	22.42	22.91	23.93	23.23	22.85	23.23	L M
261941	70± 2	17.91±0.016	17.69±0.020	18.19±0.025	0.64	2.34	1.25	25.01	25.19	28.40	26.59	25.18	26.34	L D
262022	225± 50	17.00±0.014	16.66±0.015	17.33±0.022	0.63	3.83	5.07	22.33	22.76	23.69	22.87	22.76	23.02	L M
262401	54± 10	18.45±0.027	18.23±0.037	18.72±0.044	0.70	1.53	2.14	23.17	23.81	26.73	22.56	23.82	24.23	L D
262774	248± 49	17.89±0.018	17.56±0.020	18.22±0.028	0.79	2.80	4.25	22.56	23.08	24.31	23.72	23.00	23.53	L M
263171	147± 9	17.09±0.014	16.68±0.014	17.46±0.022	0.59	3.07	4.06	22.37	22.78	23.74	23.10	22.75	23.09	L M
263531	222± 10	17.25±0.014	16.86±0.015	17.61±0.022	0.66	5.37	7.28	22.26	22.82	23.65	22.86	22.79	23.03	S M
263837	43± 11	17.25±0.015	16.80±0.015	17.63±0.023	0.71	5.06	6.17	22.30	22.58	23.14	22.57	22.53	22.71	S M

Table 4 continued on next page

**Table 4** (continued)

AGC	W50	g	r	B	b/a	h(g)	$R_{eff}(g)$	$\mu_{0,g}$	$\mu_{0,B}$	$\mu_{0,B}$	$\mu_{0,B}$	$\mu_{0,B}$	T1	T2
		(km s <sup>-1</sup> )	(mag)	(mag)		(kpc)	(kpc)	(AUTO)	( AUTO)	ISO	ISOCOR	PETRO	AVE	
263839	$170 \pm 7$	$16.53 \pm 0.010$	$16.29 \pm 0.012$	$16.82 \pm 0.017$	0.48	5.83	6.61	22.29	22.64	23.52	23.13	22.60	22.97	L M
263864	$103 \pm 5$	$15.96 \pm 0.007$	$15.45 \pm 0.007$	$16.36 \pm 0.011$	0.83	7.12	9.03	22.06	22.56	23.01	22.31	22.55	22.61	S G
263923	$128 \pm 9$	$17.14 \pm 0.014$	$16.79 \pm 0.014$	$17.47 \pm 0.021$	0.70	3.35	4.76	22.07	22.52	23.39	22.80	22.50	22.80	L M
264012	$191 \pm 22$	$17.75 \pm 0.021$	$17.30 \pm 0.021$	$18.14 \pm 0.033$	0.79	5.34	6.86	22.92	23.41	24.55	23.42	23.32	23.67	L M
264157	$101 \pm 30$	$17.80 \pm 0.020$	$17.61 \pm 0.025$	$18.06 \pm 0.032$	0.62	4.96	4.97	22.96	23.23	24.24	23.44	23.19	23.53	L M
264618	$194 \pm 40$	$17.47 \pm 0.015$	$17.08 \pm 0.016$	$17.82 \pm 0.024$	0.63	4.26	6.21	22.05	22.63	23.61	22.84	22.50	22.89	L M
264697	$36 \pm 5$	$16.78 \pm 0.009$	$16.36 \pm 0.010$	$17.15 \pm 0.015$	0.84	5.50	7.74	22.06	22.52	23.06	22.57	22.45	22.65	L G
265059	$111 \pm 12$	$17.71 \pm 0.022$	$17.30 \pm 0.020$	$18.08 \pm 0.034$	0.80	3.05	4.27	22.37	22.97	23.87	22.96	22.87	23.17	L M
267936	$195 \pm 5$	$18.47 \pm 0.027$	$18.26 \pm 0.035$	$18.74 \pm 0.043$	0.63	2.67	3.50	22.34	22.66	23.94	23.25	22.59	23.11	L M
267948	$91 \pm 8$	$16.17 \pm 0.009$	$15.75 \pm 0.009$	$16.54 \pm 0.014$	0.51	3.23	4.10	22.14	22.50	23.18	22.67	22.48	22.71	L M
267968	$101 \pm 6$	$17.59 \pm 0.016$	$17.53 \pm 0.021$	$17.79 \pm 0.025$	0.51	3.95	4.48	22.38	22.67	23.63	23.23	22.60	23.03	L M
267971	$109 \pm 9$	$18.32 \pm 0.021$	$18.13 \pm 0.029$	$18.57 \pm 0.035$	0.86	2.97	4.67	23.04	23.35	26.07	21.79	23.31	23.63	L M
267972	$67 \pm 3$	$20.24 \pm 0.039$	$20.15 \pm 0.058$	$20.45 \pm 0.064$	0.75	3.30	1.50	25.04	25.93	27.96	27.97	26.06	26.98	L D
267978	$335 \pm 33$	$16.52 \pm 0.009$	$16.15 \pm 0.009$	$16.86 \pm 0.014$	0.63	5.63	5.76	22.42	22.86	23.48	23.00	22.75	23.02	L M
268002	$35 \pm 9$	$18.43 \pm 0.031$	$18.18 \pm 0.038$	$18.71 \pm 0.050$	0.75	1.60	2.18	23.30	23.53	26.16	21.94	23.54	23.79	L D
268003	$70 \pm 7$	$17.07 \pm 0.014$	$16.75 \pm 0.016$	$17.38 \pm 0.022$	0.40	7.27	6.41	22.97	23.15	24.35	24.03	23.03	23.64	L M
268006	$110 \pm 3$	$18.02 \pm 0.024$	$17.87 \pm 0.031$	$18.25 \pm 0.038$	0.45	2.12	2.14	22.94	23.31	25.11	24.38	23.23	24.01	L D
268008	$136 \pm 8$	$16.81 \pm 0.013$	$16.57 \pm 0.016$	$17.08 \pm 0.021$	0.95	3.22	3.71	23.44	23.90	25.41	24.62	23.76	24.42	L M
268017	$116 \pm 9$	$18.75 \pm 0.031$	$18.53 \pm 0.041$	$19.02 \pm 0.050$	0.79	1.08	1.47	22.85	23.08	24.42	23.86	23.10	23.61	L D
268028	$189 \pm 5$	$17.14 \pm 0.015$	$16.78 \pm 0.015$	$17.48 \pm 0.024$	0.37	3.43	3.84	22.13	22.60	23.38	22.78	22.53	22.82	L M
268107	$185 \pm 57$	$16.86 \pm 0.011$	$16.50 \pm 0.012$	$17.20 \pm 0.018$	0.44	6.61	6.28	22.05	22.67	23.39	22.87	22.60	22.88	L G
268137	$63 \pm 7$	$17.50 \pm 0.013$	$17.61 \pm 0.024$	$17.61 \pm 0.022$	0.62	3.07	3.47	22.41	22.70	23.97	23.70	22.65	23.25	L M
268145	$37 \pm 3$	$16.78 \pm 0.013$	$16.27 \pm 0.012$	$17.19 \pm 0.020$	0.87	3.71	6.07	22.20	22.70	23.61	22.56	22.69	22.89	S M
268151	$101 \pm 3$	$17.07 \pm 0.013$	$16.74 \pm 0.015$	$17.40 \pm 0.021$	0.58	2.29	2.44	22.36	22.66	23.35	22.85	22.58	22.86	L M
268158	$330 \pm 46$	$17.67 \pm 0.015$	$17.52 \pm 0.022$	$17.91 \pm 0.025$	0.91	2.57	3.65	22.21	23.17	24.18	23.86	23.03	23.56	U M
268199	$187 \pm 6$	$16.65 \pm 0.011$	$16.29 \pm 0.012$	$16.99 \pm 0.017$	0.36	2.93	2.95	22.16	22.56	23.16	22.59	22.49	22.70	L M
268216	$46 \pm 7$	$16.71 \pm 0.013$	$16.51 \pm 0.016$	$16.98 \pm 0.020$	0.59	1.03	1.18	22.51	22.73	23.65	23.07	22.71	23.04	L D
268219	$63 \pm 6$	$17.31 \pm 0.017$	$16.94 \pm 0.016$	$17.66 \pm 0.027$	0.94	3.46	5.71	22.85	23.23	25.40	23.19	23.19	23.75	S M
268225	$42 \pm 7$	$19.18 \pm 0.036$	$18.82 \pm 0.038$	$19.51 \pm 0.057$	0.93	1.15	0.65	25.29	26.74	29.00	27.55	26.71	27.50	L D
320466	$106 \pm 2$	$16.93 \pm 0.011$	$16.72 \pm 0.014$	$17.21 \pm 0.017$	0.44	3.51	2.42	24.13	24.40	26.18	25.85	24.35	25.20	L D
321166	$114 \pm 4$	$17.29 \pm 0.023$	$16.85 \pm 0.021$	$17.67 \pm 0.035$	0.79	1.49	1.65	23.37	24.08	25.65	21.32	24.02	23.77	L D
321341	$100 \pm 14$	$17.59 \pm 0.018$	$17.31 \pm 0.022$	$17.90 \pm 0.029$	0.98	3.22	5.40	22.38	22.71	24.04	23.07	22.72	23.13	L M
321348	$74 \pm 25$	$18.74 \pm 0.037$	$18.32 \pm 0.037$	$19.10 \pm 0.057$	0.95	1.64	2.92	22.63	23.00	24.87	20.48	22.95	22.82	L D
321385	$75 \pm 8$	$17.81 \pm 0.032$	$17.48 \pm 0.025$	$18.14 \pm 0.049$	0.50	2.15	2.63	22.22	22.59	23.66	23.10	22.40	22.94	L D
321429	$38 \pm 11$	$18.94 \pm 0.035$	$18.68 \pm 0.032$	$19.23 \pm 0.055$	0.87	0.83	1.33	23.19	23.62	26.50	24.97	23.57	24.66	L D
321435	$33 \pm 3$	$18.18 \pm 0.021$	$18.11 \pm 0.028$	$18.37 \pm 0.034$	0.31	1.50	1.37	22.57	22.65	24.19	23.91	22.55	23.33	L D

**Table 4** (*continued*)

AGC	W50	g	r	B	b/a	h(g)	$R_{eff}(g)$	$\mu_{0,g}$	$\mu_{0,B}$	$\mu_{0,B}$	$\mu_{0,B}$	$\mu_{0,B}$	T1	T2
	(km s <sup>-1</sup> )	(mag)	(mag)	(mag)		(kpc)	(kpc)	(AUTO)	( AUTO)	ISO	ISOCOR	PETRO	AVE	
321438	59± 13	19.53±0.046	19.37±0.058	19.77±0.073	0.88	1.60	1.87	23.69	24.03	26.53	24.85	23.96	24.84	L D
321451	117± 15	16.90±0.011	16.65±0.012	17.19±0.017	0.68	2.70	3.16	22.19	22.55	23.04	22.62	22.53	22.69	L M
321490	159± 21	17.66±0.027	17.37±0.024	17.96±0.042	0.37	3.22	3.01	22.70	23.20	24.60	24.07	23.14	23.75	L D
321492	11± 11	18.28±0.023	17.80±0.024	18.68±0.035	0.95	0.43	0.67	22.53	23.14	23.96	22.78	23.18	23.26	L D
331052	61± 2	17.11±0.015	16.94±0.019	17.36±0.024	0.64	2.12	2.57	22.67	22.94	24.57	24.05	22.92	23.62	L D
332328	74± 6	18.41±0.022	18.04±0.024	18.75±0.034	0.55	3.73	2.22	24.97	25.31	29.30	25.06	25.35	26.25	L D
332431	197± 5	16.07±0.020	15.55±0.014	16.48±0.030	0.72	4.10	5.00	22.24	22.88	24.15	19.67	22.74	22.36	S M
332640	172± 9	17.14±0.016	16.78±0.017	17.48±0.026	0.83	3.20	4.22	22.76	23.01	24.36	23.44	22.98	23.45	L M
332761	19± 7	18.12±0.031	17.63±0.028	18.52±0.047	0.81	1.48	2.14	22.66	23.09	24.44	22.54	23.00	23.27	L D
332786	99± 11	17.76±0.025	17.28±0.024	18.15±0.039	0.43	1.34	1.55	22.21	22.57	23.42	22.21	22.70	22.72	L D
332844	166± 8	17.51±0.020	17.06±0.020	17.89±0.031	0.80	3.57	5.07	22.37	22.82	23.80	22.73	22.87	23.06	L M
332861	136± 20	17.34±0.017	16.85±0.016	17.74±0.026	0.45	3.12	3.87	22.25	22.58	23.72	22.94	22.42	22.91	S M
332879	125± 26	17.72±0.024	17.47±0.027	18.01±0.037	0.49	2.81	3.29	22.48	22.74	23.93	22.59	22.70	22.99	L M
332887	112± 8	17.73±0.022	17.43±0.026	18.05±0.035	0.92	2.08	3.22	23.13	23.42	25.62	23.19	23.37	23.90	L D
332906	122± 14	18.15±0.026	17.66±0.024	18.55±0.041	0.79	2.80	3.73	22.92	23.36	24.77	23.11	23.27	23.63	S M
333224	161± 5	17.71±0.027	17.38±0.023	18.04±0.042	0.33	3.44	3.66	22.57	22.91	24.03	23.34	22.95	23.31	L M
333318	216± 15	16.73±0.012	16.33±0.012	17.09±0.018	0.78	5.17	6.39	22.28	22.77	23.33	22.75	22.77	22.90	S G
333442	112± 6	16.96±0.012	16.64±0.014	17.29±0.020	0.95	3.01	5.89	22.13	22.68	23.94	23.32	22.63	23.14	L M
714065	238± 70	17.35±0.016	16.96±0.018	17.70±0.026	0.55	8.77	8.10	22.84	23.17	24.08	23.54	23.15	23.48	S G
714453	231± 5	15.96±0.008	15.57±0.008	16.32±0.013	0.41	9.06	8.79	22.30	22.94	23.76	23.04	22.76	23.13	S G
714568	104± 9	16.97±0.013	16.67±0.014	17.28±0.020	0.81	4.24	5.91	22.21	22.54	23.32	22.72	22.50	22.77	L M
715606	86± 8	17.64±0.021	17.16±0.019	18.03±0.033	0.87	0.99	1.45	22.67	23.00	23.85	23.00	23.14	23.25	L D
716435	181± 11	16.90±0.012	16.54±0.014	17.23±0.019	0.73	4.51	7.05	22.12	22.70	23.93	23.18	22.66	23.12	L M
716496	117± 4	17.37±0.018	17.03±0.020	17.70±0.028	0.34	1.00	1.00	22.47	22.81	23.78	23.04	22.79	23.10	L D
716572	111± 8	17.54±0.020	17.18±0.021	17.88±0.031	0.71	4.90	5.55	22.83	23.17	24.21	23.38	23.10	23.47	S M
719525	124± 3	16.31±0.009	16.09±0.011	16.59±0.014	0.92	3.51	5.40	22.50	22.92	24.12	23.57	22.86	23.37	L M
721420	102± 33	17.30±0.013	16.99±0.015	17.62±0.021	0.67	3.52	4.19	22.24	22.60	23.19	22.61	22.58	22.75	L M
721422	179± 17	16.95±0.011	16.63±0.014	17.26±0.018	0.80	3.19	5.24	22.21	22.75	23.86	23.31	22.68	23.15	L M
721463	49± 14	17.82±0.017	17.42±0.021	18.18±0.027	0.82	2.88	4.53	22.15	22.61	23.59	22.89	22.58	22.92	L M
721677	150± 12	17.18±0.020	16.76±0.017	17.55±0.031	0.86	4.98	8.01	22.44	22.75	24.17	23.32	22.73	23.24	S M
721947	188± 17	16.14±0.008	15.78±0.009	16.47±0.013	0.76	3.65	4.75	22.30	22.76	23.45	22.71	22.71	22.91	L M
721965	90± 4	17.25±0.021	16.87±0.018	17.60±0.032	0.93	2.01	3.12	22.36	22.84	23.80	23.14	22.87	23.16	S M
721972	36± 9	17.66±0.018	17.26±0.021	18.01±0.029	0.34	0.63	0.66	22.33	22.63	23.40	22.84	22.58	22.86	L D
722180	147± 41	17.78±0.018	17.45±0.024	18.11±0.029	0.57	3.85	4.63	22.37	22.74	23.72	23.11	22.74	23.08	L M
722439	98± 47	17.82±0.020	17.62±0.028	18.09±0.033	0.63	2.07	2.51	22.94	23.29	24.66	23.55	23.22	23.68	L D
722779	443± 53	16.74±0.009	15.97±0.007	17.28±0.014	0.45	6.35	7.35	21.82	22.59	23.13	22.41	22.53	22.66	E G

Table 4 continued on next page

**Table 4** (*continued*)

AGC	W50	g	r	B	b/a	h(g)	$R_{eff}(g)$	$\mu_{0,g}$	$\mu_{0,B}$	$\mu_{0,B}$	$\mu_{0,B}$	$\mu_{0,B}$	T1	T2
	(km s <sup>-1</sup> )	(mag)	(mag)	(mag)		(kpc)	(kpc)	(AUTO)	( AUTO)	ISO	ISOCOR	PETRO	AVE	
722847	117± 11	17.09±0.012	16.84±0.016	17.38±0.020	0.67	2.83	4.12	22.50	22.93	24.23	23.56	22.90	23.41	L M
723151	178± 10	17.31±0.013	17.02±0.016	17.62±0.021	0.58	3.36	4.32	22.06	22.50	23.26	22.70	22.51	22.74	L M
723565	51± 24	17.18±0.012	16.95±0.017	17.46±0.020	0.77	2.68	3.69	22.34	22.63	23.41	22.90	22.63	22.89	L M
723761	188± 12	17.39±0.019	16.89±0.016	17.79±0.030	0.61	3.62	5.42	22.33	22.63	23.78	23.29	22.63	23.08	S M
724084	259± 7	17.20±0.017	16.77±0.015	17.58±0.026	0.35	6.90	7.69	22.06	22.50	23.26	22.78	22.55	22.77	L M
724149	151± 41	17.07±0.011	16.69±0.014	17.43±0.018	0.75	4.19	5.87	22.11	22.53	23.29	22.79	22.54	22.79	S M
724279	77± 64	16.92±0.010	16.50±0.012	17.29±0.016	0.95	5.10	7.51	22.03	22.50	23.07	22.58	22.49	22.66	S G
724915	109± 14	18.16±0.022	17.78±0.025	18.51±0.034	0.55	3.14	2.39	23.21	23.53	24.39	23.94	23.31	23.79	L D
725562	115± 4	16.64±0.010	16.37±0.012	16.94±0.016	0.76	3.06	4.50	22.23	22.65	23.64	23.08	22.65	23.00	L M
725594	133± 17	17.36±0.014	17.03±0.016	17.69±0.022	0.73	3.14	4.45	22.15	22.61	23.48	22.97	22.61	22.92	L M
725708	109± 5	16.71±0.009	16.47±0.012	17.00±0.015	0.82	4.43	6.65	22.25	22.61	23.58	23.15	22.61	22.99	L M
725778	109± 7	17.50±0.015	17.29±0.019	17.77±0.024	0.82	5.18	7.36	22.52	22.99	24.14	23.64	22.90	23.42	L M
726071	151± 43	17.47±0.013	17.24±0.016	17.74±0.021	0.61	3.27	4.48	21.99	22.47	23.26	22.77	22.42	22.73	L M
726075	141± 42	17.96±0.022	17.65±0.024	18.27±0.034	0.46	3.56	4.38	22.36	22.70	23.87	23.11	22.70	23.10	L M
726344	80± 9	17.08±0.013	16.68±0.014	17.44±0.021	0.93	3.29	6.06	22.13	22.67	23.68	22.91	22.62	22.97	L M
726644	125± 12	17.55±0.016	17.35±0.019	17.82±0.025	0.76	2.63	4.18	22.07	22.53	23.49	22.92	22.43	22.84	L M
727027	165± 16	16.94±0.011	16.66±0.014	17.24±0.017	0.54	6.93	7.73	22.40	22.83	23.83	23.30	22.60	23.14	L G
727252	133± 12	17.04±0.014	16.77±0.018	17.34±0.022	0.65	4.29	4.99	23.20	23.55	25.18	23.45	23.41	23.90	L M
731387	310± 7	17.61±0.017	17.19±0.019	17.98±0.027	0.62	3.44	4.70	22.31	22.72	23.76	23.12	22.71	23.08	L M
731404	83± 5	17.38±0.017	17.03±0.019	17.71±0.027	0.83	3.06	4.38	22.91	23.34	24.71	23.51	23.31	23.72	L M
731425	77± 3	17.21±0.012	16.85±0.015	17.55±0.020	0.92	2.47	4.01	22.76	23.22	24.65	24.04	23.12	23.76	S M
731441	147± 6	17.32±0.016	16.90±0.016	17.68±0.024	0.61	2.38	3.15	22.29	22.71	23.60	22.51	22.64	22.87	L M
731444	166± 9	17.78±0.019	17.37±0.021	18.14±0.030	0.96	3.50	5.23	22.65	23.08	24.14	23.36	22.99	23.39	S M
731459	77± 5	16.40±0.008	16.06±0.009	16.73±0.013	0.79	2.97	4.14	22.09	22.48	23.09	22.53	22.47	22.64	L M
731468	146± 8	17.20±0.014	16.92±0.018	17.51±0.022	0.45	3.47	4.00	22.66	23.06	24.28	23.34	22.99	23.42	L M
731550	31± 16	17.19±0.015	16.80±0.019	17.55±0.024	0.81	0.58	0.90	22.38	22.65	23.90	23.35	22.66	23.14	L D
731554	123± 6	17.94±0.022	17.55±0.025	18.29±0.034	0.80	2.20	3.16	22.94	23.34	24.69	23.27	23.36	23.67	L D
731568	159± 8	16.86±0.011	16.42±0.012	17.24±0.017	0.58	2.60	3.57	22.03	22.69	23.42	22.93	22.57	22.90	L M
731691	105± 14	17.55±0.014	17.37±0.021	17.81±0.023	0.62	2.71	3.72	22.32	22.62	23.93	23.62	22.54	23.18	L M
731695	100± 5	17.17±0.011	16.87±0.014	17.48±0.018	0.58	2.74	3.47	22.19	22.64	23.43	22.96	22.58	22.90	L M
731702	90± 25	17.44±0.013	17.16±0.018	17.75±0.021	0.56	4.15	4.59	22.48	22.86	23.56	23.02	22.88	23.08	L M
731710	39± 10	17.33±0.012	17.02±0.015	17.64±0.019	0.76	2.26	2.92	22.16	22.51	22.96	22.67	22.53	22.67	L M
731719	122± 38	17.84±0.019	17.51±0.024	18.17±0.031	0.61	3.84	4.76	22.57	22.92	23.94	23.18	22.84	23.22	L M
731734	57± 11	17.57±0.014	17.22±0.017	17.91±0.023	0.88	3.00	4.56	22.34	22.82	23.65	23.12	22.78	23.09	L M
731735	358± 69	16.85±0.011	16.47±0.012	17.19±0.017	0.59	3.84	4.86	22.54	22.97	23.80	23.06	22.90	23.18	S M
731779	149± 10	17.39±0.013	17.05±0.016	17.72±0.021	0.70	1.98	2.74	22.13	22.50	23.25	22.76	22.47	22.75	L M

Table 4 continued on next page

**Table 4** (*continued*)

AGC	W50	g	r	B	b/a	h(g)	$R_{eff}(g)$	$\mu_{0,g}$	$\mu_{0,B}$	$\mu_{0,B}$	$\mu_{0,B}$	$\mu_{0,B}$	T1	T2
	(km s <sup>-1</sup> )	(mag)	(mag)	(mag)		(kpc)	(kpc)	(AUTO)	( AUTO)	ISO	ISOCOR	PETRO	AVE	
731797	147± 9	16.58±0.010	16.19±0.011	16.93±0.016	0.73	5.16	6.76	22.39	22.83	23.68	22.95	22.85	23.08	S M
731801	120± 6	17.41±0.013	17.15±0.018	17.70±0.021	0.80	2.65	3.78	22.20	22.55	23.37	22.99	22.61	22.88	L M
731805	116± 6	17.50±0.015	17.22±0.019	17.80±0.024	0.35	1.62	1.86	22.28	22.66	23.64	23.13	22.68	23.03	L D
731822	89± 6	17.20±0.014	17.15±0.021	17.39±0.023	0.64	2.97	3.65	22.77	23.16	24.44	23.68	23.05	23.58	L M
731831	90± 4	17.10±0.011	16.90±0.016	17.37±0.018	0.81	1.46	2.34	22.21	22.65	23.74	23.32	22.51	23.05	L D
731848	74± 5	16.42±0.008	16.06±0.010	16.76±0.013	0.72	3.45	4.51	22.28	22.66	23.24	22.64	22.67	22.80	S M
731876	105± 10	16.75±0.013	16.22±0.012	17.17±0.020	0.71	2.29	2.99	22.62	23.03	23.84	22.86	23.03	23.19	L D
731879	59± 2	17.09±0.014	16.72±0.016	17.43±0.022	0.89	2.76	4.30	22.94	23.36	24.88	23.69	23.33	23.82	S M
731941	46± 11	17.82±0.019	17.49±0.024	18.15±0.031	0.69	1.01	1.39	22.90	23.19	24.50	23.47	23.12	23.57	L D
732031	161± 32	17.16±0.014	16.78±0.016	17.51±0.022	0.41	4.52	4.76	22.85	23.30	24.61	23.54	23.22	23.67	S M
732066	172± 43	17.30±0.015	16.98±0.017	17.63±0.023	0.60	3.19	3.97	22.54	23.00	24.07	23.30	22.88	23.31	L M
732086	102± 7	16.91±0.010	16.63±0.013	17.22±0.016	0.79	2.77	4.29	22.16	22.67	23.69	23.24	22.59	23.05	L M
732102	129± 9	17.51±0.015	17.23±0.019	17.81±0.024	0.69	3.73	4.44	22.73	23.20	24.20	23.41	23.07	23.47	L M
732118	190± 6	17.68±0.018	17.43±0.022	17.97±0.028	0.54	3.57	4.55	22.44	22.84	24.08	23.25	22.83	23.25	L M
732119	139± 7	17.39±0.015	17.13±0.020	17.68±0.024	0.77	3.59	4.43	22.86	23.19	24.22	23.63	23.13	23.54	L M
732120	94± 8	17.86±0.019	17.60±0.023	18.16±0.030	0.86	1.67	2.78	22.36	22.77	23.95	23.34	22.70	23.19	L D
732134	37± 6	16.84±0.010	16.53±0.012	17.15±0.015	0.33	1.09	1.11	22.53	22.73	24.02	23.85	22.60	23.30	L D
732139	127± 19	17.40±0.014	17.03±0.016	17.75±0.022	0.56	2.61	2.83	22.42	22.77	23.39	22.88	22.77	22.95	L M
732178	155± 4	17.53±0.014	17.31±0.019	17.80±0.022	0.57	2.35	3.19	22.34	22.72	23.92	23.49	22.62	23.19	L M
732185	66± 15	17.14±0.011	17.07±0.017	17.35±0.018	0.81	3.05	4.24	22.53	22.83	24.04	23.66	22.71	23.31	L M
732188	194± 12	16.77±0.010	16.53±0.013	17.05±0.016	0.79	3.24	4.69	22.38	22.75	23.63	23.22	22.71	23.08	L M
732253	61± 9	16.74±0.011	16.48±0.014	17.03±0.018	0.69	2.96	3.84	22.48	22.82	23.62	23.09	22.82	23.09	L M
732254	149± 9	17.57±0.015	17.23±0.019	17.90±0.024	0.57	1.92	2.22	22.43	22.81	23.53	23.06	22.74	23.03	L D
732274	113± 7	16.51±0.010	15.94±0.010	16.95±0.016	0.59	3.58	5.45	22.85	23.05	24.91	23.55	22.98	23.63	L M
732305	38± 11	17.08±0.013	16.77±0.016	17.39±0.021	0.99	2.70	4.20	22.67	22.98	24.03	23.46	22.90	23.34	L M
732488	148± 24	17.07±0.011	16.86±0.016	17.34±0.019	0.59	3.13	3.57	22.51	22.79	23.59	23.13	22.78	23.07	L M
732508	103± 17	17.97±0.017	17.67±0.025	18.28±0.028	0.65	3.18	4.20	22.50	22.96	24.12	23.64	22.84	23.39	L M
732545	88± 5	17.06±0.012	16.76±0.015	17.37±0.019	0.82	2.42	3.62	22.33	22.78	23.72	23.20	22.77	23.12	L M
732593	135± 2	17.13±0.013	16.78±0.014	17.46±0.021	0.43	1.55	1.83	22.54	22.93	23.94	23.21	22.82	23.22	L D
732606	65± 17	17.62±0.017	17.27±0.021	17.96±0.028	0.73	4.07	5.04	22.89	23.19	24.46	23.84	23.19	23.67	L M
732645	82± 6	17.20±0.013	16.84±0.016	17.53±0.021	0.74	2.82	4.25	22.39	22.72	24.08	23.57	22.74	23.28	L M
732661	179± 42	17.62±0.017	17.26±0.020	17.96±0.027	0.66	3.26	4.39	22.95	23.40	24.88	23.83	23.36	23.87	L M
732677	56± 18	18.85±0.022	18.49±0.026	19.18±0.035	0.91	2.99	2.52	24.30	24.71	26.92	26.21	24.53	25.59	L D
732709	115± 15	17.51±0.016	17.20±0.020	17.83±0.025	0.69	2.70	3.69	22.46	22.88	23.96	23.40	22.81	23.26	L M
732731	55± 17	17.85±0.020	17.58±0.024	18.15±0.031	0.91	2.78	3.75	23.17	23.55	24.93	23.90	23.47	23.96	L M
732815	39± 5	16.76±0.009	16.34±0.011	17.13±0.015	0.83	3.66	5.24	22.22	22.62	23.27	22.72	22.71	22.83	S M

Table 4 continued on next page

**Table 4** (*continued*)

AGC	W50	g	r	B	b/a	h(g)	$R_{eff}(g)$	$\mu_{0,g}$	$\mu_{0,B}$	$\mu_{0,B}$	$\mu_{0,B}$	$\mu_{0,B}$	T1	T2
		(km s <sup>-1</sup> )	(mag)	(mag)		(kpc)	(kpc)	(AUTO)	( AUTO)	ISO	ISOCOR	PETRO	AVE	
732831	$33 \pm 7$	$18.01 \pm 0.021$	$17.61 \pm 0.024$	$18.37 \pm 0.034$	0.93	3.73	5.89	22.63	23.03	24.45	23.58	23.04	23.53	S M
732886	$144 \pm 6$	$16.83 \pm 0.009$	$16.54 \pm 0.012$	$17.15 \pm 0.015$	0.91	3.49	4.66	22.34	22.69	23.34	22.99	22.68	22.92	L M
732898	$23 \pm 16$	$17.78 \pm 0.018$	$17.47 \pm 0.022$	$18.10 \pm 0.029$	0.94	3.15	4.64	23.04	23.46	24.88	23.58	23.47	23.85	L M
732936	$152 \pm 10$	$16.96 \pm 0.012$	$16.63 \pm 0.014$	$17.28 \pm 0.020$	0.36	2.69	2.53	22.63	23.07	24.01	23.32	22.99	23.35	L D
732937	$148 \pm 7$	$17.13 \pm 0.015$	$16.85 \pm 0.018$	$17.44 \pm 0.024$	0.52	2.68	3.12	22.82	23.22	24.42	23.56	23.17	23.59	L D
732942	$147 \pm 3$	$16.95 \pm 0.012$	$16.61 \pm 0.013$	$17.27 \pm 0.019$	0.69	4.59	6.65	22.24	22.73	23.71	23.06	22.79	23.07	L M
732956	$78 \pm 9$	$17.31 \pm 0.013$	$16.96 \pm 0.016$	$17.65 \pm 0.021$	0.71	1.57	2.10	22.36	22.72	23.49	22.93	22.68	22.96	L D
732966	$45 \pm 2$	$17.11 \pm 0.016$	$16.85 \pm 0.020$	$17.41 \pm 0.026$	0.93	1.95	2.98	22.94	23.20	24.95	24.05	23.16	23.84	L D
733018	$21 \pm 4$	$17.19 \pm 0.014$	$16.88 \pm 0.016$	$17.51 \pm 0.023$	0.79	1.79	2.47	22.45	22.85	23.74	22.97	22.81	23.09	L D
733119	$125 \pm 11$	$17.78 \pm 0.018$	$17.48 \pm 0.022$	$18.09 \pm 0.029$	0.70	2.32	3.05	22.46	22.87	23.96	23.38	22.80	23.25	L M
733167	$214 \pm 42$	$18.06 \pm 0.021$	$17.61 \pm 0.020$	$18.43 \pm 0.032$	0.49	3.85	5.06	22.09	22.59	23.38	22.53	22.58	22.77	L M
733175	$27 \pm 4$	$17.89 \pm 0.020$	$17.54 \pm 0.023$	$18.23 \pm 0.032$	0.75	4.40	6.20	22.56	22.91	24.16	23.43	22.91	23.35	L M
733221	$24 \pm 3$	$16.73 \pm 0.011$	$16.22 \pm 0.010$	$17.14 \pm 0.017$	0.92	5.61	9.32	22.19	22.69	23.45	22.73	22.69	22.89	S G
733260	$139 \pm 18$	$17.70 \pm 0.016$	$17.43 \pm 0.018$	$18.00 \pm 0.025$	0.61	3.72	4.62	22.86	23.61	25.19	24.61	23.53	24.23	L M
733380	$142 \pm 4$	$17.42 \pm 0.018$	$17.09 \pm 0.020$	$17.75 \pm 0.029$	0.69	3.45	4.44	23.22	23.63	25.19	24.03	23.61	24.12	L M
733567	$126 \pm 30$	$17.10 \pm 0.012$	$16.80 \pm 0.013$	$17.41 \pm 0.019$	0.76	3.63	5.04	22.22	22.65	23.39	22.59	22.59	22.80	L M
733582	$244 \pm 29$	$17.03 \pm 0.014$	$16.56 \pm 0.014$	$17.42 \pm 0.022$	0.66	4.61	6.53	22.53	22.97	24.19	23.31	22.97	23.36	S M
733611	$157 \pm 15$	$17.81 \pm 0.018$	$17.55 \pm 0.022$	$18.09 \pm 0.029$	0.63	4.47	5.89	22.09	22.53	23.31	22.58	22.55	22.74	L M
733680	$188 \pm 9$	$17.83 \pm 0.020$	$17.42 \pm 0.021$	$18.20 \pm 0.031$	0.57	4.50	5.08	23.28	23.69	25.47	24.27	23.62	24.26	L M
733721	$239 \pm 15$	$17.44 \pm 0.016$	$17.08 \pm 0.018$	$17.78 \pm 0.025$	0.72	3.20	4.27	22.17	22.59	23.26	22.66	22.59	22.78	L M
733774	$137 \pm 9$	$17.20 \pm 0.013$	$16.81 \pm 0.016$	$17.55 \pm 0.021$	0.57	4.21	5.12	22.23	22.75	23.55	22.95	22.72	22.99	L M
733785	$126 \pm 44$	$17.88 \pm 0.024$	$17.59 \pm 0.026$	$18.18 \pm 0.037$	0.59	2.07	2.38	22.58	22.87	23.88	22.91	22.78	23.11	L D
733793	$227 \pm 24$	$17.41 \pm 0.014$	$17.10 \pm 0.016$	$17.73 \pm 0.022$	0.89	3.89	5.78	22.27	22.69	23.59	23.15	22.70	23.03	L M
735525	$139 \pm 15$	$16.96 \pm 0.013$	$16.65 \pm 0.016$	$17.27 \pm 0.021$	0.80	3.81	5.96	22.07	22.58	23.69	23.00	22.54	22.95	L M
740874	$158 \pm 7$	$16.95 \pm 0.011$	$16.67 \pm 0.013$	$17.25 \pm 0.017$	0.54	3.48	3.87	22.31	22.60	23.23	22.82	22.53	22.80	L M
742129	$104 \pm 39$	$17.43 \pm 0.021$	$17.10 \pm 0.020$	$17.75 \pm 0.033$	0.93	1.96	3.31	22.24	22.56	23.49	22.98	22.55	22.89	L M
742455	$55 \pm 3$	$16.44 \pm 0.013$	$16.19 \pm 0.014$	$16.72 \pm 0.021$	0.64	1.27	1.52	23.12	23.36	25.15	24.44	23.33	24.07	L D
742512	$123 \pm 3$	$16.20 \pm 0.010$	$15.83 \pm 0.009$	$16.55 \pm 0.015$	0.80	3.56	5.15	22.14	22.53	23.12	22.76	22.54	22.74	S M
743527	$44 \pm 8$	$17.64 \pm 0.019$	$17.21 \pm 0.018$	$18.01 \pm 0.030$	0.73	2.68	3.86	22.40	22.82	23.86	23.14	22.77	23.15	L M
748648	$160 \pm 7$	$18.67 \pm 0.037$	$18.50 \pm 0.043$	$18.92 \pm 0.059$	0.75	2.83	3.48	23.05	23.47	25.65	22.80	23.38	23.83	L M
748715	$119 \pm 7$	$18.87 \pm 0.033$	$18.32 \pm 0.029$	$19.30 \pm 0.050$	0.42	1.18	1.32	22.02	22.70	23.25	22.04	22.70	22.67	L D
748723	$115 \pm 19$	$17.30 \pm 0.019$	$16.96 \pm 0.019$	$17.64 \pm 0.029$	0.71	4.83	4.46	22.82	23.73	24.74	24.10	23.63	24.05	L M
748724	$102 \pm 12$	$17.76 \pm 0.022$	$17.54 \pm 0.025$	$18.03 \pm 0.035$	0.33	4.18	4.09	22.54	22.84	24.21	23.33	22.73	23.28	L M
748737	$64 \pm 4$	$17.33 \pm 0.029$	$16.93 \pm 0.026$	$17.69 \pm 0.044$	0.93	2.22	3.32	22.45	22.95	24.45	19.99	22.88	22.57	S M
748738	$27 \pm 4$	$20.03 \pm 0.063$	$19.73 \pm 0.065$	$20.34 \pm 0.099$	0.55	0.98	0.60	24.11	24.34	27.58	23.35	24.36	24.91	U D
748744	$82 \pm 6$	$17.98 \pm 0.034$	$17.56 \pm 0.030$	$18.35 \pm 0.053$	0.70	1.63	1.83	22.93	23.12	24.92	22.46	22.97	23.37	L D

Table 4 continued on next page

**Table 4** (*continued*)

AGC	W50	g	r	B	b/a	h(g)	$R_{eff}(g)$	$\mu_{0,g}$	$\mu_{0,B}$	$\mu_{0,B}$	$\mu_{0,B}$	$\mu_{0,B}$	T1	T2
	(km s <sup>-1</sup> )	(mag)	(mag)	(mag)		(kpc)	(kpc)	(AUTO)	( AUTO)	ISO	ISOCOR	PETRO	AVE	
748757	133± 2	17.03±0.017	16.86±0.017	17.28±0.027	0.30	2.28	2.56	22.29	22.57	23.69	23.38	22.52	23.04	L D
748763	148± 12	19.28±0.051	18.85±0.050	19.65±0.079	0.92	1.66	2.77	22.38	22.72	24.05	22.59	22.63	23.00	L D
748765	32± 3	18.90±0.029	18.72±0.039	19.16±0.047	0.78	1.23	1.09	24.13	24.55	27.48	25.03	24.55	25.40	L D
748766	204± 10	19.64±0.055	19.56±0.074	19.85±0.088	0.75	1.90	2.56	22.88	23.33	25.42	23.27	23.24	23.81	L D
748767	70± 12	17.84±0.019	17.64±0.024	18.10±0.031	0.82	1.51	2.40	23.07	23.37	25.36	23.79	23.30	23.95	L D
748769	19± 2	18.45±0.028	18.14±0.030	18.76±0.044	0.74	1.85	1.85	24.08	24.46	27.59	23.41	24.46	24.98	L D
748770	128± 8	18.06±0.030	17.76±0.033	18.37±0.046	0.43	4.57	4.91	22.70	23.08	24.44	22.98	22.96	23.36	L M
748777	98± 10	18.43±0.028	18.19±0.034	18.71±0.044	0.74	5.90	5.72	23.92	24.25	26.73	23.84	24.17	24.75	L M
748778	16± 3	18.17±0.061	17.79±0.061	18.52±0.086	0.88	0.05	0.04	24.06	24.54	28.02	23.93	24.71	25.30	L D
748779	23± 6	20.51±0.058	20.41±0.072	20.73±0.093	0.70	0.23	0.11	25.06	25.22	29.10	24.70	25.22	26.06	L D
748786	149± 5	17.93±0.027	17.47±0.026	18.32±0.042	0.42	3.20	3.00	23.57	23.78	25.74	23.25	23.76	24.13	L D
748788	51± 9	18.22±0.030	17.97±0.034	18.51±0.047	0.71	1.30	1.80	22.59	22.88	24.30	23.32	22.80	23.33	L D
748790	64± 29	18.42±0.031	18.30±0.040	18.65±0.050	0.35	1.92	1.91	22.82	23.11	24.85	23.76	23.08	23.70	L D
748794	85± 12	18.66±0.031	18.49±0.038	18.91±0.049	0.67	2.08	1.73	23.97	24.16	27.01	22.74	24.08	24.50	L D
748795	139± 70	18.05±0.027	17.65±0.027	18.40±0.042	0.52	3.13	4.07	22.20	22.59	23.79	22.85	22.53	22.94	L M
748798	53± 14	19.29±0.044	18.92±0.045	19.64±0.068	0.83	3.76	3.21	24.35	24.68	27.27	23.12	24.66	24.93	S D
748805	91± 6	18.62±0.036	18.26±0.036	18.96±0.056	0.76	0.85	1.42	22.64	22.83	24.59	22.26	22.73	23.10	L D
748815	144± 7	18.36±0.029	18.02±0.034	18.70±0.045	0.36	1.85	1.79	22.35	22.61	23.45	22.68	22.59	22.83	L D
748816	77± 6	18.37±0.026	18.21±0.034	18.62±0.042	0.40	3.47	2.48	23.87	24.33	26.30	25.18	24.12	24.98	L D
748817	36± 15	17.69±0.019	17.51±0.024	17.95±0.030	0.54	1.95	2.49	22.29	22.54	23.75	23.33	22.46	23.02	L D
748819	53± 2	18.37±0.024	18.10±0.028	18.66±0.038	0.33	1.86	1.03	24.33	24.64	26.85	26.10	24.62	25.55	L D
749186	116± 13	18.20±0.023	18.16±0.036	18.40±0.038	0.49	2.61	3.01	23.13	23.35	25.95	25.00	23.35	24.41	L D
749189	88± 8	20.59±0.046	20.52±0.068	20.80±0.075	0.82	0.35	0.18	25.21	25.42	28.79	26.79	25.44	26.61	L D
749194	144± 7	18.27±0.033	17.86±0.029	18.62±0.051	0.38	3.49	4.00	22.57	22.92	24.01	23.42	22.88	23.31	L M
749196	62± 10	17.93±0.020	17.77±0.029	18.17±0.033	0.64	1.72	2.20	23.30	23.67	25.67	24.20	23.62	24.29	L D
749204	139± 7	18.26±0.021	18.05±0.029	18.53±0.034	0.93	1.44	2.51	22.43	22.79	24.08	23.51	22.78	23.29	L D
749209	145± 24	18.01±0.025	17.70±0.025	18.32±0.039	0.40	2.24	2.55	22.18	22.56	23.51	23.08	22.55	22.93	L D
749220	56± 7	17.71±0.017	17.48±0.022	17.99±0.027	0.75	1.25	1.72	22.73	23.10	24.44	24.00	23.02	23.64	L D
749221	42± 8	18.36±0.025	17.98±0.029	18.71±0.040	0.42	0.97	1.10	22.27	22.51	23.16	22.45	22.57	22.67	L D
749230	127± 10	18.01±0.019	17.74±0.026	18.30±0.031	0.30	2.31	2.22	23.13	23.39	25.42	24.55	23.37	24.18	L D
749238	106± 8	20.10±0.052	19.71±0.061	20.45±0.082	0.65	0.10	0.16	22.31	22.56	23.71	23.04	22.46	22.94	L D
749241	18± 2	19.82±0.040	19.91±0.057	19.95±0.065	0.59	0.17	0.07	25.27	25.18	27.28	27.23	25.15	26.21	L D
749243	93± 8	18.35±0.022	18.16±0.031	18.62±0.036	0.61	2.53	3.12	22.96	23.29	24.88	24.33	23.15	23.91	L D
749245	85± 8	17.55±0.016	17.30±0.021	17.83±0.026	0.64	3.23	4.18	22.87	23.19	24.64	24.05	23.08	23.74	L M
749246	43± 5	20.19±0.047	20.07±0.066	20.41±0.075	0.99	1.19	1.29	23.76	23.49	26.17	25.58	23.50	24.69	U D
749247	134± 8	18.55±0.022	18.35±0.029	18.82±0.036	0.53	2.03	2.63	22.11	22.50	23.38	22.68	22.53	22.77	L D

Table 4 continued on next page

**Table 4** (*continued*)

AGC	W50	g	r	B	b/a	h(g)	$R_{eff}(g)$	$\mu_{0,g}$	$\mu_{0,B}$	$\mu_{0,B}$	$\mu_{0,B}$	$\mu_{0,B}$	T1	T2
		(km s <sup>-1</sup> )	(mag)	(mag)		(kpc)	(kpc)	(AUTO)	( AUTO)	ISO	ISOCOR	PETRO	AVE	
749256	108± 8	19.06±0.035	18.81±0.043	19.35±0.055	0.83	1.11	1.70	22.29	22.60	23.67	23.18	22.49	22.99	L D
749260	102± 3	16.92±0.014	16.64±0.018	17.22±0.023	0.34	3.23	3.06	22.65	22.92	24.28	23.30	22.93	23.36	L D
749264	145± 6	17.58±0.016	17.13±0.018	17.97±0.025	0.55	2.10	2.90	21.95	22.66	23.67	22.84	22.63	22.95	S M
749266	45± 6	18.26±0.026	17.90±0.033	18.60±0.042	0.85	1.24	1.63	22.91	23.66	25.11	24.18	23.62	24.14	L D
749269	151± 57	19.20±0.030	18.85±0.037	19.53±0.048	0.70	1.49	2.20	22.86	22.99	26.60	22.50	23.04	23.78	L D
749271	45± 5	17.66±0.017	17.51±0.023	17.90±0.028	0.95	2.18	3.05	22.56	23.43	24.53	24.07	23.36	23.85	L M
749279	69± 11	20.60±0.053	20.66±0.084	20.75±0.088	0.65	1.31	0.88	24.04	24.18	26.50	26.18	24.16	25.25	L D
749282	128± 5	18.29±0.028	18.05±0.034	18.57±0.044	0.82	1.57	2.27	23.07	23.29	25.02	23.56	23.20	23.77	L D
749284	145± 7	17.28±0.015	16.95±0.017	17.61±0.024	0.81	5.52	8.94	22.41	22.91	24.32	23.37	22.89	23.37	L G
749287	149± 7	18.05±0.022	17.78±0.025	18.35±0.034	0.37	2.43	2.53	22.42	22.83	23.79	23.18	22.77	23.14	L D
749288	39± 3	17.90±0.020	17.70±0.026	18.16±0.033	0.55	3.65	4.43	23.28	23.57	26.05	24.25	23.54	24.35	L M
749297	136± 41	18.01±0.020	17.80±0.026	18.29±0.032	0.72	2.52	3.84	22.21	22.60	23.75	23.05	22.58	22.99	L M
749299	55± 7	18.31±0.034	18.06±0.034	18.60±0.053	0.42	3.34	3.67	22.58	22.88	24.41	23.88	22.84	23.50	L M
749303	49± 7	18.47±0.023	18.17±0.029	18.77±0.037	0.44	0.78	0.45	24.40	24.67	27.60	25.63	24.66	25.64	L D
749304	64± 9	18.72±0.029	18.54±0.038	18.97±0.046	0.60	0.42	0.58	22.47	22.77	23.88	23.09	22.70	23.11	L D
749308	141± 10	17.92±0.021	17.71±0.026	18.19±0.033	0.35	4.85	5.13	22.49	22.92	24.21	23.53	22.81	23.37	L M
749313	96± 6	17.79±0.018	17.57±0.024	18.06±0.029	0.87	1.63	2.36	22.30	22.57	23.43	23.04	22.51	22.89	L D
749316	41± 12	18.07±0.020	17.96±0.031	18.29±0.033	0.41	0.48	0.53	22.40	22.57	23.43	23.07	22.53	22.90	L D
749318	91± 6	19.62±0.046	19.23±0.054	19.97±0.073	0.63	1.82	2.18	23.57	24.07	25.96	23.40	23.94	24.34	S D
749322	121± 3	19.24±0.032	19.15±0.049	19.45±0.052	0.85	1.36	1.79	23.19	23.32	25.61	25.17	23.32	24.36	L D
749323	49± 8	16.99±0.013	16.53±0.015	17.38±0.020	0.89	0.82	1.16	22.85	23.18	24.22	23.26	23.07	23.43	L D
749324	56± 5	17.23±0.015	17.01±0.019	17.51±0.024	0.49	0.81	0.90	22.60	22.85	23.75	23.01	22.78	23.10	L D
749329	76± 7	19.80±0.042	19.50±0.048	20.12±0.066	0.57	1.40	1.26	23.94	24.15	27.38	23.09	24.19	24.70	L D
749330	32± 7	19.85±0.057	19.41±0.060	20.23±0.088	0.40	0.46	0.54	22.68	23.11	24.27	23.09	22.95	23.35	L D
749333	45± 7	18.61±0.028	18.38±0.036	18.89±0.044	0.49	2.46	2.91	22.46	22.74	23.69	23.10	22.57	23.03	L D
749336	71± 6	18.04±0.023	17.72±0.027	18.36±0.036	0.67	1.25	1.77	22.48	22.70	23.79	23.13	22.66	23.07	L D
749339	190± 56	18.04±0.019	17.68±0.023	18.37±0.030	0.76	3.46	4.70	22.43	22.87	23.66	23.02	22.84	23.10	L M
749343	38± 11	18.67±0.027	18.43±0.031	18.96±0.043	0.54	2.86	2.48	23.84	24.23	26.54	24.22	24.17	24.79	L D
749344	82± 11	18.84±0.027	18.55±0.037	19.14±0.043	0.99	3.62	3.00	24.45	24.65	26.74	25.30	24.51	25.30	L D
749347	38± 7	17.79±0.019	17.54±0.026	18.08±0.031	0.67	0.94	1.07	23.19	23.45	25.01	23.96	23.34	23.94	L D
749349	27± 5	18.64±0.027	18.30±0.030	18.97±0.042	0.86	0.87	0.89	24.30	23.38	25.96	21.85	23.36	23.64	L D
749354	109± 7	18.12±0.021	17.90±0.027	18.40±0.034	0.71	3.97	5.68	22.51	22.91	24.25	23.56	22.86	23.40	L M
749356	139± 6	18.11±0.020	17.75±0.022	18.44±0.032	0.54	1.78	2.48	22.30	22.77	23.84	23.36	22.68	23.16	L D
749358	88± 7	18.19±0.024	17.89±0.027	18.50±0.038	0.95	3.94	5.90	23.41	23.85	25.75	24.04	23.79	24.36	L M
749362	175± 8	17.54±0.016	17.32±0.020	17.82±0.026	0.52	3.93	4.73	22.69	23.02	24.42	23.86	22.98	23.57	L M
749363	103± 5	17.36±0.015	17.06±0.018	17.67±0.024	0.50	2.72	4.06	22.64	23.14	25.05	24.00	23.03	23.80	L D

Table 4 continued on next page

**Table 4** (*continued*)

AGC	W50	g	r	B	b/a	h(g)	$R_{eff}(g)$	$\mu_{0,g}$	$\mu_{0,B}$	$\mu_{0,B}$	$\mu_{0,B}$	$\mu_{0,B}$	T1	T2
	(km s <sup>-1</sup> )	(mag)	(mag)	(mag)		(kpc)	(kpc)	(AUTO)	( AUTO)	ISO	ISOCOR	PETRO	AVE	
749366	34± 8	20.04±0.061	19.71±0.066	20.36±0.095	0.69	0.67	0.95	23.20	23.53	25.64	21.83	23.54	23.63	L D
749368	51± 3	18.73±0.026	18.51±0.034	19.01±0.042	0.47	1.50	1.76	23.28	23.63	25.83	24.72	23.58	24.44	L D
749376	33± 7	20.45±0.057	20.11±0.067	20.78±0.090	0.88	1.23	0.75	25.08	25.57	28.63	24.31	25.58	26.02	L D
749377	98± 11	18.10±0.022	17.87±0.030	18.38±0.035	0.75	1.83	2.63	22.25	22.61	23.72	23.26	22.61	23.05	L D
749380	140± 4	17.97±0.021	17.63±0.022	18.30±0.033	0.30	2.17	2.34	22.19	22.59	23.62	22.88	22.66	22.94	L D
749383	97± 6	18.25±0.023	17.94±0.027	18.57±0.037	0.57	3.89	3.81	23.38	23.61	25.32	24.38	23.50	24.20	L M
749388	56± 7	18.49±0.031	18.24±0.039	18.78±0.049	0.52	1.89	2.12	23.20	23.50	25.30	23.13	23.47	23.85	L D
749390	100± 21	18.60±0.035	18.21±0.037	18.95±0.055	0.85	1.58	1.93	23.45	23.65	25.74	23.73	23.59	24.18	U D
749396	75± 4	18.82±0.027	19.10±0.057	18.86±0.048	0.66	0.69	0.75	23.21	23.48	26.05	25.29	23.42	24.56	L D
749397	58± 2	17.22±0.014	16.94±0.019	17.52±0.023	0.77	1.80	1.64	23.96	24.21	26.55	25.32	24.18	25.06	L D
749404	198± 14	17.96±0.020	17.70±0.026	18.25±0.033	0.38	3.56	4.00	22.26	22.56	23.60	23.04	22.52	22.93	L M
749405	147± 10	18.02±0.029	17.63±0.026	18.38±0.044	0.35	1.61	1.65	22.69	23.11	24.35	23.63	23.05	23.53	L D
749406	26± 6	20.62±0.063	20.44±0.081	20.87±0.101	0.86	0.60	0.25	25.84	25.97	28.69	27.47	25.99	27.03	L D
749408	23± 3	16.85±0.018	16.45±0.015	17.21±0.027	0.69	0.85	0.98	22.91	23.22	24.17	23.49	23.24	23.53	L D
749409	56± 9	18.96±0.038	18.81±0.043	19.20±0.060	0.58	1.73	1.81	23.62	23.96	26.24	25.37	23.90	24.87	L D
749410	27± 2	17.01±0.013	16.62±0.015	17.37±0.020	0.60	0.65	0.93	22.33	22.76	23.81	23.07	22.56	23.05	L D
749419	47± 6	18.07±0.021	17.67±0.025	18.42±0.033	0.62	3.50	3.86	22.87	23.79	24.95	24.30	23.72	24.19	S M
749423	106± 12	17.31±0.015	16.93±0.016	17.65±0.023	0.52	3.55	3.67	22.94	23.29	24.28	23.62	23.30	23.62	S M
749424	151± 7	17.34±0.015	17.07±0.019	17.64±0.024	0.69	2.43	3.30	22.48	22.82	23.97	23.34	22.79	23.23	L M
749425	96± 9	20.38±0.042	20.28±0.065	20.59±0.070	0.33	1.62	0.91	24.06	24.45	27.45	26.66	24.51	25.77	L D
749426	114± 9	18.32±0.021	18.07±0.027	18.60±0.034	0.51	1.74	2.12	22.38	22.64	23.61	23.18	22.54	22.99	L D
749428	89± 15	18.88±0.041	18.61±0.042	19.17±0.064	0.86	1.31	2.00	22.76	23.17	24.49	23.83	23.05	23.64	L D
749430	143± 43	16.88±0.014	16.52±0.013	17.22±0.021	0.38	6.37	6.63	22.72	23.40	24.52	24.17	23.13	23.81	L M
749433	26± 6	19.15±0.033	18.80±0.039	19.48±0.052	0.36	1.46	1.56	22.23	22.54	23.27	22.81	22.51	22.78	L D
749435	24± 9	19.23±0.032	19.10±0.048	19.46±0.053	0.52	0.49	0.64	22.54	22.89	24.12	23.60	22.86	23.37	L D
749436	39± 2	19.29±0.031	19.08±0.040	19.56±0.049	0.86	0.55	0.37	25.17	25.42	27.70	25.90	24.96	25.99	L D
749437	40± 3	17.28±0.014	17.03±0.019	17.57±0.023	0.68	4.63	5.43	23.61	24.03	26.23	24.34	24.00	24.65	L M
749438	106± 7	18.09±0.020	17.88±0.028	18.36±0.033	0.58	1.05	1.32	22.51	22.83	23.79	23.22	22.80	23.16	L D
749439	55± 8	18.28±0.014	18.26±0.023	18.46±0.024	0.82	1.00	1.16	22.98	23.13	24.26	24.20	22.89	23.62	L D
749440	126± 19	16.93±0.011	16.58±0.013	17.27±0.017	0.89	2.10	3.02	22.23	22.61	23.26	22.82	22.57	22.82	L M
749446	82± 7	18.25±0.027	17.80±0.027	18.64±0.041	0.65	1.56	1.91	23.20	23.60	25.09	22.96	23.47	23.78	L D
749447	122± 16	17.81±0.020	17.52±0.024	18.12±0.032	0.51	2.11	2.33	23.11	23.47	25.06	23.95	23.40	23.97	L D
749450	38± 3	18.02±0.022	17.84±0.031	18.27±0.036	0.30	1.59	1.56	22.89	23.07	24.72	23.89	23.02	23.67	L D
749452	80± 7	18.17±0.022	18.10±0.034	18.37±0.037	0.53	1.18	1.50	23.34	23.65	25.83	24.87	23.54	24.47	L D
749453	31± 3	18.31±0.022	18.03±0.028	18.61±0.036	0.75	1.96	2.89	22.61	23.04	24.34	23.70	22.99	23.52	L D
749464	129± 10	18.35±0.034	18.13±0.035	18.63±0.053	0.32	2.80	2.60	22.94	23.27	24.91	24.02	23.31	23.88	L D

Table 4 continued on next page

**Table 4** (*continued*)

AGC	W50	g	r	B	b/a	h(g)	$R_{eff}(g)$	$\mu_{0,g}$	$\mu_{0,B}$	$\mu_{0,B}$	$\mu_{0,B}$	$\mu_{0,B}$	T1	T2
	(km s <sup>-1</sup> )	(mag)	(mag)	(mag)		(kpc)	(kpc)	(AUTO)	( AUTO)	ISO	ISOCOR	PETRO	AVE	
749471	98± 5	19.16±0.030	18.94±0.037	19.43±0.048	0.77	2.09	1.84	24.57	25.44	28.78	24.58	25.51	26.08	L D
749475	117± 8	18.54±0.027	18.32±0.033	18.81±0.043	0.50	3.12	3.71	22.39	22.65	23.59	22.86	22.65	22.94	L M
749479	39± 5	18.47±0.034	17.31±0.018	19.18±0.050	0.69	2.58	3.94	22.94	23.98	25.14	20.73	24.02	23.46	E D
749480	25± 2	20.13±0.045	20.03±0.063	20.35±0.073	0.72	0.68	0.38	25.05	25.27	28.44	24.46	25.31	25.87	L D
749481	35± 5	18.10±0.026	17.65±0.026	18.49±0.040	0.94	3.73	5.14	23.41	23.49	25.56	21.24	23.42	23.43	L M
749483	89± 2	17.79±0.020	17.49±0.023	18.10±0.031	0.64	1.34	1.72	22.58	22.89	23.83	22.88	22.81	23.10	L D
749485	36± 6	18.83±0.035	18.57±0.041	19.13±0.055	0.38	0.38	0.44	22.58	22.73	24.18	23.52	22.75	23.29	L D
749486	32± 8	18.56±0.031	18.36±0.037	18.83±0.049	0.75	1.43	1.76	23.50	23.76	25.34	24.38	23.54	24.25	L D
749492	126± 4	18.68±0.034	18.62±0.038	18.88±0.053	0.68	2.30	3.13	22.31	22.62	23.87	23.59	22.55	23.16	L M
749494	126± 7	18.08±0.019	17.76±0.023	18.39±0.031	0.94	1.33	2.26	22.07	22.51	23.38	22.79	22.43	22.78	L D
749495	110± 14	18.59±0.026	18.31±0.032	18.90±0.042	0.71	0.98	1.58	22.13	22.52	23.56	22.93	22.46	22.87	L D
749503	55± 12	18.68±0.042	18.39±0.039	18.99±0.064	0.99	4.25	4.20	24.11	24.42	26.80	25.81	24.37	25.35	L M
749505	107± 11	18.83±0.029	18.50±0.033	19.15±0.046	0.66	2.57	2.61	23.09	23.42	24.58	24.01	23.26	23.82	L D
749508	53± 7	18.18±0.021	17.83±0.022	18.52±0.032	0.98	8.68	6.45	24.60	24.93	26.61	25.52	24.73	25.45	L M
749509	96± 9	18.30±0.025	17.98±0.026	18.62±0.039	0.79	3.10	4.56	22.72	23.85	25.57	24.60	23.77	24.45	L M
749510	59± 6	17.81±0.022	17.47±0.023	18.13±0.034	0.62	2.12	2.82	23.20	23.52	25.58	24.01	23.46	24.14	L D

## REFERENCES

- Aaronson, M. & Mould, J., 1983, ApJ, 265, 1
- Abazajian, K. N., Adelman-McCarthy, J. K., Agers, M. A., et al., 2009, ApJS, 182, 543
- Adelman-McCarthy, J. K., Agers, M. A., Allam, S. S., et al., 2006, ApJS, 162, 38A
- Bertin, E., & Arnouts, S., 1996, A&AS, 117, 393
- Begum, A., Chengalur, J. N., Karachentsev, I. D., & Sharina, M. E., 2008, MNRAS, 386, 138
- Bell, E. F. & de Jong, R. S., 2001, ApJ, 550, 212
- Bergvall, N., Ronnback, J., Masegosa, J., & Ostlin, G., 1999, A&A, 341, 697
- Boissier, S., Boselli, A., Ferrarese L., et al., 2016, A&A, 593, 126
- Bothun, G. D., 1982, ApJS, 50, 39
- Bothun, G. D., Impey, D. C., Malin, F. D. & Mould, R. J., 1987, AJ, 94, 1
- Bothun, G. D., Schombert, J. M., Impey, C. D. & Schneider, S. E., 1990, ApJ, 360, 427
- Bothun G. D. et al., 1997, PASP, 109, 745
- Bottinelli, L., Gouguenheim, L., Paturel, G., & Teerikorpi, P., 1986, A&A, 156, 157
- Broeils A. H., 1992, PhD thesis, Univ. Groningen
- Burkholder, V., Impey, C. & Sprayberry, D., 2001, AJ, 122, 2318
- Burstein, D., 1982, ApJ, 253, 539
- Ceccarelli L., Herrera-Camus R., Lambas D. G., Galaz G., Padilla N. D., 2012, MNRAS, 426, 6
- Chung, A., van Gorkom, J. H., O'Neil, K., & Bothun, D. G., 2002, AJ, 123, 2387
- Courteau, S., 1997, AJ, 114, 2402
- Courteau, S., Dutton, A. A., van den Bosch, F. C., et al. 2007, ApJ, 671, 203
- Courtois, M. H., Tully, B. R., Fisher, R. J., Bonhomme, N., & Zavodny, M. 2009, AJ, 138, 1938
- Das M. et al., 2009, ApJ, 693, 1300
- de Blok, W. J. G., van der Hulst, J. M., & Bothun, G. D., 1995, MNRAS, 274, 235
- de Blok, W. J. G., McGaugh, S. S., & van der Hulst, J. M., 1996, MNRAS, 283, 18
- de Vaucouleurs G., 1959, Handbuch der Physik, 53, 311
- de Vaucouleurs G., 1974, IAU Symp., 58, 1
- de Vaucouleurs G., 1975, ApJS, 29, 193
- de Vaucouleurs G., de Vaucouleurs A., & Corwin H. G., 1976, Second Reference Catalogue of Bright Galaxies. University of Texas Press, Austin
- Dobrycheva et al., 2017, arXiv:1712.08955
- Driver, S. P., et al., 2011, MNRAS, 413, 971
- Du, W., Wu, H., Lam, Man I., et al., 2015, AJ, 149, 199
- Dunn M. J., 2010, MNRAS, 408, 392
- Fouque, P., Bottinelli, L., & Gouguenheim, L., 1990, ApJ, 349, 1
- Freedman, L. W., 1990, ApJ, 355, L35
- Galaz, G., Dalcanton, J. J., Infante, L., & Treister, E., 2002, AJ, 124, 1360
- Galaz G. et al., 2011, ApJ, 728, 74
- Galaz, G., Milovic, C., Suc, V. et al. 2015, ApJL, 815, 29
- Giovanelli, R., Haynes, M. P., Herter, T. et al., 1997, AJ, 113, 53
- Giovanelli, R., Haynes, M. P., Kent, B. R., et al., 2005, AJ, 130, 2598
- Gurovich, S., Freeman, K., Jerjen, H., Staveley-Smith, L., & Puerari, I., 2010, AJ, 140, 663
- Haberzettl L. et al., 2007, A&A, 471, 787
- He, Y. Q., Xia, X. Y., Hao, C. N., et al., 2013, ApJ, 773, 37
- Haynes, M. P., Giovanelli, R., Martin, A. M. et al., 2011, AJ, 142, 170
- Haynes, M. P., Giovanelli, R., Kent, B. R. et al., 2018, ApJ, 861, 49
- Ho, Luis, 2007, ApJ, 668, 94
- Hubble, E. 1926, ApJ, 64, 321
- Impey, C. D., Bothun, G. D. & Malin, F. D., 1988, ApJ, 330, 634
- Impey, C. D., Sprayberry, D., Irwin, M. J., & Bothun, G. D., 1996, ApJS, 105, 209
- Impey, C. & Bothun, G., 1997, AR&AA, 35, 267
- Impey C., Burkholder V., Sprayberry D., 2001, AJ, 122, 2341
- Infante L 1987, A&A, 183, 177
- Knezek P. M., 1993, PhD thesis, Univ. Massachusetts
- Kniazev, A. Y., Grebel, E. K., Pustilnik, S. A. et al., 2004, AJ, 127, 704
- Kron R. G. 1980, ApJ, 43, 305
- Lei F. J., Wu H., Du W., et al., 2018, ApJS, 235, 18
- Liske, J., et al., 2015, MNRAS, 452, 2087
- Lisker, T., Grebel, E. K., Binggeli, B., & Katharina, G., 2007, ApJ, 660, 1186
- Liu, F. S., Xia, X. Y., Mao, S., Wu, H., & Deng, Z. G., 2008, MNRAS, 385, 23
- Malhotra, S., Spergel, D. N., Rhoads, J. E., & Li, J., 1996, ApJ, 473, 687
- Masters et al., 2008, AJ, 135, 1738
- Matthews, L. D., van Driel, W., & Gallagher, J. S., 1998, AJ, 116, 2196
- Matthews, L. D., van Driel, W., Monnier-Ragaigne, D., 2001, A&A, 365, 1
- McGaugh, S. S., & Bothun, G. D., 1994, AJ, 107, 530
- McGaugh, S. S., Bothun, G. D., & Schombert, J. M., 1995, AJ, 110, 573

- McGaugh S. S., 1996, MNRAS, 280, 337
- McGaugh, S. S., Schombert, J. M., Bothun, G. D., & de Blok, W. J. G., 2000, ApJ, 533, 99
- McGaugh, S. S., 2005, ApJ, 632, 859
- McGaugh, S. S., 2012, AJ, 143, 40
- Minchin, R. F. et al., 2004, MNRAS, 355, 1303
- Nair, B. P. & Abraham, G. R., 2010, ApJS, 186, 427
- O'Neil, K., Bothun, G. D., & Schombert J., 2000, AJ, 119, 136
- O'Neil, K., Bothun, G. D., van Driel, W., & Monnier Ragaigne, D., 2004, A&A, 428, 823
- Papastergis, E., Adams, E. A. K., & van der Hulst, J. M., 2016, 593, 39
- Pizagno, J., Prada, F., Weinberg, D. H. et al., 2007, AJ, 134, 945
- Peng, C. Y., Ho, L. C., Impey, C. D., & Rix, H., 2002, AJ, 124, 266
- Pohlen, M. & Trujillo, I., 2006, A&A, 454, 759
- Ponomareva et al., 2017, MNRAS, 469, 2387
- Ponomareva, A. 2017, Understanding disk galaxies with the Tully-Fisher relation [Groningen]: Rijksuniversiteit Groningen
- Sabatini S., Roberts S., & Davies J., 2003, Ap&SS, 285, 97
- Sandage, a. & Binggeli, B., 1984, AJ, 89, 919
- Sakai, S., Mould, J. R., Hughes, S. M. G., et al., 2000, ApJ, 529, 698
- Schlafly, E. F. & Finkbeiner, D. P., 2011, ApJ, 737, 103
- Schlegel D., Finkbeiner D., & Davis M., 1998, ApJ, 500, 525
- Schombert J. et al., 1992, AJ, 103, 1107
- Schombert J. et al., 2013, AJ, 146, 41
- Shao, Z. Y., Xiao, Q. B., Shen S. Y. et al., 2007, ApJ, 659, 1159
- Simons R. C., Kassin S. A., Weiner B. J. et al., 2015, MNRAS, 452, 986
- Smith, J. A., Tucker, D. L., Kent, S., et al., 2002, AJ, 123, 2121
- Sorce, J. G., Tully, R. B., Courtois, H. M., 2012, ApJ, 758, 12
- Sorce, J. G., Courtois, H. M., & Tully, R. B., 2012, AJ, 144, 133
- Sorce, J. G., Courtois, H. M., Tully, R. B., et al., 2013, ApJ, 765, 94
- Sprayberry, D., Impey, D. C., Irwin, M. J., McMahon, R. G. & Bothun, D. G., 1993, ApJ, 417, 114
- Sprayberry, D., Bernstein, M. G. & Impey, D. C., 1995, ApJ, 438, 72
- Theureau, G., Hanski, M. O., Coudreau, N., Hallet, N., & Martin, J. M., 2007, A&A, 465, 71
- Tiley, A. L., Bureau, M., Saintonge, A. et al., 2016, MNRAS, 461, 3494
- Trachternach, C., Bomans, D. J., Haberzettl, L., & Dettmar, R. J., 2006, A&A, 458, 341
- Trachternach, C., de Blok, W. J. G., McGaugh, S. S., van der Hulst, J. M., & Dettmar, R. -J., 2009, A&A, 505, 577
- Tully R. B. & Fisher J. R., 1977, A&A, 54, 661
- Tully R. B. & Fouque P., 1985, ApJS, 58, 67
- Tully, R. B., Pierce, M. J., Huang, J. S. et al., 1998, AJ, 115, 2264
- van der Hulst J. M. et al., 1993, AJ, 106, 548
- van Dokkum P., Abraham R., Merritt A. et al., 2015, ApJL, 798, L45
- Verheijen, M. A., 1997, PhD thesis, Univ. Groningen
- Williams, R. P., Baldry, I. K., Kevin, L. S., et al., 2016, MNRAS, 463, 2746
- Willick, 1994, ApJS, 92, 1
- Wu, H., Burstein, D., Deng, Z. G., et al., 2002, AJ, 123, 1364
- Zaritsky, D., Courtois, H., Munoz-Mateos, J. -C., et al., 2014, AJ, 147, 134
- Zheng, Z. Y., Shang, Z. H., Su, H. J., et al., 1999, AJ, 117, 2757
- Zhong, G. H., Liang, Y. C., Liu, F. S., et al., 2008, MNRAS, 391, 986
- Zwaan, M., van der Hulst, J., de Blok, W., & McGaugh, S., 1995, MNRAS, 273, L35